Doctoral School in Molecular, Cellular and Environmental Biology

Accademic year 2017/2018

XXXI cycle

Study on the evolution of explosive defensive systems in Coleoptera through functional anatomy and ultrastructure.

Studio sull'evoluzione dei sistemi difensivi esplosivi nei coleotteri mediante anatomia funzionale ed ultrastruttura.

Ph.D. Student: Maurizio Muzzi

Tutor: Prof. Andrea Di Giulio

Maurizio Muzzi (2018). **Study on the evolution of explosive defensive systems in Coleoptera through functional anatomy and ultrastructure.**

Doctoral thesis. Department of Science, Roma Tre University, Rome, Italy.

Maurizio Muzzi

Department of Science, Roma Tre University,

Viale Guglielmo Marconi, 446,

00146 Rome, Italy.

e-mail: maurizio.muzzi@uniroma3.it

INDEX

Preface

This thesis is focused on the anatomycal, morpho-functional and evolutive study of the pygidial explosive defensive systems of the bombardier beetles Paussinae and Brachinine (Carabidae). The thesis is structured as follow:

General introduction. Brief introduction on the issues related to evolution of explosive defensive systems in beetles.

Chapter 1. The chapter is conform to the published paper: Di Giulio, A., & Muzzi, M. (2018). Two novel approaches to study arthropod anatomy by using dualbeam FIB/SEM. Micron, 106, 21-26.

Chapter 2. The chapter is conform to the published paper: Di Giulio, A., Muzzi, M., & Romani, R. (2015). Functional anatomy of the explosive defensive system of bombardier beetles (Coleoptera, Carabidae, Brachininae). Arthropod structure & development, 44(5), 468-490.

Chapter 3. The chapter is conform to the published paper: Muzzi, M., Moore, W., & Di Giulio, A. (2019). Morpho-functional analysis of the explosive defensive system of basal bombardier beetles (Carabidae: Paussinae: Metriini). Micron 119, 24-38.

Chapter 4. The chapter is conform to the submitted paper: Muzzi, M., & Di Giulio, A. The ant nest "bomber": explosive defensive system of the flanged bombardier beetle Paussus favieri (Coleoptera, Carabidae). Arthropod structure & development.

Conclusions. This section briefly highlights and discusses the main outcomes of the present work.

Summary

I coleotteri carabidi appartenenti alle sottofamiglie Brachininae e Paussinae sono conosciuti con il nome di coleotteri bombardieri per via del loro particolarissimo meccanismo di difesa. Questi insetti, infatti, rispondono ad attacchi predatori ed a sollecitazioni meccaniche producendo esplosivamente una miscela chinonica finemente nebulizzata ed avente temperature prossime o pari a quelle dell'acqua in ebollizione. Il rilascio di questo getto vaporizzato è inoltre accompagnato da un crepitio facilmente percettibile ed è proprio grazie a questo scoppiettante rumorio ed alla natura caustica delle loro secrezioni che l'appellativo di bombardieri appare quanto mai appropriato. La sopraccitata strategia difensiva è resa possibile grazie ad una forma estremamente specializzata del sistema di ghiandole difensive pigidiali presente nella totalità dei carabidi. Tali ghiandole derivano da complesse invaginazioni cuticolari associate a cellule epidermiche e si presentano sempre come strutture dorsali pari, situate nell'area posteriore dell'addome e sboccanti al livello dell'ottavo segmento addominale. Solitamente, un sistema difensivo pigidiale di un coleottero carabide è composto da: una porzione ghiandolare, un dotto collettore, un reservoir ed una valvola. Le sostanze difensive prodotte dalla porzione ghiandolare vengono convogliate da un lungo dotto nel reservoir, una camera sacciforme atta all'immagazzinamento di queste ultime e ricoperta da uno strato muscolare. Il reservoir, assottigliandosi prossimalmente porta ad una valvola associata a muscoli che ne regolano l'apertura. La contrazione sincrona della muscolatura di valvola e reservoir permette al carabide di controllare l'espulsione delle sostanze difensive immagazzinate nel reservoir. Il sistema dei coleotteri bombardieri, tuttavia, appare eccezionalmente divergente da quello di altri carabidi grazie alla presenza di una seconda camera fortemente sclerotizzata detta camera di reazione. Essa è separata dal reservoir (considerato come la prima camera) grazie ad una valvola ed è associata a cellule ghiandolari accessorie secernenti gli enzimi catalasi e perossidasi. A seguito di un disturbo o di una minaccia i bombardieri contraggono i muscoli del reservoir, permettendo agli idrochinoni ed all'acqua ossigenata, contenuti al suo interno, di raggiungere la seconda camera (di reazione) contenente catalasi e perossidasi. Il mescolamento dei due gruppi di sostanze chimiche causa una reazione fortemente esotermica che, accompagnata dai caratteristici crepitii, porta alla produzione di chinoni, ossigeno, acqua e calore con conseguente innalzamento della temperatura fino a 100°C.
A dispetto della loro unicità, le ghiandole esplosive si ritrovano in due sottofamiglie distinte di coleotteri carabidi: Brachininae e Paussinae. La

condivisione del sistema esplosivo è resa particolarmente interessante dal fatto che i rapporti filogenetici tra paussini e brachinini sono ancora oggi controversi ed oggetto di dibattito. Da un lato, l'unicità strutturale del sistema esplosivo, con la sua organizzazione bi-compartimentalizzata e le sorprendenti analogie chimiche alla base della reazione esplosiva hanno spinto diversi autori ad ipotizzare un'evoluzione unica del sistema esplosivo e pertanto a considerare Paussinae e Brachininae come gruppi fratelli. D'altro canto le innumerevoli analisi morfologiche basate su caratteri di adulti e stadi pre-immaginali, suggeriscono una forte lontananza tra le due linee filetiche con paussini considerati come carabidi basali e brachinini considerati come carabidi particolarmente derivati. Questo supporterebbe invece l'ipotesi di una duplice evoluzione del sistema all'interno dei coleotteri carabidi. Analisi molecolari non sono state ancora in grado di fornire risposte convincenti in merito alla posizione di queste due sottofamiglie per riconosciuti problemi di "long branch attraction".

Sorprendentemente, mentre il sistema esplosivo è stato ben descritto e studiato dal punto di vista chimico e funzionale, studi dettagliati sulla sua morfologia non sono mai stati eseguiti. Il presente lavoro è volto a colmare queste carenze, analizzando per la prima volta ed in maniera comparativa la morfologia fine e l'ultrastruttura del sistema ghiandolare pigidiale di difesa in specie chiave rappresentative della diversità dei due gruppi di coleotteri bombardieri Paussinae e Brachininae. Le informazioni relative ai dettagli strutturali del sistema sono state ottenute grazie ai contributi congiunti di diverse tecniche di microscopia: dissezioni, analisi istologiche, microscopia a fluorescenza, microscopia a scansione (SEM) e microscopia a fascio ionico focalizzato (FIB/SEM). L'uso di tecniche complementari ha permesso di esplorare i diversi gradi di complessità anatomica del sistema. In particolare sono stati implementati due nuovi metodi che hanno permesso di analizzare l'ultrastruttura delle regioni cellulari utilizzando esclusivamente il microscopio FIB/SEM in luogo del microscopio elettronico a trasmissione (TEM).

Uno dei principali risultati del presente lavoro consiste nella caratterizzazione delle camere di reazione e del loro diverso grado di complessità nelle due sottofamiglie. L'analisi comparativa ha inoltre permesso di evidenziare molteplici differenze tra le due sottofomiglie per ognuna delle componenti del sistema (ghiandole, dotto, reservoir, valvola, camera di reazione, cellule accessorie), non solo al livello della morfologia generale ma anche al livello di morfologia cuticulare fine ed ultrastruttura. Inoltre l'analisi del sistema in più membri appartenenti alla stessa sottofamiglia conferma la posizione basale dei Metriini all'interno dei Paussinae; la posizione basale dei

Crepidogastrini all'interno dei Brachininae ed una condizione particolarmente derivata per quanto riguarda il genere *Paussus* all'interno dei Paussinae. Concludendo, nonostante le sorprendenti analogie chimiche, la mancanza di similarità morfologiche tra i sistemi esplosivi suggerisce che la produzione esplosiva di chinoni si sia evoluta indipendentemente in Paussinae e Brachininae, probabilmente in risposta a differenti pressioni ecologiche.

Abstract

Bombardier beetles exhibit one of the most extraordinary examples of defensive strategies ever evolved in animals: when disturbed, they abruptly produce hot quinones and release them as a caustic spray against offenders and potential predators. This unique ability is made possible by a particular kind of pygidial defensive system that represents an extreme specialization of the simple and non-explosive defensive pygidial glands found in other carabid and adephagan beetles. Though Brachininae represent the most renowned bombardier beetles group, a similar explosive defensive system is also present in the members of the ground beetle subfamily Paussinae, commonly known as "flanged bombardier beetles" for the presence of an elytral fold used to forwardly direct the defensive secretions. Whether the bombarding mechanism evolved only once or twice in the history of carabid beetles, is still a matter of controversy. Some authors emphasize the astonishing chemical and functional similarities of the two explosive defensive systems and favour the hypothesis that Paussinae and Brachininae are sister groups, and therefore the bombarding mechanism evolved only once. However, analyses of adult and larval morphological characters lead other authors to hypothesize that the Paussinae and Brachininae are more distantly related, and therefore the bombarding mechanism evolved two times independently. Molecular phylogenetic work has not yet resolved this question, largely because the subfamily Paussinae is subtended by a long branch in trees inferred by molecular sequence data and therefore it is prone to long branch attraction issues and the phylogenetic placement of this subfamily relative to all other carabids is uncertain. Surprisingly, while the system has been thoroughly analysed from chemical and functional points of view, a detailed morphological study has never been made. Fine morphological characterization is still incomplete in Brachininae and has never been performed in Paussinae while the ultrastructural features are still unknown in both groups. In order to supplement the partial and scattered information, the explosive defensive systems of key species belonging to the two bombardier beetles subfamilies Paussinae and Brachininae have been comparatively analysed using the contribution of complementary microscopy techniques. Dissections, histology, fluorescence microscopy, scanning electron microscopy (SEM) and focused ion beam microscopy (FIB/SEM) have been used to describe and illustrate various levels of anatomical complexity. Novel methods using FIB/SEM microscope were implemented to analyse ultrastructural features of the cellular regions, replacing the classical use of transmission electron microscopy (TEM). Explosive

defensive systems consist of two independent, symmetrical glands composed of secretory lobes, long collecting duct, reservoir chamber, cuticular valve, sclerotized reaction chamber, and an accessory glands.

One of the main results of the present work is the characterization of the fine morphology of the reaction chambers in Brachininae and Paussinae that allowed a deeper knowledge of the different level of complexity found in these two subfamilies. Equally important differences have been found comparing the other part of the system at gross and fine morphological scales, showing that the two systems differ in many ways, not only in their relative position within the abdomen, gross morphology and discharging method, but also in fine cuticular morphology and ultrastructural features. Similar comparative analysis within each bombardier beetle subfamily clearly confirmed the basal position of Metriini within Paussinae and the basal position of Crepidogastrini within Brachininae as well as the derived condition of the myrmecophilous genus *Paussus* within Paussinae. In conclusion, despite the remarkable chemical analogies, the lack of morphological similarity between the explosive defensive systems suggests that the bombarding mechanism may very well have evolved independently in the Paussinae and the Brachininae, perhaps in response to different ecological pressures.

Introduction

Members of the ground beetle subfamily Brachininae are commonly known as "bombardier beetles" thanks to their remarkable ability to produce and explosively discharge hot quinonoid substances from glandular openings near their abdominal tip (Eisner, 1958; Dean, 1980a,b; Eisner and Aneshansley, 1999).

This derived system represents an extreme specialization of the simple (non-explosive) pygidial defensive glands universally present in Carabidae (Forsyth 1970, 1972; Balestrazzi et al., 1985; Will et al. 2000). Pygidial glands are complex cuticular invaginations of the body wall lined by epidermal cells continuous with those of the integument. They open into the eighth abdominal tergum, posterolateral to the tergite and are always represented by paired dorsal structures located near the posterior end of the abdomen, above the reproductive organs and one on each side of the hindgut (Forsyth, 1972). Each structure is usually composed of a glandular system, a collecting duct, a reservoir and a valve. Every glandular system consists of an aggregation of acinous or finger-like secretory lobes producing defensive secretions. Differences among carabid groups are often matched by differences in the chemistry of the produced secretions; nevertheless, some chemicals appear to be quite common among a vast array of carabid beetles. For example, the followings are rather widespread: unsaturated acids, salicyl aldehyde, formic acid, ethyl phenol, hydrocarbons, quinones, methacrylic and tiglic acid (Moore and Wallbank, 1968; Will et al., 2000). One long and flexible collecting duct transfers the secretions, produced by the glands, into the reservoir chamber, a sac-like structure covered by a muscle coat of variable thickness. The reservoir usually narrows proximally and leads to an opening valve located anterior to the exit pores. The valve and the reservoir muscles allow the beetles to control the ejection of the defensive substances that are usually sprayed or oozed from the beetle body. The defensive gland system of Brachininae is unique in having a second, highly sclerotized compartment associated with numerous accessory glands. This second chamber is known as the reaction chamber and is separated from the reservoir (representing the first chamber) by a one-way valve similar to the one present in other Carabidae. This two-chambered system allows brachinines to explosively produce quinones at the moment of the ejection mixing two sets of chemicals stored separately. The first set of chemicals is composed by hydroquinones and hydrogen peroxide, which are produced by the secretory

lobes and stored in the reservoir. The second set of chemicals, instead, is made of catalases and peroxidases, produced by the accessory glands surrounding the reaction chamber and stored in the latter. When bombardier beetles are disturbed, muscles surrounding the reservoir chamber contract, allowing the aqueous solution of hydroquinones (10%) and hydrogen peroxide (25%) to pass through the one-way valve and enter the reaction chamber. When the fluid from the reservoir is squeezed into the reaction chamber, where enzymes are stored, a strong explosive exothermic reaction takes place and leads to the production of benzoquinones, free oxygen, water and heat up to 100°C (Schildknecht and Holoubek, 1961; Aneshansley et al., 1969). The explosive reaction is accompanied by audible crepitating sounds, thus the name "bombardier beetles", and consists in the instantaneous series of events reported in the following. The catalase reacts with aqueous hydrogen peroxide, promoting its decomposition and producing water and freed oxygen. At the same time, the liberated oxygen is used by the peroxidase to force the oxidation of the hydroquinones to their respective quinones. This oxidation leads to production of molecular hydrogen that will combine with oxygen to produce water. As already mentioned, this fast catalytic reaction is strongly exothermic and is capable of heating the defensive spray up to the temperature of boiling water. Considering that quinones are intrinsically repellent, even when cold, it is apparent that the thermal properties of the bombardier beetles spray greatly contribute to the overall defensive potential of the secretion. Another fascinating feature of the Brachininae defensive system is that its efficiency does not only depend on the caustic nature of the secretion or its high temperature. In fact, another key factor in the success of this exceptional anti-predator adaptation is represented by the remarkable ability to precisely aim the spray. These beetles are, in fact, capable of hitting a target at long distance, thanks to the great mobility of their abdominal tip, and to the speed at which the chemical spray is ejected (Eisner, 1958; Dean, 1980a,b; Eisner and Aneshansley, 1999; Eisner et al., 2006). The degree of precision is so high that the insect can aim its spray in any direction, including potential targets located towards its back and even the individual segment of the leg stimulated by the predator (Eisner and Aneshansley, 1999). Furthermore, a last peculiarity, responsible for the success of the bombardier beetles pygidial system, is the capacity to perform up to 20 multiple consecutive discharges; an ability that surely plays an important role in facing numerous small aggressors like ants. So, what may seem just an unusual habit to the untrained eye, is the expression of an highly refined defensive strategy capable of deterring a vast array of predators (Eisner, 1958; Dean, 1980a,b; Eisner et al., 2006). The quinonoid spray, in

fact, is capable of repelling a broad range of arthropod attackers ranging from smaller ants to bigger aggressors such as sizable beetles, praying mantes or spiders. It is also noteworthy that among the predators discouraged by the obnoxious Brachininae spray there are even vertebrates such as frogs and little birds. Even a human being may feel discomfort or even painful sensations when sprayed by bigger species or hit in more sensitive areas such as eyes, mucous surfaces and sites of injured skin. The story goes that among the people who "painfully met" with bombardier beetles there is the famous naturalist Charles Darwin. In fact, one anecdote relates how Darwin, in the stress of handling three rare beetles at a time, put one of them in his mouth. This specimen was likely a bombardier beetle that, feeling under threat, released its hot spray down Darwin's throat forcing him to deal with two unfortunate consequences: severe pain and the loss of the specimens (Desmond et al., 1994). A similarly uncomfortable experience is mentioned by the entomologist and archaeologist John Obadiah Westwood (1839) that, quoting a traveller, reported that certain south American bombardier beetles were able to burn the flash to such a degree that only a few specimens could be captured with bare hands.

Even if exceptional and anomalous, the defensive mechanism of Brachininae bombardier beetles is not strictly unique: a similar two chambered explosive system has been indeed observed in another single group of beetles. These are members of ground beetle subfamily Paussinae, commonly known as the “flanged bombardier beetles”, so named for their distinctive subapical elytral fold they use to direct their spray taking advantage of the Coanda effect (Eisner and Aneshansley, 1982), the tendency of moving fluids to cling to curved surfaces and move along them. Paussinae beetles use these curved flanges as launching guides to forwardly direct the hot quinones released from the lateral opening of their pygidial glands; a completely different “aiming strategy” if compared to the hypermobile abdomen of Brachininae, precisely addressing the caustic spray from the almost joined apical pores of their pygidial glands. Despite completely distinct from the one of Brachininae, even the Paussinae defensive system allows the beetle to precisely aim the defensive system spray against the source of disturbance and to repeatedly attack the same or multiple aggressors with great efficiency. As stressed in the past by several authors (Eisner et al., 1977, 1989, 1991, 2000), there are striking general similarities between Paussinae and Brachininae defensive systems, including the presence of the unique sclerotized reaction chamber and the nature of the chemicals involved in the explosive reaction. However, the phylogenetic relationship between Brachininae and Paussinae remains unclear (Maddison et al., 1999; Eisner et

al., 2000, 2001); it is possible that these two lineages of bombardier beetles are products of convergent evolution, or it is also possible that they represent each other's sister groups. Therefore, in spite of the exclusiveness of the bombarding mechanism, there are still two mutually exclusive hypotheses. The first one is that the explosive defensive system evolved only once, thus Brachininae and Paussinae must be considered as a monophyletic lineage. The second hypothesis, instead, sustains that the explosive defensive system evolved independently in Brachininae and Paussinae. Some authors (Eisner et al., 1977, 2000, 2001; Aneshansley et al., 1983; Erwin and Sims, 1984; Bousquet, 1986), emphasizing the astonishing chemical and functional similarities of the two explosive defensive systems, favoured the hypothesis of single evolution, and considered Paussinae and Brachininae as sister groups. On the contrary, the analyses of adult (Forsyth, 1972; Ball and McCleve, 1990; Deuve, 1993; Liebherr and Will, 1998) and larval morphological characters (Beutel, 1992, 1993; Arndt, 1998), lead other authors to consider Paussinae and Brachininae as distant and unrelated taxa, favouring the hypothesis of a double evolution of the bombarding mechanism.

Due to their distribution and cryptic habits, Paussinae are unknown to many; on the contrary, even those unfamiliar with entomology are aware of the existence of the much more common Brachininae also thanks to a recent "popularization". In fact, brachinines are becoming a worldwide famous textbook example of sophisticated defensive mechanism, thanks also to the striking similarities with human weapons. In fact, even if the beetle cannot shoot real bullets, the audible pops, the abrupt production of hot chemicals, and their ejection as a fine aerosolized spray, resembling swirling smoke produced by small cannons, may lead the observer to think that the bombardier beetles are using little weapons against the enemies. Even the astonishing accuracy of these beetles in aiming the spray against enemies (Eisner and Aneshansley, 1982, 1999), recalls the precise pointing of a gun turret. It is also interesting to note that Brachininae have been even repeatedly studied as a biomimetic model for human applications (Beheshti and McIntosh, 2007; Lai, 2010; Booth et al., 2012; Schroeder et al. 2018). In particular, the reaction chambers have been used as a model to improve the efficiency of impact and shockwave absorbing engineering designs related to the production of military and motorcycle helmets and to the production of crumple zones in automobiles and locomotives (Lai, 2010). The discharging apparatus, instead, inspired the development of liquid spray atomization technologies with potential applications in fuel injectors, drug delivery

systems, consumer aerosols and even in fire extinguishers (Booth et al., 2012).
In the past, scientists thoroughly analysed and widely investigated this system and, to a minor extent, the one of paussines from both chemical and functional points of view (Eisner, 1958; Moore and Wallbank, 1968; Aneshansley et al., 1969, 1983; Schildknecht, 1970, Eisner et al., 1977, 1989, 1991, 2000, 2001; Eisner and Aneshansley, 1982, 1999; Arndt et al., 2015), leading to a precise identification of the precursors (hydroquinones and hydrogen peroxide) and the catalytic enzymes (catalases and peroxidases) causing the exothermic reaction that generates the ejected products (benzoquinones, free oxygen, water and heat) (Schildknecht and Holoubek, 1961; Schildknecht et al., 1968, 1970; Aneshansley et al., 1969). Anyway, fine morphology and ultrastructural features of these systems have been greatly overlooked and morpho-anatomical data are still surprisingly limited and partial, indeed, the majority of the available information is limited to gross morphology and is based on dissections of dried specimens observed by optical microscopy (Forsyth, 1972; Eisner et al. 1989, 1991). Concerning fine morphological data obtained with SEM, few scattered and incomplete pieces of information are found in publications dealing with chemistry or functional aspects of the system, but most of them are limited to micrographs used for illustrative purposes (Eisner et al., 2000, 2001). Unfortunately, ultrastructural and anatomical data concerning the defensive system at cellular and sub-cellular levels are totally missing.

In view of the above the aims of the present work are:

- Provide a first comparative and detailed morphological and ultrastructural analysis of the explosive pygidial defensive system of Brachininae, analysing species belonging to three different subtribes representative of the Brachininae diversity.

- Characterize with the same level of detail the explosive defensive system of Paussinae, analysing pygidial glands in two different tribes, the most basal Metriini and the highly derived Paussini.

- Investigate if the morphology of the explosive defensive system and its anatomical features are stable within the same bombardier lineage, checking for differences among members of the same sub-family.

- Explore if the system of myrmecophilous paussines and the one of free living species is similar or not and if potential differences mirror different life strategies.

- Provide functional interpretation of pygidial glands components in Paussinae and Brachininae.

- Compare the explosive defensive systems of the two bombardier groups, identifying similarities and differences, contributing to the debate on the evolution of the bombarding mechanism.

- Evaluate how the integrated contribution of different and complementary microscopy techniques can be used to address the problems related to morphological and anatomical characterization.

Methodological note:

In this work a comparative morphological analysis of different defensive systems in bombardier beetles is presented, crossing standard optical and electron microscopy techniques with cutting edge technologies to obtain complementary morpho-anatomical data.
Dissections have been performed on a great number of dried material coming from museums and private collections in order to obtain a first gross morphological data on cuticular parts of the system. Live specimens, collected during different expeditions, have been used to obtain other gross morphological data on tissues and, especially, to perform histological analysis of the system and to study its ultrastructure using electron microscopy. The classical use of transmission electron microscopy (TEM) was replaced by the use of the focused ion beam scanning electron microscope (FIB/SEM), and two novel approaches to study arthropod anatomy by using this instrument have been implemented. Fluorescence microscopy, was used to check for the presence of resilin in the two systems, exploiting its autofluorescence under UV excitation. The possibility to detect the presence of this elastomeric protein allowed a better understanding of the functional anatomy of the two bombardier beetles systems pointing out regions subject to high mechanical stress.
Additionally, during the last three years, more than 30 species representative of the main genera and lineages of the two bombardier beetle subfamilies Paussinae and Brachininae have been scanned by X-ray micro-tomography using both synchrotron and laboratory micro-CT. The resulting virtual thin slices will provide a precise three-dimensional data on both external and

internal anatomy of the whole insects. Scanning of the beetles will also allow creating three-dimensional models that will facilitate the comparison of different explosive defensive systems. The analysis of these data is still in progress and will be presented in future papers in combination with ultrastructural and fine morphological data.

References

Aneshansley, D.J., Eisner, T., Widom, J.M. and Widom, B., 1969. Biochemistry at 100°C: explosive secretory discharge of bombardier beetles (*Brachinus*). Science 165, 61-63.

Aneshansley, D.J., Jones, T.H., Alsop, D., Meinwald, J. and Eisner, T., 1983. Thermal concomitants and biochemistry of the explosive discharge mechanism of some little known bombardier beetles. Experientia 39, 366-368.

Arndt, E., 1998. Phylogenetic investigation of Carabidae (Coleoptera) using larval characters. Phylogeny and classification of Caraboidea (Coleoptera: Adephaga). In: Ball, G.E., Casale, A., Taglianti, A.V. (Eds.), International Congress of Entomology, Phylogeny and Classification of Caraboidea (Coleoptera:Adephaga): Proceedings of a Symposium, 28 August 1996, Florence, Italy: XX International Congress of Entomology. Museo regionale di scienze naturali, Torino, pp. 171-190.

Arndt, E.M., Moore, W., Lee, W.K. and Ortiz, C., 2015. Mechanistic origins of bombardier beetle (Brachinini) explosion-induced defensive spray pulsation. Science 348, 563-567.

Balestrazzi, E., Valcurone Dazzini, M.L., Bernardi, M.D., Vidari, G., Vita-Finzi, P., Mellerio, G., 1985. Morphological and chemical studies on the pygidial defence glands of some Carabidae (Coleoptera). Naturwissenschaften 72, 482-484.

Ball, G.E. and McCleve, S., 1990. The middle American genera of the tribe Ozaenini, with notes about the species in southwestern United States and selected species from Mexico. Quest. Ent. 26, 30-116.

Beheshti, N. and McIntosh, A.C., 2007. A biomimetic study of the explosive discharge of the bombardier beetle. Int. J. Des. Nat. Ecodyn. 1, 61-69.

Beutel, R.G., 1992. Study on the systematic position of Metriini based on characters of the larval head (Coleoptera: Carabidae). Syst. Entomol. 17, 207-218.

Beutel, R.G., 1993. Phylogenetic analysis of Adephaga (Coleoptera) based on characters of the larval head. Syst. Entomol. 18, 127-147.

Booth, A., McIntosh, A.C., Beheshti, N., Walker, R., Larsson, L.U. and Copestake, A., 2012. Spray technologies inspired by bombardier beetle. In: Bhushan, Bharat (Ed.), Encyclopedia of Nanotechnology. Springer, Heidelberg, New-York, pp. 2495-2503.

Bousquet, Y., 1986. Description of first-instar larva of *Metrius contractus* Eschscholtz (Coleoptera: Carabidae) with remarks about phylogenetic relationships and ranking of the genus Metrius Eschscholtz. Can. Entomol. 118, 373-388.

Dean, J., 1980a. Effect of thermal and chemical components of bombardier beetle chemical defense: glossopharyngeal response in two species of toads (*Bufo americanus*, *B. marinus*). J. Comp. Physiol. 135, 51-59.

Dean, J., 1980b. Encounters between bombardier beetles and two species of toads (*Bufo americanus*, *B. marinus*): speed of prey-capture does not determine success. J. Comp. Physiol. 135, 41-50.

Desmond, A., Darwin, J.M. and Kingsland, S.E., 1994. The life of a tormented evolutionist. Bulletin of the History of Medicine, 68, 533.

Deuve, T., 1993. L'abdomen et les genitalia des femelles de Coléoptères Adephaga. Mémoires du Muséum national d'histoire naturelle. Editions du Muséum, Paris.

Eisner, T., 1958. The protective role of the spray mechanism of the bombardier beetle, *Brachynus ballistarius* Lec. J. Insect Physiol. 2, 215-220.

Eisner, T., Jones, T.H., Aneshansley, D.J., Tschinkel, W.R., Silberglied, R.E. and Meinwald, J., 1977. Chemistry of defensive secretions of bombardier beetles (Brachinini, Metriini, Ozaenini, Paussini). J. Insect Physiol. 23, 1383-1386.

Eisner, T. and Aneshansley, D.J., 1982. Spray aiming in bombardier beetles: jet deflection by Coanda effect. Science 215, 83-85.

Eisner, T., Ball, G.E., Roach, B., Aneshansley, D.J., Eisner, M., Blankespoor, C.L. and Meinwald, J., 1989. Chemical defense of an ozaenine bombardier beetle from New Guinea. Psyche 96, 153-160.

Eisner, T., Attygalle, A.B., Eisner, M., Aneshansley, D.J. and Meinwald, J., 1991. Chemical defense of a primitive Australian bombardier beetle (Carabidae): *Mystropomus regularis*. Chemoecology 2, 29-34.

Eisner T. and Aneshansley, D.J., 1999. Spray aiming in the bombardier beetle: photographic evidence. P. Natl. Acad. Sci. U.S.A. 96, 9705-9709.

Eisner, T., Aneshansley, D.J., Eisner, M., Attygalle, A.B., Alsop, D.W. and Meinwald, J., 2000. Spray mechanism of the most primitive bombardier beetle (*Metrius contractus*). J. Exp. Biol. 203, 1265-1275.

Eisner, T., Aneshansley, D.J., Yack, J., Attygalle, A.B. and Eisner, M., 2001. Spray mechanism of crepidogastrine bombardier beetles (Carabidae: Crepidogastrini). Chemoecology 11, 209-219.

Eisner, T., Aneshansley, D.J., del Campo, M.L., Eisner, M., Frank, J.H. and Deyrup, M., 2006. Effect of bombardier beetle spray on a wolf spider: repellency and leg autotomy. Chemoecology 16, 185-189.

Erwin, T.L. and Sims, L.L., 1984. Carabid beetles of the West Indies (Insects: Coleoptera): a synopsis of the genera and checklists of tribes of Caraboidea, and of the West Indian species. Quaest. ent. 20, 351-466.

Forsyth, D.J., 1970. The ultrastructure of the pygidial defence glands of the carabid *Pterostichus madidus* F. J. Morphol. 131, 397-415.

Forsyth, D.J., 1972. The structure of the pygidial defence glands of Carabidae (Coleoptera). Trans. Zool. Soc. Lond. 32, 249-309.

Lai, C., 2010. Potential Applications of the Natural Design of Internal Explosion Chambers in the Bombardier Beetle (Carabidae, *Brachinus*) (Doctoral dissertation). Massachusetts Institute of Technology.

Liebherr, J.K. and Will, K.W., 1998. Inferring phylogenetic relationships within Carabidae (Insecta, Coleoptera) from characters of the female reproductive tract. Phylogeny and classification of Caraboidea (Coleoptera: Adephaga). In: Ball, G.E., Casale, A., Taglianti, A.V. (Eds.), International Congress of Entomology, Phylogeny and Classification of Caraboidea (Coleoptera:Adephaga): Proceedings of a Symposium, 28 August 1996, Florence, Italy : XX International Congress of Entomology. Museo regionale di scienze naturali, Torino, pp. 107-170.

Maddison, D.R., Baker, M.D. and Ober, K.A., 1999. Phylogeny of carabid beetles as inferred from 18S ribosomal DNA (Coleoptera: Carabidae). Syst. Entomol. 24, 103-138.

Moore, B.P. and Wallbank, B.E., 1968. Chemical composition of the defensive secretion in carabid beetles and its importance as a taxonomic character. Proc. R. Entomol. Soc. Lond. Ser. B 37, 62-72.

Roach, B., Dodge, K.R., Aneshansley, D.J., Wiemer, D., Meinwald, J. and Eisner, T., 1979. Chemistry of defensive secretions of ozaenine and paussine bombardier beetles (Coleoptera: Carabidae). Coleopts. Bull. 33, 17-19.

Schildknecht, H. and Holoubek, K., 1961. Die Bombardierkäfer und ihre Explosionschemie V. Mitteilung über Insekten-Abwehrstoffe. Angew. Chem. Ger. Ed. 73, 1-7.

Schildknecht, H., Maschwitz, E. and Maschwitz, U., 1968. Die Explosionschemie der Bombardierkäfer (Coleoptera, Carabidae) III. Mitt.: Isolierung und Charakterisierung der Explosionskatalysatoren. Z. Naturforsch. B 23, 1213-1218.

Schildknecht, H., 1970. The defensive chemistry of land and water beetles. Angew. Chem. Int. Ed. 9, 1-9.

Schildknecht, H., Maschwitz, E. and Maschwitz, U., 1970. Die Explosionschemie der Bombardierkäfer: Struktur und Eigenschaften der Brennkammerenzyme. J. Insect Physiol. 16, 749-789

Schroeder, T.B., Houghtaling, J., Wilts, B.D. and Mayer, M., 2018. It's Not a Bug, It's a Feature: Functional Materials in Insects. Advanced Materials, 30, 1705322.

Westwood, J.O., 1840. An introduction to the modern classification of insects: founded on the natural habits and corresponding organisation of the different families (Vol. 2). Longman, Orme, Brown, Green, and Longmans.

Will, K.W., Attygalle, A.B. and Herath, K., 2000. New defensive chemical data for ground beetles (Coleoptera: Carabidae): interpretations in a phylogenetic framework. Biol. J. Linn. Soc. Lond. *71*, 459-481.

Micron 106 (2018) 21–26

Contents lists available at ScienceDirect

Micron

journal homepage: www.elsevier.com/locate/micron

Two novel approaches to study arthropod anatomy by using dualbeam FIB/SEM

Andrea Di Giulio[a,b,*], Maurizio Muzzi[a,b]

[a] Department of Science, University Roma Tre, Viale G. Marconi, 446, 00146 Rome, Italy
[b] Laboratorio Interdipartimentale di Microscopia Elettronica (LIME), University Roma Tre, Rome, Italy

ARTICLE INFO

Keywords:
Anatomy
Electron microscopy
Exoskeleton
Methods
Morphology
Ultrastructure

ABSTRACT

Transmission Electron Microscopy (TEM) has always been the conventional method to study arthropod ultrastructure, while the use of Scanning Electron Microscopy (SEM) was mainly devoted to the examination of the external cuticular structures by secondary electrons. The new generation field emission SEMs are capable to generate images at sub-cellular level, comparable to TEM images employing backscattered electrons. The potential of this kind of acquisition becomes very powerful in the dual beam FIB/SEM where the SEM column is combined with a Focused Ion Beam (FIB) column. FIB uses ions as a nano-scalpel to slice samples fixed and embedded in resin, replacing traditional ultramicrotomy. We here present two novel methods, which optimize the use of FIB/SEM for studying arthropod anatomy.

1. Introduction

Traditionally, anatomical studies of arthropod fine structures have always been conducted using Scanning Electron Microscopy (SEM) combined with Transmission Electron Microscopy (TEM). In particular, minute external structures (such as pores, sensilla, scales, ommatidia) have been thoroughly described thanks to the use of SEM while TEM has been widely used to investigate the internal anatomy of the animal analysing ultrastructural features.

The presence of a hard exoskeleton facilitates the study of arthropod external morphology reducing the risk of artefacts and making easier to observe small cuticular structures employing SEM. However, the hardness of the integument and its thickness may represent an obstacle for the processing of arthropod samples; specifically, the chitinous nature of the exoskeleton (sclerotized and often mineralized) can cause not only several difficulties regarding the penetration of fixatives but it makes also very challenging to obtain satisfactory thin and ultrathin sections during the ultramicrotomy process.

These problems have affected the progresses of the anatomical studies of arthropods leading to a lack of balance between the analysis of external and internal features favouring fine morphological SEM studies over ultrastructural analyses of tissues and cells.

Over the past twenty years microscope technology has developed new instruments especially for physics and engineering applications (like scanning probe microscopy, focused ion beam microscopy, ultrasonic microscopy, X-ray microscopy), some of them combining more technology in a single complex system. However, biological studies rarely profited of these new technologies being more tied to the use of the classical microscopy techniques like optical, confocal, scanning or transmission microscopy.

In the last few years, as highlighted by Friedrich et al. (2014), entomologists showed a renewed interest in insect morphology and anatomy partly thanks to the possibility to combine complementary techniques ranging from the traditional approaches (dissections, histology and maceration) to the use of modern and advanced instruments like Confocal Laser Scanning Microscopy (CLSM), Micro Computed Tomography (μ-CT) or FIB/SEM. In particular, the possibilities offered by these new techniques allowed researchers to thoroughly analyse anatomical features that otherwise would be very hard or almost impossible to inspect. For example CLSM permits to three-dimensionally visualize the insect morphology and even the internal anatomy of small and delicate samples that are very troublesome to dissect and/or extremely hard to prepare for a successful histological analysis (Grzywacz et al., 2014; Smolla et al., 2014). Micro-CT instead makes it possible to acquire a complete series of virtual thin sections that are almost free of artefacts, perfectly aligned and obtained in a very short time compared to lengthy and often unsuccessful acquisition of histological sections (Martín-Vega et al., 2017). Other than providing a three dimensional data of both internal and external structures this analysis is non-destructive, so it can be performed on rare material (Simonsen and Kitching, 2014) and can be used even on ancient or fossil samples embedded in amber (Tafforeau et al., 2006; Pohl et al., 2010).

* Corresponding author at: Department of Science, University Roma Tre, Viale G. Marconi, 446, 00146 Rome, Italy.
E-mail address: andrea.digiulio@uniroma3.it (A. Di Giulio).

https://doi.org/10.1016/j.micron.2017.12.007
Received 16 November 2017; Received in revised form 18 December 2017; Accepted 18 December 2017
Available online 21 December 2017

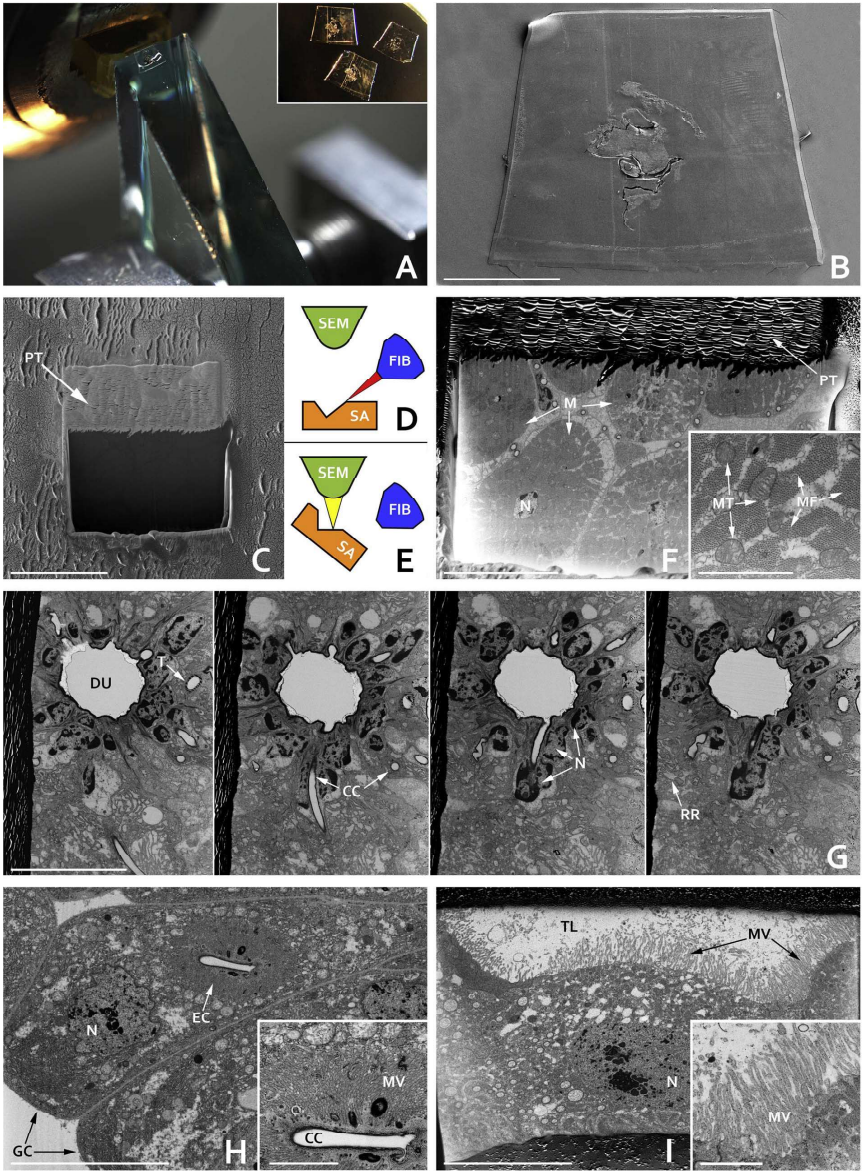

(caption on next page)

Fig. 1. Slice&Mill method. A. Ultramicrotome slicing of the embedded sample with a glass knife. The inset box shows three thick slices (20 μm) glued on a stub and gold sputtered. B. SEM picture of a thick resin slice of an included abdomen of *Brachinus elongatulus* (visible in the centre). C. SEM image of the thick slice after platinum coating and subsequent milling. D. Schematic representation of ion milling performed at a tilt angle of 0°. E. Illustration of the micrograph acquisition using the backscattered electron detector. Note that, compared to the milling process the stage is tilted by +38°. F. Milled surface observed by backscattered electrons showing the anatomy *B. elongatulus* abdominal muscles; the inset box shows a close-up of myofibrils with visible microfilament arrays and the associated mitochondria. G. Four sequential images of *B. elongatulus* abdominal glands at the level of the collecting ductules, obtained by backscattered electrons after FIB sectioning (approximately 800 nm between the slices). H. Backscattered electron image showing extracellular cavity (EC) and conducting canal (CC) inside an abdominal gland cell (GC) of *B. elongatulus*; the inset box shows a close-up of the conductive canal (CC) surrounded by microvilli (MV). I. Backscattered electron image showing part of a malpighian tubule of *B. elongatulus*; the box shows a close-up of the microvilli (MV) inside the lumen.
Acronyms: CC conducting canal, DU ductule, EC, extracellular cavity, FIB ion beam, GC, gland cell, M muscles, MF myofibrils, MT mitochondria, MV microvilli, N nucleus, PT platinum layer, RR rough endoplasmic reticulum, SA sample, SEM electron beam, TL lumen of the Malpighian tubule.
Scale bars: B = 1 mm; C = 20 μm; F = 10 μm; F, close up = 2 μm; G = 10 μm; H = 10 μm; H, close up = 2 μm; I = 10 μm; I, close up = 2 μm.

One of the most promising combined instruments for biological applications, especially in the field of morphology and anatomy, is by far the Focused Ion Beam/Scanning Electron Microscope (FIB/SEM) representing a revolutionary instrument that facilitates structural analysis of any biological sample at sub-micron scale (Kizilyaprak et al., 2014; Narayan and Subramaniam, 2015; Titze and Genoud, 2016). In fact, FIB/SEM integrates a field emission SEM column, used for imaging, with a Focused Ion Beam column, used as a nano-scalpel for sectioning the sample. The FIB column replaces the diamond knife of the ultramicrotome thanks to the milling process, while the SEM column, combined with an appropriate sample preparation and backscattered electrons (BSE) detector, can be used to produce TEM-like images (Villinger et al., 2012). For these reasons, the FIB/SEM simplifies and speeds up the sample processing avoiding artefacts due to the most critical parts of the preparation and provides a complete set of serial ultrastructural sections that can be used for 3D reconstruction and visualization of any microstructures (Medeiros et al., 2012; Takemura et al., 2015; Tamada et al., 2017).

During the past 15 years the FIB/SEM was only seldom employed by biologists, especially for the visualization of organelles and cells (Villinger et al., 2012; Wei et al., 2012; Kizilyaprak et al., 2014; Narayan and Subramaniam, 2015; Tamada et al., 2017), while we pioneered the use of FIB/SEM as a replacement of the combined use of SEM and TEM in the morpho-anatomical characterization of insects (Di Giulio et al., 2015; Must et al., 2017).

We present here two new techniques for the study of arthropod cells and tissues that exploit the FIB/SEM capability of analysing arthropod structural anatomy, overcoming the possible technical pitfalls and artefacts due to the presence of a hard exoskeleton. These techniques represent an improvement of those already employed in our previous studies (Di Giulio et al., 2012; Di Giulio et al., 2015; Must et al., 2017).

2. Two novel methods and results

The methods here presented were developed at the electron microscopy laboratory of the Roma Tre University (LIME, Rome, Italy) by using the Dual Beam (FIB/SEM) Helios Nanolab (FEI Company, Hillsboro – US).

Prior to analyse the samples with FIB/SEM, the specimens must be processed and embedded in epoxy or acrylic resins by using any standard TEM protocol including en-bloc staining. This technique allows creating contrasted images increasing the number of backscattered electrons emerging from biological samples subsequent to the interaction between sample surface and focused electrons (Lešer et al., 2009; Kizilyaprak et al., 2014). The samples here reported for illustrating the new methods were processed using the following protocol. Insects were euthanized with CO2 prior to dissecting. Antennae and abdomen were removed from the specimens, submerged in cacodylate buffer 0.1 M, immersed in Karnovsky's fixative solution for 2 h at 4 °C, post-fixed in 1% Osmium tetroxide for 1 h at 4 °C, stained en-bloc with 2% aqueous Uranyl acetate, dehydrated in a graded ethanol series and embedded in epoxy resin with propylene oxide as a bridging solvent.

2.1. "Slice&Mill" method (Fig. 1)

Although this method is suitable for any kind of biological sample, including soft homogeneous tissues, its application is especially recommended for the characterization of complex cellular structures associated to hard integument (exocrine glands, sensilla, external genitalia, etc.). It is based on the production of large thick slices (see below) of voluminous resin embedded samples ranging from single appendages (i.e. legs, antennae, wings, elytrae, gills, mandibles) to entire regions (i.e. head capsule, abdomen, thorax). A single thick slice of an entire body region contains different tissues and several regions of interest that can be easily localized using the SEM column, and subsequently sectioned, following different orientations, using the FIB column. This possibility is exemplified by the results presented in Fig. 1, in fact, using a single thick slice we imagined: muscles (Fig. 1F); different gland systems (Fig. 1G, H); and Malpighian tubules (Fig. 1I) of the ground beetle *Brachinus elongatulus* Chaudoir, 1876. The opportunity to analyse different tissues using a single thick slice may not only save a lot of time but may also spare many samples and the materials needed for fixation, staining and resin infiltration.

a) Block sectioning: the resin block is trimmed with a razor blade until the sample is exposed, then it is cut by using an ultramicrotome and a glass knife (Fig. 1A) until the target area is reached. The observation of stained semi-thin slices (ranging from 0.5 to 2 μm) by an optical microscope allows to assure that the area of interest has been reached checking for the presence of the desired tissues.
b) Slicing: thick slices of 15–20 μm are cut with the ultramicrotome using a glass knife and mounted on a conventional SEM-stub by using double sided adhesive carbon disks (Fig. 1A–B). The increased thickness of the sections diminishes the risk of damaging the brittle fine cuticular structure during the cutting process.
c) Gold sputtering: in order to make the samples conductive the stubs with the slices are sputter coated with 30 nm of gold and observed at the FIB/SEM (Fig. 1A box on top right corner; B).
d) Platinum protection coating: the target structures present on each thick slice are identified by the secondary electrons. Stained histological sections obtained in step "a" are useful as a guide to identify the regions of interest. Once defined, the region of interest is coated with a platinum layer 0.5–1 μm thick (Fig. 1C) by Electron Beam Induced Deposition (EBID), in order to protect the sample from the ion beam damage during the milling process.
e) Milling: the area protected by the platinum layer is transversally etched ("cross sectioned" according to the FIB/SEM software) by the focused ion beam operated at 30 kV and a current range 0.92–6.5 nA (Fig. 1D).
f) Imaging: SEM pictures are taken after tilting the stage of +38° compared to the stage tilt used during the milling process. Since the two columns are oriented at 52° the supplementary tilt of 38° is required to bring the cut surface perpendicular to the SEM column (Fig. 1E). The "cross section" pictures are acquired by using BSE and through-the-lens (TLD) detector, with an operating voltage of 2 kV, at a working distance of 2 mm, and a beam current of 0.17 nA (Fig. 1F–I). In order to make the pictures similar to the ones

obtained with a conventional TEM, the contrast was inversed. Images are acquired with a frame size ("resolution" according to FIB/SEM software) of 1024 × 884 or 2048 × 1768 and a dwell time of 20–80 μs according to the number of slices, magnification and level of details required.

g) Serial imaging: repeating steps "e" and "f" allows obtaining a series of sequential images of arbitrary step (Fig. 1G). The milling process can be paused at will in order to obtain serial sectioning of the sample ranging from a few nanometers (useful for further 3D reconstructions) to hundreds of microns.

2.2. "Outside-In" method (Fig. 2A–G)

This method is based on the extraction of the sample from the resin block, exploiting the hardness of the arthropod exoskeleton and the low adhesion between the resin and the waxy cuticular surfaces. The extraction process removes only the external embedding medium, keeping the tissues and cells intact and still embedded in the previously infiltrated resin. This method was developed for the complete characterization of single cuticular microstructures and it proved to be particularly suitable for the study of arthropod sensorial organs as it is able to provide information on both the external and the internal anatomy of the same structure. In fact, after the extraction process the sample surface is entirely exposed allowing to: precisely localize target structures; characterize their external morphology; and ablate the surface to reveal their inner portion by using the focused ion beam. After the ablation performed by the FIB column, the freshly milled surface can be used to image the ultrastructural features of the sensilla by using backscattered electrons. To illustrate the potential of this method we analysed an antenna of the ground beetle *Paussus favieri* Fairmaire, 1851, targeting coeloconic sensilla (Fig. 2A–G).

a) Extraction: the first step is the extraction of the sample from the resin block (Fig. 2A). After heating the block in oven at 50 °C for 5–7 min, the resin is roughly cut out with a blade or a scalpel until the sample is close to the surface. After that, the sample is gently removed, first needling the area surrounding the sample by using fine and sharp entomological pins (Fig. 2A) or other sharp tools, and then by using fine tipped tweezers acting as levers. When the sample is close to the surface, the removal can be performed by using fine entomological pins without trimming the block. A small brush is useful to remove resin residues from the sample.
b) Mounting: the extracted sample is mounted on a conventional SEM-stub by using double-sided adhesive carbon disks (Fig. 2A box on top right corner).
c) Gold sputtering: in order to make the samples conductive the stubs with the antennae are sputter coated with 30 nm of gold and observed at the FIB/SEM (Fig. 2A box on top right corner; B).
d) Platinum protection coating: The SEM column allows an easy recognition of the external cuticular structures (*e.g.* pores, sensilla, scales, ommatidia) although some of them might be damaged after the extraction (Fig. 2B). Once localized, the area of interest is coated by Electron Beam Induced Deposition (EBID), with a platinum layer of 0.5–1 μm (Fig. 2C), in order to protect the sample from the ion beam damage during the milling process.
e) Milling: the area protected by the platinum layer is cross sectioned by the focused gallium ion beam operated at 30 kV and a current range 0.92–2.8 nA (Fig. 2D).
f) Imaging: see point "f" of the above Slice&Mill method (Fig. 2E–G).
g) Serial imaging: see point "g" of the above Slice&Mill method (Fig. 2G).

Tough these techniques were developed using manual controls, involving the presence of an operator that ensures the optimisation of every step, the new generation software "Auto Slice and View" can be used to automate these methods making it easier to obtain a three dimensional data (Xu et al., 2017).

3. Discussion

While the original application of FIB/SEM was mainly related to material science and semiconductor industries, an increasing number of biological applications appeared during the last 10 years. The capability to selectively ablate small areas of the sample, using high-energy ions, combined with the possibility to create images, using both secondary and backscattered electrons, provides excellent results for biological specimens. However, considering that FIB/SEM is a relatively new technique it has been optimized only for a limited number of biological samples, mainly vertebrate tissues and cells. Most of these papers have been recently reported in reviews or book chapters concerning the use of FIB/SEM for the study of biological samples (Kizilyaprak et al., 2014; Peddie and Collinson, 2014; Narayan and Subramaniam, 2015; Titze and Genoud, 2016).

Arthropods, due to their hard exoskeleton, represent a group of animals particularly difficult to be processed and analysed for ultrastructural studies. Besides the problems related to the penetration of fixative and resin (mostly in terrestrial arthropods due to hydrophobic external layers), also the ultramicrotome sectioning represents a complex and critical step. Indeed, it is very common that the ultra-thin sections get fractured and that the sample itself separates from the resin. Moreover, the presence of pollutant and formation of precipitates in the liquids used for rinsing and staining the ultra-thin sections represent other typical problems along with slice loss and blade damage during the ultramicrotome cut. The methods presented here, based on the use of Dual Beam FIB/SEM microscope, allow overcoming most of these technical problems, adding the following new powerful advantages:

a) It is possible to analyse large-volume (up to 10^6 μm^3, see Xu et al., 2017) of three-dimensional samples. The inspection of the sample can be performed by the SEM column with secondary electrons and allows finding the target structure/tissue even if it is very small and rare, as is the case of single sensilla, pores, scales, glands, etc. For example, for a sensillum it is possible to morphologically characterize both the external structure (by the secondary electrons) and the ultrastructure of the nervous cells (by backscattered electrons) (Must et al., 2017). This can be very useful for electrophysiological studies as ideally it could be possible to target the same sensillum of the same arthropod specimen, first to record the electrical data, and then to perform an anatomical characterization.
b) The orientation of sample sectioning (i.e. cross, longitudinal, oblique), can be chosen at will with extreme ease and precision by using the stage control and visualization by secondary electrons before FIB milling.
c) The absence of artefacts related to ultramicrotome sectioning (mechanical damages, loss of sections, specimen detachment).
d) The absence of contaminations due to section staining (Uranyl acetate and Lead citrate precipitates or pollution of distilled water).
e) The milling process can be interrupted at will every few nanometers to take high-resolution pictures of the fresh milled surface using BSE providing a series of sequential images of cellular and subcellular structures.

These methods proved to be extremely useful for the analysis of arthropods but their application should not be limited to these samples, in fact, the Outside-In method could easily be applied to other organisms having a hard cuticle or shell (i.e. molluscs, nematodes, corals, lophophorates), while the Slice&Mill method can be virtually employed for any tissue.

Moreover, the FIB/SEM has been successfully used for the analysis of cuticular parts of sensorial organs to visualise hidden structures in dried insect specimens (Romani et al., 2009; Di Giulio et al., 2012;

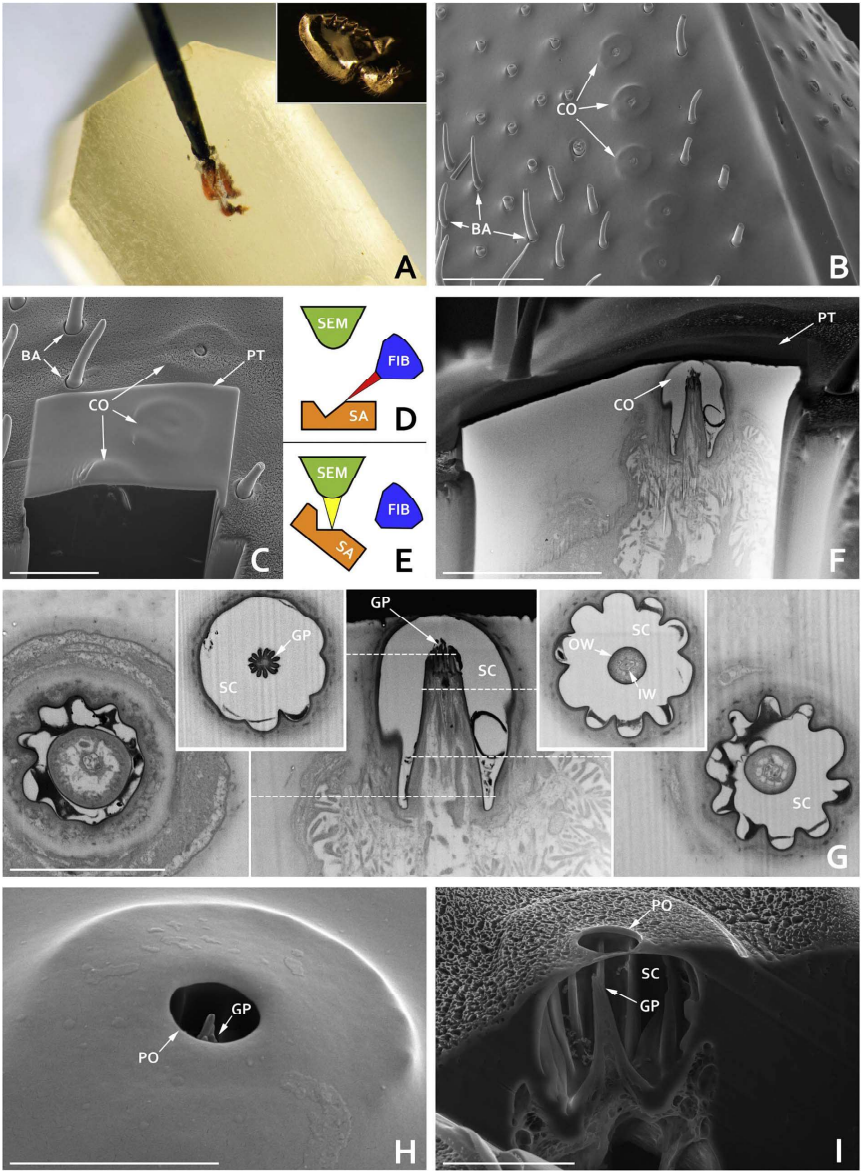

(caption on next page)

Fig. 2. A–G: Outside-In method applied to an antenna of the beetle *Paussus favieri*. A. Extraction from resin block of an embedded antenna. The inset box shows the antenna on a stub after gold sputtering. B. SEM micrograph of the beetle antenna after extraction. Note that, after the extraction, many basiconic sensilla remain intact while the coeloconic sensilla appear filled with resin. C. SEM image showing a coeloconic sensillum protected by a platinum layer and milled by using FIB. D. Schematic representation of ion milling performed at a tilt angle of 0°. E. Illustration of the micrograph acquisition using the BSE detector. Note that, compared to the milling process the stage is tilted by +38°. F. Milled surface observed by backscattered electrons showing the anatomy of a longitudinally sectioned coeloconic sensillum. G. Detail of sensillum in F surrounded by four cross sections of an adjacent coeloconic sensillum. H-I: FIB/SEM application on dried specimens without fixation or inclusion. H. Secondary electron detail of a coeloconic sensillum in a dried specimen of *P. favieri* antenna. I. Milled coeloconic sensillum in H showing the dried internal grooved peg.
Acronyms: BA basiconic sensillum, CO coeloconic sensillum, FIB ion beam, GP grooved peg, IW inner wall, OW outer wall, PO pit orifice, PT platinum layer, SA sample, SEM electron beam, SC sub-cuticular chamber.
Scale bars: B = 40 μm; C = 10 μm; F = 10 μm; G = 5 μm; H = 4 μm; I = 4 μm.

Nagel and Kleineidam 2015; Nurme et al., 2015). We show in Fig. 2(H–I) an example of this application for the visualization of a coeloconic sensillum and its grooved peg.

In the face of numerous advantages, the use of FIB/SEM shows only minor drawbacks related to the destructive nature of the analysis, the resolution limits and the acquisition times needed for obtaining the micrographs that are slower compared to the ones of TEM. In fact, while FIB/SEM micrographs are created using secondary or backscattered electrons, acquiring pixel by pixel in series, TEM pictures are obtained using higher voltages and transmitted electrons, acquiring all the pixels in parallel, so leading to a higher electron flux and subsequently shorter times for the creation of the final picture. Another restriction of FIB/SEM ultrastructural analysis is related to the maximum resolving power of the instrument, in fact, even if perfectly adequate for the analysis of organelles, the lateral resolution of a FIB/SEM is limited to 3 nm and it is definitely inferior to the sub-nanometric resolution of TEM (Peddie and Collinson, 2014). Apart from these small constrains, the results of an ultrastructural analysis performed by a FIB/SEM is effectively comparable to the one of TEM allowing sub cellular investigations including immunohistochemical studies (Sonomura et al., 2013).

In conclusion, the FIB/SEM proved to be a complete laboratory for biological samples, capable not only to overcome the technical pitfalls typical of TEM analysis but also to provide additional capabilities to the ultrastructural analysis at the expense of very small and negligible constrains.

Acknowledgements

We are deeply indebted to Francesco Tatti for his precious technical suggestions. We are grateful to Sandra Moreno for the help in preparing the biological samples, and Daniele De Felicis for the kind availability and technical assistance in the LIME lab. We thank Johan Billen and Francesco Tatti for the critical review of the manuscript. We extend our thanks to three anonymous reviewers who improved the manuscript. The research was possible thanks to the A. Di Giulio research grants (CAL, University Roma Tre, Rome, IT) and the co-funding of the Department of Science of Roma Tre University for the use of LIME electron microscopy facilities.

References

Di Giulio, A., Maurizi, E., Stacconi, M.V.R., Romani, R., 2012. Functional structure of antennal sensilla in the myrmecophilous beetle *Paussus favieri* (Coleoptera, Carabidae, Paussini). Micron 43, 705–719.
Di Giulio, A., Muzzi, M., Romani, R., 2015. Functional anatomy of the explosive defensive system of bombardier beetles (Coleoptera, Carabidae, Brachininae). Arthropod Struct. Dev. 44, 468–490.
Friedrich, F., Matsumura, Y., Pohl, H., Bai, M., Hörnschemeyer, T., Beutel, R.G., 2014. Insect morphology in the age of phylogenomics: innovative techniques and its future role in systematics. Entomol. Sci. 17, 1–24.
Grzywacz, A., Góral, T., Szpila, K., Hall, M.J., 2014. Confocal laser scanning microscopy as a valuable tool in Diptera larval morphology studies. Parasitol. Res. 113, 4297–4302.
Kizilyaprak, C., Daraspe, J., Humbel, B.M., 2014. Focused ion beam scanning electron microscopy in biology. J. Microsc. 254, 109–114.
Lešer, V., Drobne, D., Pipan, Ž., Milani, M., Tatti, F., 2009. Comparison of different preparation methods of biological samples for FIB milling and SEM investigation. J. Microsc. 233, 309–319.
Martín-Vega, D., Simonsen, T.J., Hall, M.J., 2017. Looking into the puparium: Micro-CT visualization of the internal morphological changes during metamorphosis of the blow fly, Calliphora vicina, with the first quantitative analysis of organ development in cyclorrhaphous dipterans. J. Morphol. 278, 629–651.
Medeiros, L.C.S., De Souza, W., Jiao, C., Barrabin, H., Miranda, K., 2012. Visualizing the 3D architecture of multiple erythrocytes infected with plasmodium at nanoscale by focused ion beam-scanning electron microscopy. PLoS One 7, e33445.
Must, A., Merivee, E., Nurme, K., Sibul, I., Muzzi, M., Di Giulio, A., Williams, I., Tooming, E., 2017. Encoding noxious heat by spike bursts of antennal bimodal hygroreceptor (dry) neurons in the carabid *Pterostichus oblongopunctatus*. Cell Tissue Res. 368, 29–46.
Nagel, M., Kleineidam, C.J., 2015. Two cold-sensitive neurons within one sensillum code for different parameters of the thermal environment in the ant *Camponotus rufipes*. Front. Behav. Neurosci. 9, 240.
Narayan, K., Subramaniam, S., 2015. Focused ion beams in biology. Nat. Methods 12, 1021–1031.
Nurme, K., Merivee, E., Must, A., Sibul, I., Muzzi, M., Di Giulio, A., Williams, I., Tooming, E., 2015. Responses of the antennal bimodal hygroreceptor neurons to innocuous and noxious high temperatures in the carabid beetle, *Pterostichus oblongopunctatus*. J. Insect Physiol. 81, 1–13.
Peddie, C.J., Collinson, L.M., 2014. Exploring the third dimension: volume electron microscopy comes of age. Micron 61, 9–19.
Pohl, H., Wipfler, B., Grimaldi, D., Beckmann, F., Beutel, R.G., 2010. Reconstructing the anatomy of the 42-million-year-old fossil† Mengeatertiaria (Insecta, Strepsiptera). Naturwissenschaften 97, 855–859.
Romani, R., Stacconi, M.V.R., Riolo, P., Isidoro, N., 2009. The sensory structures of the antennal flagellum in *Hyalesthes obsoletus* (Hemiptera: Fulgoromorpha: Cixiidae): a functional reduction? Arthropod Struct. Dev. 38, 473–483.
Simonsen, T.J., Kitching, I.J., 2014. Virtual dissections through micro-CT scanning: a method for non-destructive genitalia 'dissections' of valuable Lepidoptera material. Syst. Entomol. 39, 606–618.
Smolla, M., Ruchty, M., Nagel, M., Kleineidam, C.J., 2014. Clearing pigmented insect cuticle to investigate small insects' organs in situ using confocal laser-scanning microscopy (CLSM). Arthropod Struct. Dev. 43, 175–181.
Sonomura, T., Furuta, T., Nakatani, I., Yamamoto, Y., Unzai, T., Matsuda, W., Iwai, H., Yamanaka, A., Uemura, M., Kaneko, T., 2013. Correlative analysis of immunoreactivity in confocal laser-scanning microscopy and scanning electron microscopy with focused ion beam milling. Front. Neural Circuits 7.
Tafforeau, P., Boistel, R., Boller, E., Bravin, A., Brunet, M., Chaimanee, Y., Cloetens, P., Feist, M., Hoszowska, J., Jaeger, J.J., Kay, R.F., Lazzari, V., Marivaux, L., Nel, A., Nemoz, C., Thibault, X., Vignaud, P., Zabler, S., 2006. Applications of X-ray synchrotron microtomography for non-destructive 3D studies of paleontological specimens. Appl. Phys. A 83, 195–202.
Takemura, S.Y., Xu, C.S., Lu, Z., Rivlin, P.K., Parag, T., Olbris, D.J., Plaza, S., Zhao, T., Katz, W.T., Umayam, L., Weaver, C., Hess, H.F., Horne, J.A., Nunez-Iglesias, J., Aniceto, R., Chang, L., Lauchie, S., Nasca, A., Ogundeyi, O., Sigmund, C., Takemura, S., Tran, J., Langille, C., Le Lacheur, K., Mclin, S., Shinomiya, A., Chklovskii, D., Meinertzhagen, I.A., Weaver, C., 2015. Synaptic circuits and their variations within different columns in the visual system of *Drosophila*. Proc. Natl. Acad. Sci. U. S. A. 112, 13711–13716.
Tamada, H., Kiryu-Seo, S., Hosokawa, H., Ohta, K., Ishihara, N., Nomura, M., Mihara, K., Nakamura, K.I., Kiyama, H., 2017. Three-dimensional analysis of somatic mitochondrial dynamics in fission-deficient injured motor neurons using FIB/SEM. J. Comp. Neurol. 525, 2535–2548.
Titze, B., Genoud, C., 2016. Volume scanning electron microscopy for imaging biological ultrastructure. Biol. Cell 108, 307–323.
Villinger, C., Gregorius, H., Kranz, C., Höhn, K., Münzberg, C., von Wichert, G., Mizaikoff, B., Wanner, G., Walther, P., 2012. FIB/SEM tomography with TEM-like resolution for 3D imaging of high-pressure frozen cells. Histochem. Cell Biol. 138, 549–556.
Wei, D., Jacobs, S., Modla, S., Zhang, S., Young, C.L., Cirino, R., Caplan, J., Czymmek, K., 2012. High-resolution three-dimensional reconstruction of a whole yeast cell using focused-ion beam scanning electron microscopy. BioTechniques 53, 41.
Xu, C.S., Hayworth, K.J., Lu, Z., Grob, P., Hassan, A.M., García-Cerdán, J.G., Niyogi, K.K., Nogales, E., Weinberg, R.J., Hess, H.F., 2017. Enhanced FIB-SEM systems for large-volume 3D imaging. Elife 6.

Arthropod Structure & Development 44 (2015) 468–490

Contents lists available at ScienceDirect

Arthropod Structure & Development

journal homepage: www.elsevier.com/locate/asd

Functional anatomy of the explosive defensive system of bombardier beetles (Coleoptera, Carabidae, Brachininae)

Andrea Di Giulio [a, *], Maurizio Muzzi [a], Roberto Romani [b]

[a] Department of Science, University Roma Tre, Viale G. Marconi, 446, 00146 Roma, Italy
[b] Department of Agricultural, Food and Environmental Sciences, University of Perugia, Borgo XX Giugno 74, 06121 Perugia, Italy

ARTICLE INFO

Keywords:
Bombardier beetles
Brachininae
Brachinus
Pheropsophus
Aptinus
Explosive glands
FIB/SEM
Ultrastructure
Pygidial glands
Carabidae

ABSTRACT

This paper provides the first comparative anatomical study of the explosive pygidial defensive system of bombardier beetles in species classified in three brachinine subtribes: *Brachinus* (Brachinina), *Pheropsophus* (Pheropsophina) and *Aptinus* (Aptinina). We investigated the morphology and ultrastructure of this system using optical, fluorescence, and focused ion beam (FIB/SEM) microscopy. In doing so, we characterized and comparatively discussed: (1) the ultrastructure of the gland tissues producing hydroquinones and hydrogen peroxide (secretory lobes), and those producing catalases and peroxidases (accessory glands); (2) the complex anatomy of the collecting duct; (3) the arrangement of the muscular bundles and the folding of the cuticle of the reservoir, suggesting a functional division of this chamber (dynamic part and storage part); (4) the great structural diversity of sculpticles inside the reaction chamber, where we could recognize six main types of microsculpture located in specific districts of the chamber. Additionally, using fluorescence microscopy, we highlighted the presence of resilin in two structures strongly subjected to mechanical stress during the discharge, the valve and the turrets of the reaction chamber. The results of this paper give a solid anatomic overview of the most popular beetle defensive system, contributing to the debate on its evolution within the Carabidae.

1. Introduction

The Brachininae, commonly known as “bombardier beetles,” have the remarkable ability to explosively discharge hot quinones from glandular openings near their abdominal tip (Eisner, 1958; Dean, 1980a,b; Eisner and Aneshansley, 1999). This derived system represents an extreme specialization of the simple (non-explosive) paired pygidial defensive glands found in all Adephaga (Forsyth, 1968, 1970, 1972; Balestrazzi et al., 1985; Bonacci et al., 2011), each of which is composed of secretory cells, a collecting duct and a reservoir chamber. The defensive gland system of bombardier beetles is unique in having a second, highly sclerotized chamber known as the reaction chamber, which is separated from the reservoir chamber by a one-way valve. The reaction chamber is also associated with secretory cells, which produce catalases and peroxidases that are stored in the reaction chamber. When bombardier beetles are disturbed muscles surrounding the reservoir chamber contract, allowing the hydroquinones and hydrogen peroxide, which are stored in the reservoir chamber, to pass through the one-way valve and enter the reaction chamber and mix with catalases and peroxidases. This results in an explosive exothermic reaction, producing benzoquinones, free oxygen, water and heat up to 100 °C (Schildknecht and Holoubek, 1961; Schildknecht et al., 1968, 1970; Aneshansley et al., 1969), accompanied by a characteristic popping sound.

Only one other group of carabid beetles is capable of such remarkable defense. These are members of ground beetle subfamily Paussinae, commonly known as the “flanged bombardier beetles”, so named for their unique subapical elytral fold (flange of Coanda), which they use to direct their spray (Eisner and Aneshansley, 1982). The striking similarities between the defensive systems of the Brachininae and the Paussinae, including the sclerotized reaction chamber and the nature of the chemicals themselves, have been stressed in the past by several authors (Eisner et al., 1977, 1989, 1991, 2000). In fact in both groups the secretory cells produce hydroquinones, hydrogen peroxide and various hydrocarbons such as alkanes, alkenes and alkadienes

* Corresponding author.
E-mail addresses: andrea.digiulio@uniroma3.it, digiulio@uniroma3.it (A. Di Giulio).

http://dx.doi.org/10.1016/j.asd.2015.08.013
1467-8039/

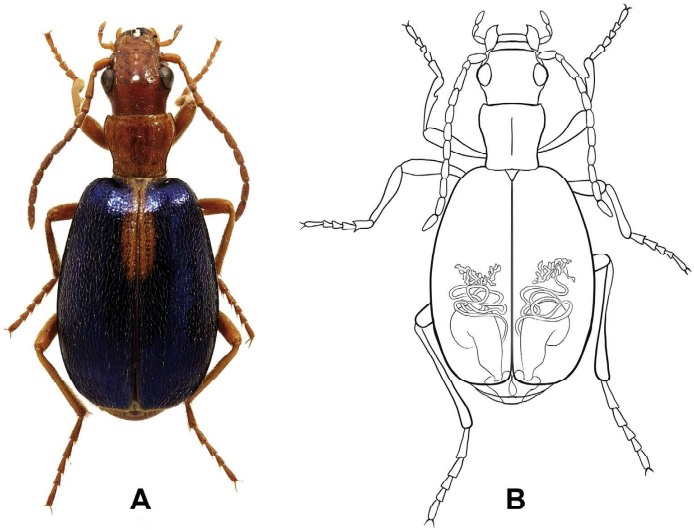

Fig. 1. Localization of the pygidial defensive system in a representative brachinine bombardier beetle. A. Habitus of *Brachinus sclopeta*. B. Schematic line drawing of the same species with defensive system outlined.

(Eisner et al., 2000). However, the phylogenetic relationship between the Brachininae and the Paussinae remains unclear (Maddison et al., 1999; Eisner et al., 2000, 2001), and it is possible that these two lineages of bombardier beetles are products of convergent evolution, or it is also possible that they represent each other's sister groups.

It is remarkable that no other animal is capable of sustaining a hot explosion inside its body and that one of the substances essential for the reaction is hydrogen peroxide, a potent cytotoxin.

The effectiveness of the Brachininae defensive system against both vertebrate and invertebrate predators is also related to the precise aiming of the spray. These beetles are, in fact, capable of

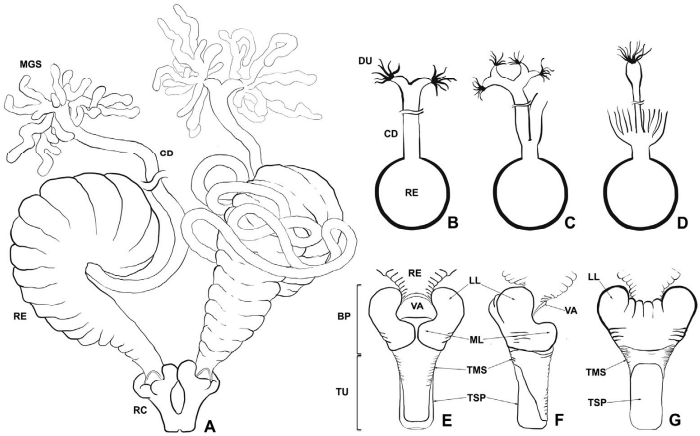

Fig. 2. Line drawings of the pygidial defensive system in a generalized brachinine. A. Pygidial defensive system in dorsal view, showing the main components and their relative position. B–D. Main different types of collecting system found in brachinines: *Brachinus* type (B), *Aptinus* type (C), *Pheropsophus* type (D). E–G. Reaction chamber showing the external structure from dorsal (E), right lateral (F), and ventral (G) views. *BP* basal part, *CD* collecting duct, *DU* ductule, *LL* lateral lobe, *MGS* multilobed glandular system, *ML* medial lobe, *RE* reservoir, *RC* reaction chamber, *TMS* turret membranous sheath, *TSP* turret sclerotised plate, *TU* turret, *VA* valve.

hitting a target at long distance, thanks to the great mobility of their abdominal tip, and to the speed at which the chemical spray is ejected (Schildknecht and Holoubek, 1961; Dean, 1980b; Eisner et al., 2006).

The exceptional nature of this explosive defensive system has long attracted the attention of generations of scientists and has been repeatedly studied as a biomimetic model for human applications (Beheshti and McIntosh, 2007; Lai, 2010; Booth et al., 2012).

The first publication on the structure of Brachinine defensive system dates back to the nineteenth century (Dierckx, 1899). But it was not until the 1960–70s that interest in bombardier beetles reached its peak, with the remarkable contributions of several authors (Eisner, 1958; Aneshansley et al., 1969; Schildknecht, 1970; Forsyth, 1972; Eisner et al., 1977). Most of the early investigations were focused on the chemical and functional aspects of the system, while only little attention was paid to the fine morphology of the components (Forsyth, 1972; Eisner et al., 2000, 2001; Arndt et al., 2015), and their ultrastructure was not studied with the only exception of the secretory cells of *Brachinus crepitans* (Schnepf et al., 1969). In fact, the majority of the available information was obtained by optical microscopy (Forsyth, 1972), while the SEM was only occasionally used as a tool to illustrate single aspects of the system in papers dealing with either understanding the chemistry or the functional morphology of the system (Eisner et al., 2000, 2001).

In this paper we provide the first detailed comparative study of the fine morphology and ultrastructure of the pygidial defensive gland systems of several lineages of Brachininae, including *Brachinus* (Brachinina), *Pheropsophus* (Pheropsophina) and *Aptinus* (Aptinina), integrating contributions of different microscopic techniques. Histology and optical microscopy were used to study the general structure of the system and the organization of tissues; while scanning electron microscopy (SEM) combined with focused ion beam microscopy (FIB) was used to characterize the ultrastructural details of the system. In this study the FIB/SEM microscopy replaced the traditional use of transmission electron microscopy (TEM) thanks to the possibility to obtain complete section series of single structures. Additionally, fluorescence microscopy was used to check for the presence of resilin (Neff et al., 2000; Michels and Gorb, 2012) at the level of the valve and other cuticular structures subject to repeated mechanical stress.

2. Materials and methods

2.1. Material examined

This study is based on the analysis of *Brachinus sclopeta* (25 specimens, from Latium, central Italy; Fig. 1A), *Brachinus elongatulus* (6 specimens, from Arizona, USA), *Pheropsophus hispanus* (2 specimens, from Morocco), *Pheropsophus occipitalis* (10 specimens, from China) *Pheropsophus africanus* (2 specimens, from Morocco), *P.* sp. (2 from China), *Aptinus bombarda* (3 specimens, from Slovenia) and *Aptinus creticus* (2 specimens from Turkey). The material is preserved in the A. Di Giulio collection (Rome, Italy).

2.2. Dissections

Dried specimens were examined with a streomicroscope (Olympus SZX16), dissections were made as follows: (1) dried beetles were rehydrated by boiling them in distilled H_2O for a few minutes (the time to properly hydrate the specimen is based on body size); (2) the abdomen was removed and transferred to an aqueous solution of 10–15% KOH (at 50 °C) or in Pancreatin solution (at 36 °C, see Alvarez-Padilla and Hormiga, 2007) for a time sufficient to properly digest the specimen based on size; (3) the cleared abdomen was rinsed three times in dH_2O and the different parts of the system were isolated, stained in Chlorazol Black for 1 h (in order to visualize the unsclerotized cuticular parts) and rinsed again; (4) the parts were dehydrated in a graded series of EtOH solutions, from 20% to 100%, and (5) mounted on slides with Euparal for the study with a light microscope (Olympus BX51). In order to rehydrate specimens preserved in 75% or 100% EtOH for dissections, we rehydrated them slowly, placing them in cold distilled H_2O, but all other steps of the procedure were the same as described above.

2.3. Histology

For the histological analysis 6 specimens (3 males and 3 females) of *Brachinus sclopeta* and 2 *Brachinus elongatulus* (1 male and 1 female) were anesthetized with CO_2, fixed with Bouin's solution, dehydrated in a graded ethanol series, and embedded in paraffin. 5–7 μm thick serial sections were obtained by rotary microtome and were stained with haematoxylin and eosin.

Sections were observed using the light microscope Olympus BX51 and photographed with the 5 megapixel digital camera Olympus ColorView II.

2.4. Focused ion beam/scanning electron microscope (FIB/SEM)

The gland systems of bombardier beetles were analyzed with the Dualbeam (FIB/SEM) Helios Nanolab (FEI Company, Eindhoven, The Netherlands) at the L.I.M.E. (Roma Tre University, Rome, Italy). The FIB/SEM is equipped with two columns including one electron beam (SEM column) and one ion beam (FIB column), oriented at 52°, and focused on the same point of the sample. This apparatus is capable of selectively ablating (milling process) a previously marked region of the sample by using a focused ion current from a gallium source. The milling process can be interrupted every few nanometers to take high-resolution images of the cross sections by the SEM column.

This instrument was used for (1) obtaining high-resolution SEM images of the cuticular components of the defensive system and for (2) analyzing the ultrastructure of the glandular tissues of the defensive system from abdomens previously fixed and embedded in epoxy resin.

For high resolution SEM images the different structures of the defensive system (dissected following the procedure illustrated in paragraph 2.2) were dehydrated to 100% EtOH by passing through a graded ethanol series, critical point-dried in a Balzer Union CPD 030 unit, gold coated in an Emitech K550 unit, and finally examined by using the field emission SEM column of the dualbeam FIB/SEM, with secondary electrons (SE) and an operating voltage of 5 kV.

For FIB ultrastructural analysis of the pygidial defensive system embedded in Epon–Araldite resin we followed a procedure similar to the one normally used for TEM preparation (Di Giulio et al., 2012). The specimens were CO_2 anesthetized and immediately immersed in a solution of 5% glutaraldehyde and 2.5% paraformaldehyde in cacodylate buffer +5% sucrose, pH 7.2–7.3. The abdomens were promptly removed, cut longitudinally in two halves to improve penetration, and held in the fixative for 2 h at 4 °C. They were then rinsed overnight in cacodylate buffer, post-fixed in 1% osmium tetroxide for 1 h at 4 °C and rinsed in a cacodylate buffer. Samples were en bloc stained with 2% aqueous uranyl acetate for about 2 h at 4 °C and dehydrated in a graded ethanol series followed by embedding in Epon–Araldite with propylene oxide as a bridging solvent. Thick sequential slices of about 15–20 μm were cut with a glass knife on a Leica Ultracut T ultramicrotome, and mounted on stubs with self-adhesive carbon disks. Slices containing glandular tissues were gold coated in an Emitech K550 unit and analyzed with FIB/SEM. Glandular tissues present on

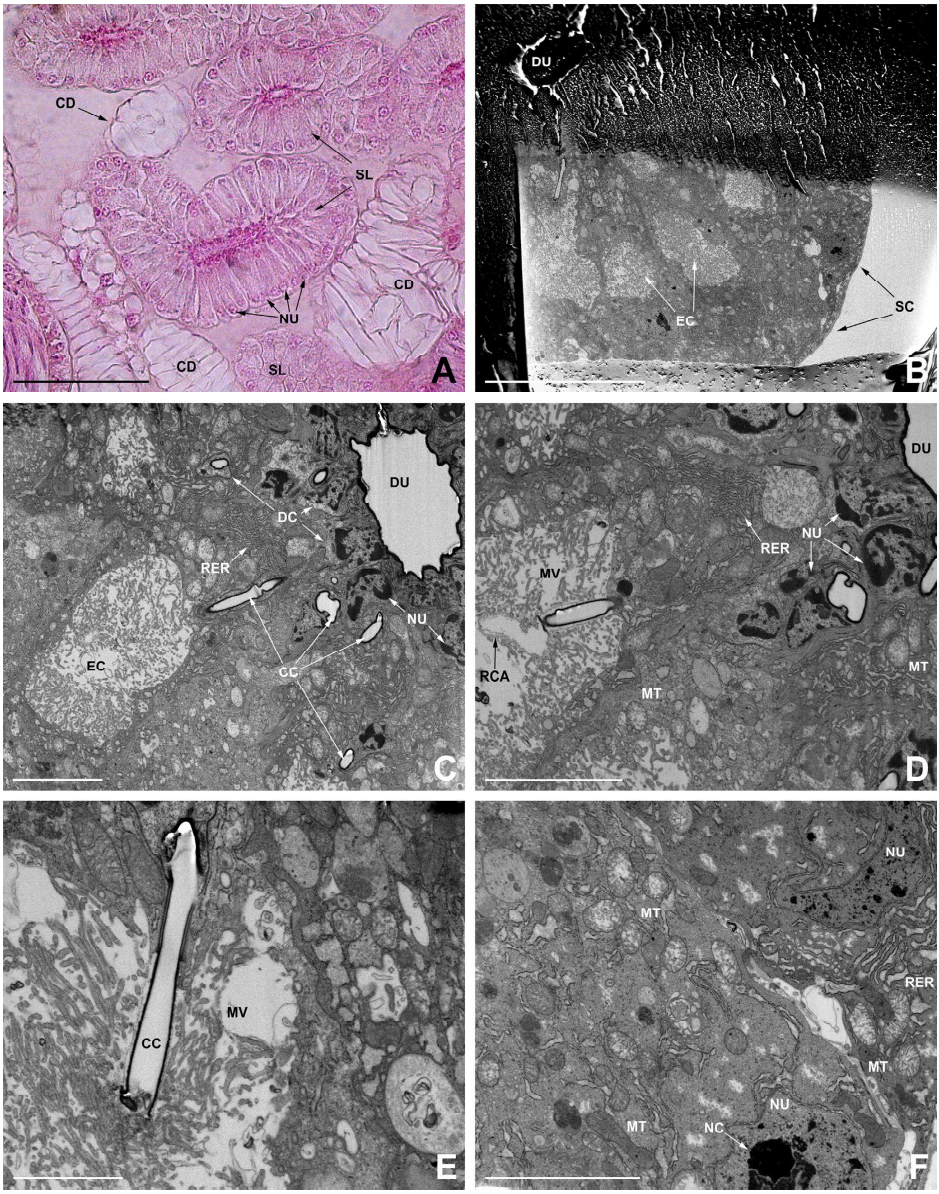

Fig. 3. Secretory lobes anatomy. A. Histological section of *Brachinus sclopeta* showing several secretory lobes; note the tight packing of the secretory cells and the peripheral position of the nuclei. B–F. FIB/SEM analysis of one, cross sectioned secretory lobe of *B. elongatulus*, showing the anatomy of several secretory cells, duct cells and ductules at different magnifications; note the great amount of heterochromatin inside the duct cell nuclei. *CC* conducting canal, *CD* collecting duct, *DC* duct cell, *DU* ductule, *EC* extracellular cavity, *MT* mitochondrion, *MV* microvilli, NC nucleolus, NU nucleus, *SC* secretory cell, *SL* secretory lobe, *RER* rough endoplasmic reticulum. Scale bars: A = 50 μm; B = 20 μm; C = 5 μm; D = 5 μm; E = 2 μm; F = 4 μm.

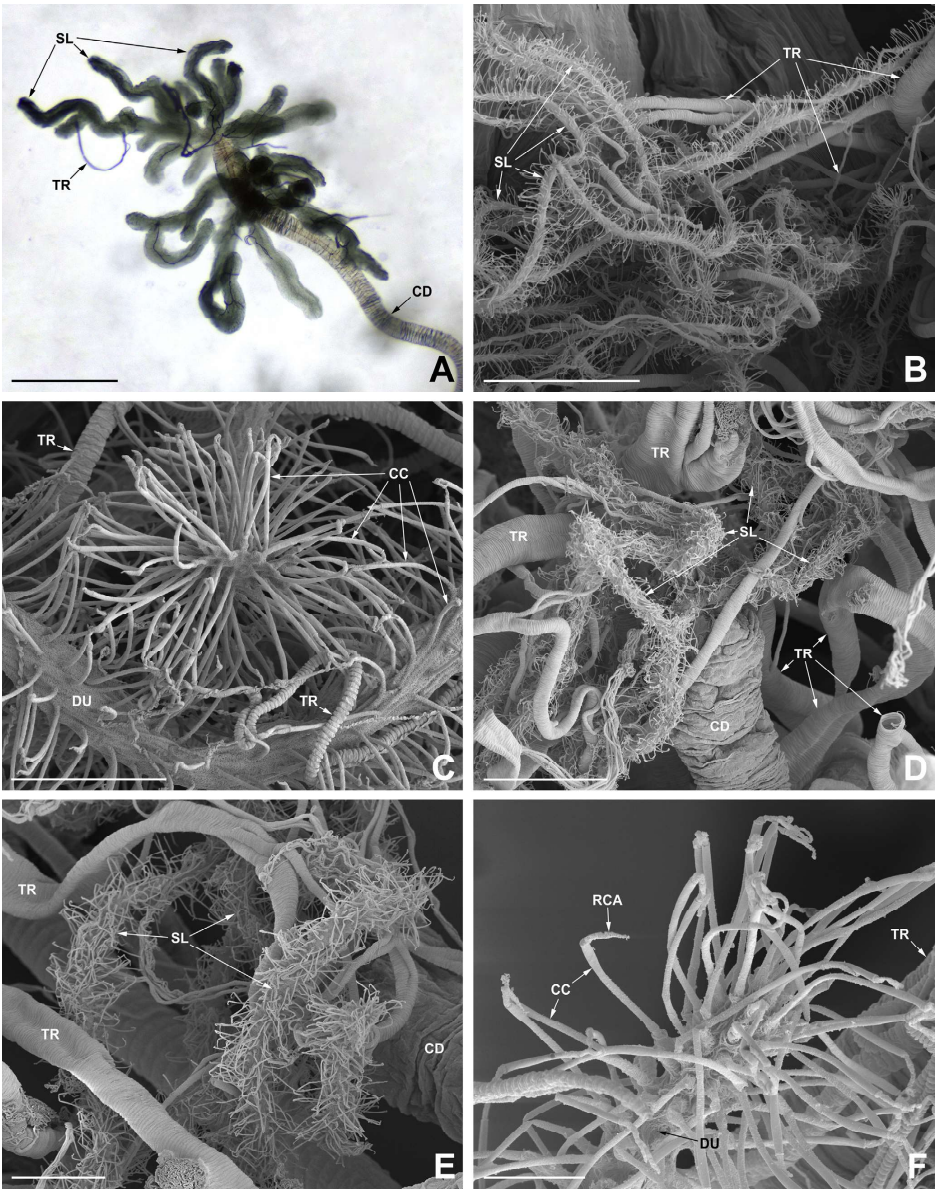

Fig. 4. Secretory lobes structure. A. Secretory lobe of *Brachinus sclopeta* freshly dissected after chlorazol black staining. B–F. Secretory lobes of brachinines after KOH digestion. B. Several secretory lobes of *B. elongatulus* tangled with tracheae. C. Apex of a secretory lobe of *B. elongatulus* showing the different arrangement of the conducting canals around the ductule: crowded and radial at the apex and regularly spaced and transversal along the trunk. D–E. Insertion of the secretory lobes into the collecting duct in *Pheropsophus occipitalis*. F. Close-up of a conducting canal of *P. occipitalis*, showing the cuticular part of the receiving canals of the duct cells. *CC* conducting canals, *CD* collecting duct, *DU* ductule, *RCA* receiving canal, *SL* secretory lobes, *TR* tracheae. Scale bars: A = 250 μm; B = 100 μm; C = 20 μm; D = 100 μm; E = 50 μm; F = 10 μm.

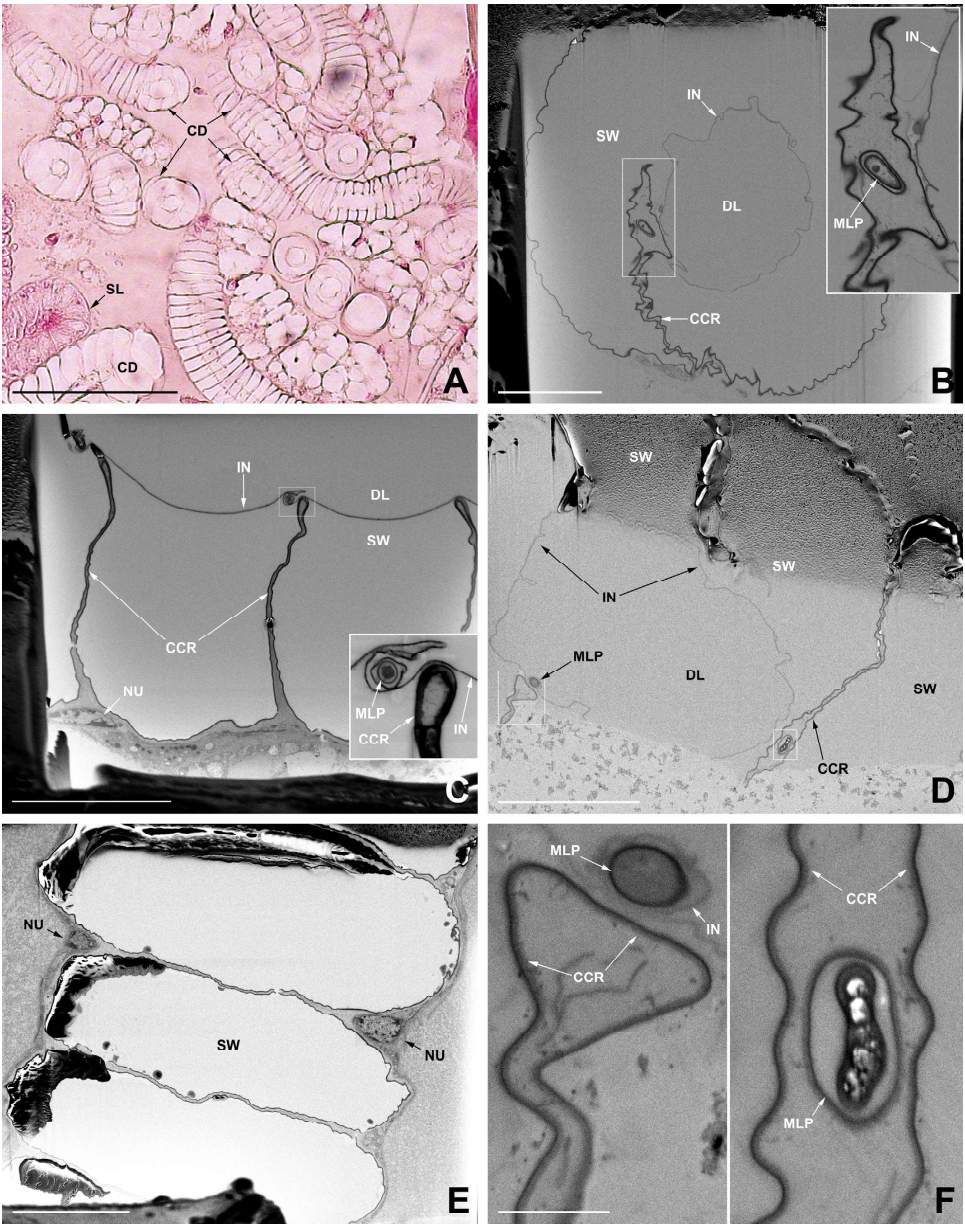

Fig. 5. Collecting duct anatomy. A. Histological section of *Brachinus sclopeta* showing the collecting duct knot, cut at different levels and with different orientations. B–F. FIB/SEM sectioning of the brachinine collecting duct. B. Cross section of *Pheropsophus hispanus* collecting duct; the lateral box shows a close-up of a match-like projection, covered by the

each thick slice were cross sectioned approximately every 100 nm of milling (horizontal feed) by the focused gallium ion beam (FIB) operating at 30 kV and 0.92 nA; SEM pictures were taken by using backscattered electrons (BSE) and a through-the-lens (TDL) detector with an operating voltage of 2 kV, a working distance of 2 mm, and an applied current of 0.17 nA.

2.5. Fluorescence microscopy

Resilin, an elastomeric protein that shows autofluorescense, was visualized using fluorescence microscopy. Slide mounted slices prepared for the histological analysis (see paragraph 2.3) of *Brachinus sclopeta* were observed using either a Olympus BX51 microscope with a DAPI filter (excitation 340–380 nm, 420 nm longpass emission filter). Resilin appears in blue color under UV excitation (Neff et al., 2000; Michels and Gorb, 2012). Images were captured with a Leica digital camera.

2.6. Acronyms

AE: aedeagus; AF: alveolate floor; AG: accessory gland; AGI: accessory gland insertion; AGO: accessory gland opening; AM: addressing muscles; BP basal part; BRS: branched spines; BS: bumped surface; CC: conducting canal; CCR: cuticular crista; CD: collecting duct; CDT: collecting duct trunk; CL: cuticular layers; CS: collecting system; DC: duct cell; DL: duct lumen; DO: duct opening; DRE: dynamic reservoir; DU: ductule; EC: extracellular cavity; FS: flattened spines; GO: gonostylus; HC: heterochromatin; HG: hindgut; HW: haired walls; IN: intima; LL: lateral lobe; MGS: multilobed glandular structure; ML: medial lobe; MLP: match-like projection; MP: multi-perforated plate; MS: membranous strip; MT: mitochondrion; MV: microvilli; NC: nucleolous; NU: nucleus; PS: particulate secretion; RC: reaction chamber; RCA: receiving canal; RCL: reaction chamber lumen; RE: reservoir; RER: rough endoplasmic reticulum; RF: reservoir fold; RM: reservoir muscles; SC: secretory cell; SH: spiny hairs; SL: secretory lobe; SPH: spherule; SPL: spiny lobes; SPN: spinule; SRE: storage reservoir; SW: spiralled wall; TMS: turret membranous sheath; TR: tracheae; TSP: turret sclerotized plate TU: turret; VA: valve; VDL: valve dorsal layer; VM: valvular muscles; VVL: valve ventral layer.

3. Results

3.1. General structure of the defensive system of Brachinini

As in all Adephaga, the defensive system (Figs. 1B and 2A) is composed of two, independent glandular systems, positioned laterally in the distal half of the abdomen, flanking the hindgut. Each system is a functional unit, composed of a multilobed system of secretory cells connected to one long, tangled collecting duct, which is attached to a voluminous reservoir chamber; a valve separates the reservoir chamber from a strongly sclerotized, funnel-shaped reaction chamber (Fig. 2E–G) which is surrounded by many elongate accessory glands, and followed by a system for discharging the spray. The general structure of the system (Fig. 2A) is very similar in different brachinine genera and, other than having different relative dimensions, there are only a few small differences concerning the structure of the reservoir, the branching of the collecting duct (Fig. 2B–D) and the number of the secretory lobes.

In the following, a detailed comparative description for each functional structure is given at a gross, fine and ultrastructural level.

3.2. Secretory lobes (SL)

Each glandular system is represented by several elongate secretory lobes (SL) (Figs. 3 and 4). SEM investigations of cleared specimens revealed that each SL is composed of one blind-ended cuticular ductule (DU) (Fig. 4C); ductules from the same glandular system are somewhat packed and intertwined one another (Figs. 3A and 4A–B), and converge altogether into the CD (Fig. 4A–D). The number and length of the ducts vary among different genera and species, being higher in larger bodied species, while their diameter remains almost constant (about 40 μm). Each ductule receives secretions from many secretory units, which are composed of two types of cells, a secretory cell and a medial duct cell (Fig. 3). Secretory cells are located externally and have a conical shape (Fig. 3A–B). The cytoplasm contains abundant mitochondria, vesicles and regions of rough endoplasmic reticulum (Fig. 3D–F). The rounded nucleus is located on the periphery of the cell body (Fig. 3A–B) and includes an evident nucleolus. The apical part of the secretory cell is organized in a wide extracellular cavity (EC) filled with hundreds of microtubules (Fig. 3B–E), which appear irregularly twisted and converge with one another medially towards the receiving canal of the duct cell. The duct cell (DC) is quite short (about 20 μm) and contains only a little cytoplasm, and a heterochromatic nucleus positioned medially and close to the tubule wall (Fig. 3C–D). Each conducting canal (CC) enters the secretory cell inside the extracellular cavity (Fig. 3C–E), and receives the secretions at the level of the multi-perforated, irregular, receiving canal (RCA) (Fig. 3D). The RCA is attached to a linear, thin CC, which inserts radially into the ductule (DU) (Figs. 3C, E and 4C, F). All CCs are equally spaced along and around the DU, except at the DU apex, where they are distinctly and tightly crowded (Fig. 4C, F). The surface of the CC appears smooth at SEM (Fig. 4F), while that of the DUs seems irregularly rough (Fig. 4C, F).

3.3. Collecting system (CS)

The collecting system (CS) (Figs. 5 and 6) is composed of one long collecting duct (CD), connecting the secretory lobes (SL) to the reservoir chamber (RE). The CD branches distally into the blind-ended DUs inside the SLs, that receive the secretions from the CCs of the glandular units (Figs. 4A, D and 6A).

The CD is generally represented by an extraordinarily long corrugated cuticular tube (Figs. 5A and 6A–B), longer than the entire insect, twisted on itself, tangled with a finely branched tracheal system and the malpighian tubules, and in close association with the hind gut.

We identify the following main parts of the CD, each of which has different structural arrangements in the species and genera examined (Fig. 2A–D).

thin intima and invaginated into the cuticular crista of the duct cell. C. Longitudinal section of *Brachinus elongatulus* collecting duct showing three cuticular cristae and the peripheral duct cell; the lateral box shows a close-up of a match-like projection entering the cuticular intima. D. Oblique, peripheral section of *P. hispanus* collecting duct. E. Longitudinal peripheral section of *B. elongatulus* collecting duct made at the level of the spiralled wall; note the thin layer of duct cells with their almost empty cytoplasm filling the narrow space among the cuticular cristae of the spiralled wall. F. Close-ups of the two boxes of D, showing match-like projections entering the cuticular intima before (left picture) and after (right picture) insinuating into the cuticular cristae. *CCR* cuticular crista, *CD* collecting duct, *DL* duct lumen, *IN* intima, *MLP* match-like projection, *NU* nucleus, *SL* secretory lobe, *SW* spiralled wall. Scale bars: A = 100 μm; B = 10 μm; C = 10 μm; D = 10 μm; E = 10 μm; F = 1 μm.

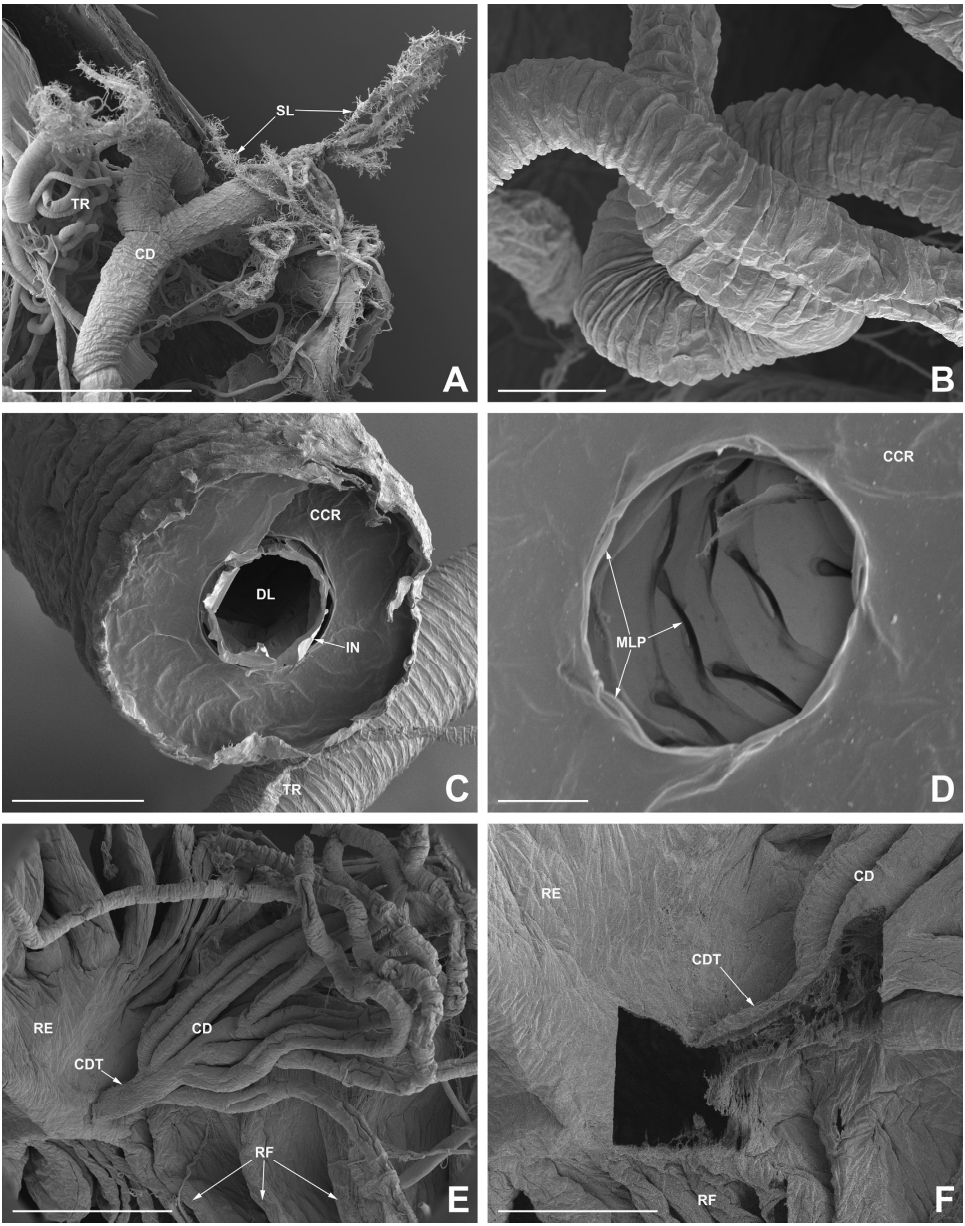

Fig. 6. Collecting duct fine structure. A. Apical part of the collecting duct of *Aptinus bombarda*, showing the peculiar branching of this duct at the level of the secretory lobes. B. Collecting duct of *B. sclopeta*, external structure. C. Cross section of *Pheropsophus occipitalis* collecting duct, showing the spiralled wall of cuticular cristae. D. Close-up of the

1. basal part, the thicker part of the CD, at the level of the RE;
2. medial part, usually constant in diameter, represented by the main duct length;
3. distal part, subapical part of the CD, thinner than medial part, at the level of the SL;
4. apical part, just before connection with the DUs.

In *Brachinus* spp. the CD is simple (see Fig. 2B) with the exception of the bilobed apical part. In *Aptinus* the basal part CD can be simple (*A. bombarda*) or divided into two branches (*A. creticus*); the distal part is always divided into two thin apically bifurcate branches, (Fig. 2C). In the genus *Pheropsophus* the CD is basally divided into 8 (*P. africanus*), 12 (*P. occipitalis* and *P.* sp. from China) or 16 (*P. hispanus*) equally long branches (Fig. 6E); each branch is apically undivided and bulged (Fig. 2D).

The SLs are always separate from, and not tangled with the CD. The DUs, usually single or bilobed apically, are arranged in clusters of 10–15 that converge at the apical part of the CD.

The diameter of the CD, though slightly irregular, is quite constant in both, the species with an undivided CD and those with branched CD; in fact the diameter of the CD in species with a simple, basally undivided duct is similar to the diameter of each branch of the CD in species with a basal division.

In all species examined the CD attaches to the medial wall of the RE (Fig. 7A, C); where the CD is not only in contiguity with the RE wall, but a small portion of the tube enters inside the reservoir lumen. Here the internal wall of the CD is organized in a dense net that is the result of the overlapping of multiple cuticular spiculae (Fig. 6F). Contrary to the irregularly furrowed surface of the DUs, the surface of the CD is regularly corrugated (Fig. 6B) as a result of the cellular structure of the tube. In cross section the CD appears to be composed of a single layer of modified epidermal cells (Fig. 5C, E). These cells have only little cytoplasm and a flattened nucleus containing electron-dense clumps of heterochromatin. Each cell has (toward the lumen of the CD) a thin, electrondense epicuticular layer (Fig. 5B–F). In longitudinal section, the cuticle forms an elongated arm ending in a small bulged apex (Fig. 5C). Cross sections of the CD reveal that cells are positioned such that they form a continuous, radially arranged ring, which spirals around the lumen of the CD (Fig. 5D). Contiguous cells produce cuticular cristae which are deeply invaginated into the lumen of the CD (Fig. 5C–E). The arms of adjacent cells define apparently empty chambers (Fig. 5B, E). This wall extends along the entire length of the CD and forms a continuously spiralled barrier that insulates the CD from the hemolymph. The internal lumen of the CD is lined by a thin layer of cuticular intima (Figs. 5B–D and 6C), which separates the lumen from the CD cells. At regular intervals, the internal cristae (Figs. 5B–F and 6C) are transformed into curved projections that, due to their basal stick and their wider, suboval “head”, resemble the shape of a match (Figs. 5B–D, F and 6D). These “match-like” projections attach the intima to the cuticular wall of the CD (Fig. 6D). The internal lumen of the CD is filled with a slightly electrondense secretion (Fig. 5B).

3.4. Reservoir (RE)

The reservoir chamber (RE) is tubular, strongly curved, multifolded, bellows-like (Fig. 7B–E). It is composed of a thin cuticular layer (Fig. 7F), which is internally smooth and externally covered by a complex muscular sheath (Fig. 7A). The number of folds of the RE varies widely among genera and species, with the largest species *Pheropsophus* showing the highest number of folds, which are also deeper than observed in other species (Fig. 7E–F). The only two openings of the RE are: (1) a small entrance opening, represented by the basal part of CD (Fig. 7A), which fills the RE with hydrogen peroxide and hydroquinones; and (2) a wider opening into the RC which allows the passage of the stored chemicals when permitted by a complex cuticular valve (VA) (Figs. 7A and 8). The insertion point of the CD is positioned almost in the middle (Fig. 7A) of the tubular RE and represents the boundary level between two functional parts (Fig. 7A–D): the distal part and the basal part. The distal part is shorter and wider, strongly bent downward, and blind ending: this represents the storage compartment. The basal part is longer and narrower, ending at the valve, and represents the more active dynamic compartment. The basal part has a higher number of regularly spaced folds (Fig. 7C–D). The compression of the two compartments is regulated by different sets of muscles (Fig. 7A): the storage compartment is surrounded by a complex muscular sheath, composed of irregularly oriented fibers, including short longitudinal fibers attached between adjacent folds; the dynamic compartment is controlled by two dorsolateral, longitudinal bundles of fibers distally attached to the dorsal layer of the VA, external to the valve muscles.

3.5. Valve (VA)

A cuticular valve (VA) (Fig. 8) regulates the flow of fluids from the RE into the RC. It is responsible of the physical separation of the chemical reacting substances (hydroquinones + hydrogen peroxide + hydrocarbons in the RE, and catalases + peroxidases in the RC) in two compartments. The VA is a complex structure, connected to the basal part of the RE wall (Figs. 7A and 8D). It is composed of a dorsal and ventral layer of cuticle (Fig. 8A–B, E–F), tightly overlapping when in repose: (1) the dorsal layer is a semicircular plate, with a heavily sclerotized rounded margin and appearing as a curved, flexible bar in transverse section (Fig. 8A); (2) the ventral layer is composed of a very thin flap, without heavy sclerotization. Two wide, short and broadly arched bundles of muscles (Figs. 7A and 8A–C) open and close the valve. Fibers of each bundle insert distally on the RE and proximally on sides of dorsal layer of VA; contraction of these curved muscles cause the dorsal layer of the VA to rise, thereby opening the valve. The fluorescence analysis (Fig. 8B) of the histological slices of *Brachinus sclopeta* shows the presence of resilin at the level of the thin ventral layer of the VA.

The structure of the VA is identical in all examined species, and it is also very similar to the valvular structure present in the pygidial defensive system of the other Carabidae.

3.6. Reaction chamber (RC)

The reaction chamber (RC) is a funnel-shaped structure (Figs. 2E–G and 9), basally widened, and distally narrowed toward the abdominal apex. The RC has two main parts (Fig. 9C–D): a wide, cordiform basal part, and a cylindrical apical part, also called turret or exit duct, which ends at the tip of the abdomen above the anus.

P. occipitalis duct lumen, showing the peculiar way of sewing the intima (almost transparent in this picture) to the spiralled wall, through curved match-like projections of the cuticular cristae. E. Multiple collecting duct in *Pheropsophus occipitalis*, showing the confluence of the collecting duct branches into a single wider trunk before inserting into the reservoir chamber. F. Close-up of the collecting duct trunk shown in E, after selective ablation through FIB/SEM to show the cuticular microsculpture inside this trunk, very different from the regularly spiralled wall of the collecting duct branches. *CD* collecting duct, *CCR* cuticular crista, *CDT* collecting duct trunk, *DL* duct lumen, *IN* intima, *MLP* match-like projection, *RE* reservoir, *RF* reservoir fold, *SL* secretory lobe, *TR* tracheae. Scale bars: A = 200 μm; B = 50 μm; C = 20 μm; D = 5 μm; E = 500 μm; F = 200 μm.

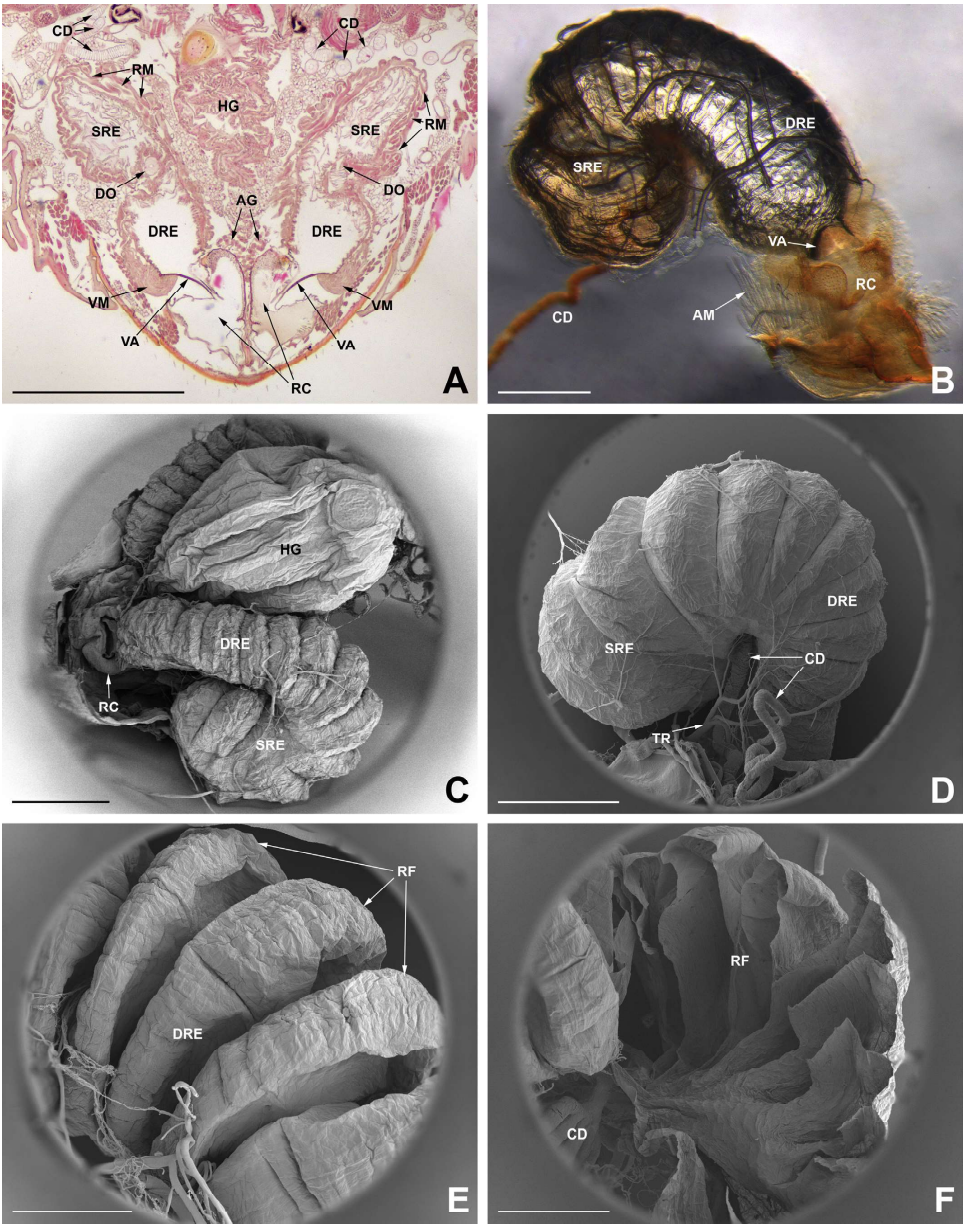

Fig. 7. Reservoir chamber structure. A. Horizontal histological section of *Brachinus sclopeta* abdomen, showing the two reservoir chambers, and their subdivisions into storage and dynamic parts; note the different types of muscles acting on the two different functional parts of the reservoir. B. Distal part of the left explosive system dissected and imaged at the

- The basal part of the RC (Figs. 2E–G, 9, 10 and 11) anteriorly encircles the valve with a ring of slightly sclerotized cuticle. It is somewhat inflated on the ventral surface and extends dorsolaterally in two rounded, convex lobes, which meet medially in some species. The basal part is heavily sclerotized, except for a thin longitudinal, mesodorsal, membranous strip (Fig. 9A), and the cuticular wall is multilayered (Fig. 11F). The internal surface of the RC has very complex patterns of microsculpture (Figs. 10 and 11) and pores leading into the accessory gland ducts, which are often grouped in clusters (Fig. 10E–F), as described in the following paragraph. The pores are more abundant dorsolaterally near the lobes. Concerning the microsculpture, the same areas of the RCs (ventral wall, lateral lobes, valve ring, posterior area), in different species and genera of brachinines, show similar types of sculpticles (Fig. 10A–B), with only slight variations in density and size among the species. In particular, the following five main types of microsculpture can be recognized:
  1. Spiny hairs (Fig. 10C–E). Spiny hairs are thin, elongate, flexible, conical hairs, which are sharp and sometimes slightly branched at the apex, They are directed into the lumen of the RC and arise perpendicularly from the cuticular surface. They are extremely variable in size, following a gradient of length, with longer hairs in the proximal part (where the RC is wider) and shorter hairs in the distal part, where they are replaced by flattened spines. The spiny hairs are widespread in the basal part of the RC, covering the surface of both lobes and the ventral wall, where they represent the most common type of microsculpture. All examined genera show spiny hairs in this part of the RC.
  2. Spiny lobes (Figs. 9E–F, 10D and 11E). Flattened cuticular lobes, thinner at the base and apically expanded, rounded and microspinulated, positioned only on the ring of cuticle encircling the valve. All examined genera show spiny lobes in this part of the RC.
  3. Haired walls (Figs. 9A, F, 10A and 11A–B). Wide, laminar, cuticular walls tipped by fringes of elongate, hair-like projections, emerge from the basal part of the RC and directed toward the middle of the cavity.
     In *Brachinus* these structures are represented by 5–6 subparallel, longitudinal, hair-tipped carinae, present medially on the ventral surface of RC, and associated with furrows on the outside of the RC. In *Pheropsophus* the cuticular walls are greater in number and are tipped by dense tufts of cuticular filaments, more abundant and elongate on the medial part (in association with the valve) and gradually shorter and thinner on the sides (near the lateral lobes). In Aptinus these structures are absent but are replaced by branched spines as described below.
  4. Branched spines (Fig. 10B). These structures, only present in Aptinus, are in a similar location and presumable serve the same function as the haired walls of *Brachinus* and *Pheropsophus*, but they are structurally quite different. They are represented by stout, conical, tree-like cuticular projections, especially branched distally, and extending into elongate, flexible filaments.
  5. Flattened spines (Fig. 10A, C). Subtriangular flattened cuticular spines, acute at the tip (rarely 2- or 3-spinulated), partially imbricate and posteriorly directed, present at the interface between basal part and turrets, especially in the mesodorsal wall of RC.
  6. Alveolate floor (Figs. 9E–F and 11A, C–D). While in *Brachinus* and *Aptinus* the internal surface of the expanded part of the RC is flat and smooth, mainly covered by spiny hairs, in *Pheropsophus* it is covered by a honeycomb structure that increases the internal surface area. A large number of rounded compartments compose this complex surface, decreasing in size from the proximal part to distal part of the RC. Each compartment is limited by raised walls variously fringed, especially at the tip, by scattered short cuticular projections usually not greater in height than the height of the wall. The bottom of each compartment is deeply concave, and there is a corresponding external convexity on the RC (Fig. 11B).
     There is a lot of particulate secretion attached to the microsculpture, often filling almost all the cavity (Figs. 8A and 9A), representing the accessory gland products. The secretion appears multilayered, with boundaries between layers visible in the FIB images (See Fig. 12); more electron dense layers are located near the RC walls while less electron dense layers are present towards the RC lumen. Embedded in this secretion, especially in the lobes, electron dense spheres (*Pheropsophus*, see Fig. 12A–B) or dark dotted globules (*Brachinus*, see Fig. 12C) are present.
- Apical part (Figs. 2E–G and 13). This part is basically represented by the turrets, which are tubular structures composed of a thin, membranous, expandable cuticular layer that is simple dorsally, but tightly encloses ventrally an additional cuticular, highly sclerotized, subrectangular plate (Figs. 9D and 13C–E), concave in the middle, extended up to the apex of the abdomen. The two turrets run subparallel and appear completely fused medially in males (Fig. 13A, C), or only apically in females (Fig. 13B). Sclerotized parts of this section appear internally smooth or with only scattered, flat, microspinulate microsculpture (Fig. 13F), especially located close to the opening. The fluorescence microscopy analysis of *Brachinus sclopeta* shows the presence of resilin associated with the thin expandable parts of the turrets (Fig. 9B).

3.7. Accessory glands (AG)

The AGs are bicellular glands associated with the basal part of the RC (Fig. 14A), not forming a true tissue, but laying individually in the hemolymph. Each secretory unit is composed of a secretory cell (SC) and a duct cell (DC) (Fig. 14C, D). In KOH treated specimens, the medial part of the reaction chamber is characterized by the presence of a dense net of thin tubules representing the conducting canals (CC) of the DCs (Fig. 15A–D). Each CC is quite long, and it is proximally connected with the external wall of the reaction chamber (Fig. 15A, D). In all examined species we observed that bundles of CC often insert inside the reaction chamber at the same site (Fig. 15A, B, D), where a rounded circular depression was observed (Fig. 15A). In cross section the conducting canals (CC) can appear either empty or filled with electrondense secretion (Fig. 15F). Distally each CC is connected with a secretory cell.

Each SC is quite large and of various shape (most of them are elliptical or elongated) (Fig. 14B–C). Ultrastructural features of the SCs include a large nucleus (Fig. 14C), located basally with an evident nucleolus, abundant stacks of rough endoplasmic reticulum (RER) (Fig. 14D, F), often located close to the nucleus itself, and several mitochondria (Fig. 14C–D, F).

stereomicroscope, from a fresh specimen of *B. sclopeta*; note the structure of the reservoir filled with air, and the sclerotization of valve and reaction chamber as compared to the membranous reservoir. C–F. FIB/SEM pictures of KOH digested reservoirs of: *B. sclopeta* (C, D) and *Pheropsophus occipitalis* (E–F); note the different tipes of foldings in *Brachinus* and *Pheropsophus*. *AG* accessory gland, *AM* addressing muscles, *CD* collecting duct, *DO* duct opening, *DRE* dynamic reservoir, *HG* hindgut, *RC* reaction chamber, *RF* reservoir fold, *RM* reservoir muscles, *SRE* storage reservoir, *TR* tracheae, *VA* valve, *VM* valvular muscles. Scale bars: A = 600 μm; B = 300 μm; C = 500 μm; D = 500 μm; E = 500 μm; F = 500 μm.

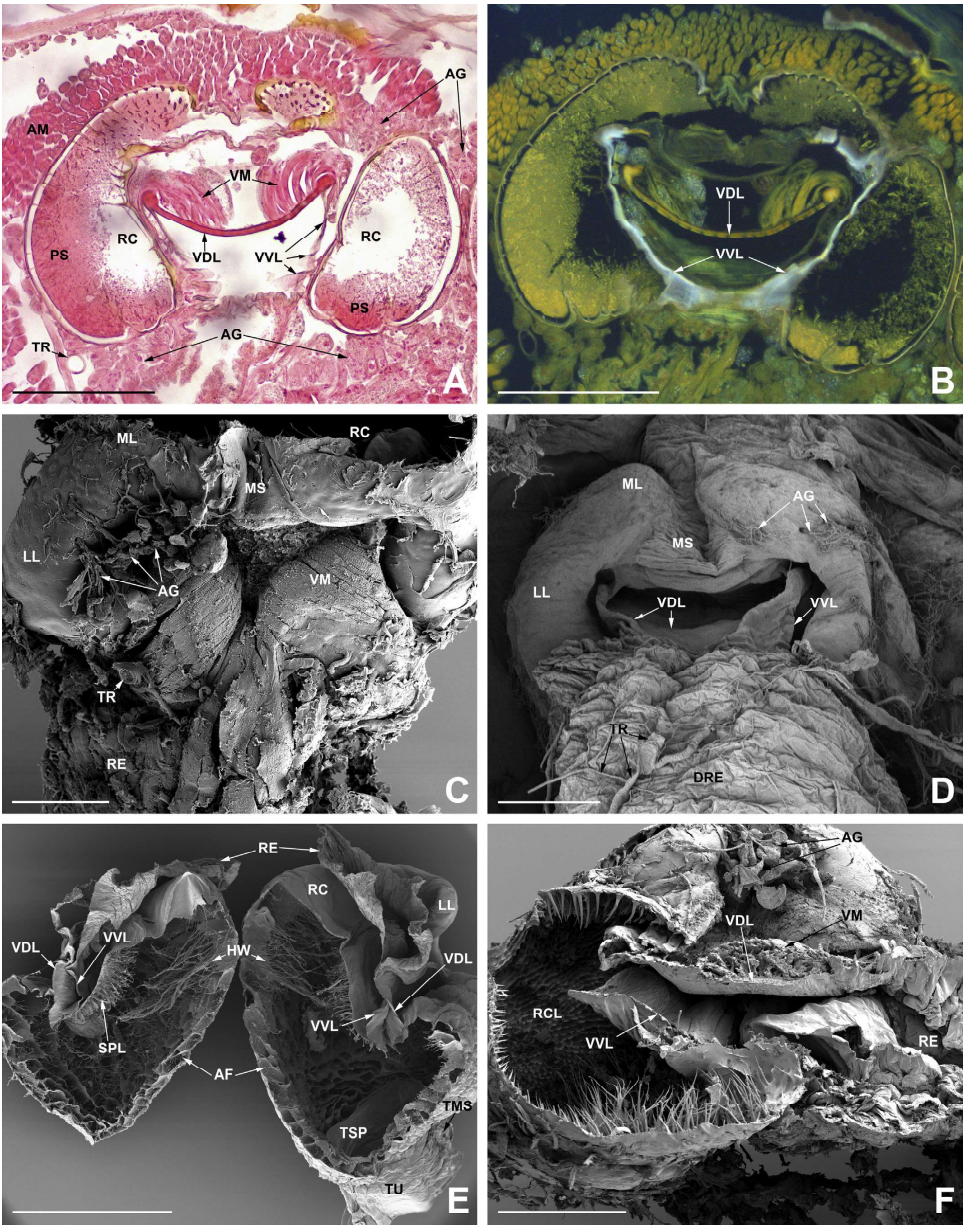

Fig. 8. Cuticular valve structure. A. Histological cross section of *Brachinus sclopeta* reaction chamber, showing the two layers (dorsal and ventral) of the valve; note the thickness of the dorsal layer as compared to the membranous ventral one, and the attachment of the two bundles of valvular muscles on the dorsal layer. B. Same as A, but observed by

The apical region of the secretory cell has a large extracellular cavity (EC) with a dense array of microvilli arranged in a radiate pattern (Fig. 14B). The microvilli show in cross section microtubules, and converge towards the receiving canal (RCA) of the DC (Fig. 14E). The RCA is made up of a thin layer of endocuticle and a complex, multilobed, clustered structure (Fig. 15C). The RCA is made by the associated duct cell (DC) and is directly connected to the CC (Figs. 14E and 15C). The CCs are isodiametric and run in bundles to the RC (Fig. 15B, D). The DC has a reduced cytoplasm and a single, heterocromatic nucleus usually positioned medially, close to the CC wall (Fig. 14D).

4. Discussion

In this paper we analyzed the explosive pygidial defensive system of Carabidae Brachininae, comparing different representative species, genera and subtribes of Brachininae in order to check for structural differences among taxa and possibly relate them to sex, dimensions or their evolutionary history.

The terminal part of the system is represented by multilobed glands, which consists of an aggregation of secretory lobes, organized in branches radially converging into a larger collecting duct. Each secretory lobe is represented by a thin elongate tubule, receiving the secretions from a surrounding monolayer of glandular tissue. This last is composed of hundreds of bicellular, conical units consisting of a secretory cell and a duct cell, assignable to gland type III according to the terminology of the gland structures (Noirot and Quennedey, 1974, 1991; Quennedey, 1998).

The presence of a single type of glandular unit in the secretory lobes suggests that the same cells produce both hydroquinones and hydrogen peroxide. The general organization of the multilobed glands appears very similar in all examined genera, with only slight differences related to the increased number and length of the secretory lobes in larger species (especially *Pheropsophus*).

In the present study we paid particular attention to the ultrastructure of the collecting duct, also called efferent duct by Eisner et al. (2001), in order to infer about the significance of its extreme length, that can easily reach two times the length of the entire body. It is worth noting that also other carabids show a long collecting duct (Forsyth, 1972; Balestrazzi et al., 1985). In the past it was speculated that the increased length of this structure could be related either to a possible maturation of the secretions passing through the collecting duct from the secretory lobe to the reservoir (Forsyth, 1970), or to avoid recoil and moderate the effects of the backflow of the toxic substances during the contraction of the reservoir, thus avoiding possible damages to the secretory lobe cells (Forsyth, 1970). Our morphological and ultrastructural analyses do not support either of the aforementioned hypotheses in Brachinini.

The duct is represented by a thick, round and spirally corrugated tube, resulting from the adhesion and interlocking of thousands of closely packed cuticular cristae, each one secreted by epidermal cells. This spring-like structure gives resistance and elasticity to the duct, that can be folded multiple times and undergo high pressures without clogging or collapsing. Epidermal cells forming the duct are very thin and depleted forming an ultra thin, flat, continuous monolayer of cells enclosing the spiralled, hollow wall of the duct. The scarce or absent metabolic activity of these cells is demonstrated by the great reduction of cytoplasm and organelles. For this reason, a possible influence of these cells in the transformation of the secretions can be ruled out. However, we cannot exclude that a maturation of the secretions can be favored by the slow passage through the long tube before the products reach the reservoir.

A fine net of cuticular projections partially closes the end of the duct facing inside the reservoir, possibly allowing the flowing of the secretion towards the reservoir and avoiding the backflow of the secretion during the reservoir contraction. This would make the “recoil” hypothesis of collecting duct length unlikely as well. It seems likely that the cuticular valve, which isolates the reservoir from the reaction chamber, also protects the reservoir from any recoil. The impact of the explosion can be absorbed by the reaction chamber wall, given the presence of the elastic resilin shown by fluorescence microscopy at the level of the turrets.

We describe for the first time in Brachininae the presence of unusual match-like projections of the cuticular cristae, sewing the intima to the spiralled wall of the collecting duct. As far as we know, these peculiar structures have not been described in other insects, but may be present also in homologous ducts of other Carabidae.

The presence of regularly spaced folds on the cuticular wall of the reservoir, combined with the action of a complex sheath of variously oriented muscles, facilitates the expansion and compression of the reservoir. The contraction of the muscles squeezes the reservoir, forcing the secretions to flow into the reaction chamber, while the muscular relaxation possibly helps the secretions to be sucked from the duct into the reservoir.

We functionally divided the reservoir into two parts: a wider storage chamber, with its own separate complex layer of muscles, and a distal dynamic chamber, the latter is more folded and regulated by the muscles attached distally to the cuticular valve and in continuity with the arched valve muscles. It is very likely that the synchronous contraction of all these muscles causes both the combined opening of the valve and the squeezing of the reactive chemical mixture into the reaction chamber.

The cuticular valve is composed of two layers of cuticle tightly overlapping; the aforementioned muscles are attached to the dorsal one, which is strongly sclerotized and thus more resistant to the mechanic stress. However, it is worth noting that the fluorescence microscopy analysis showed the presence of resilin only in the thin, unsclerotized ventral layer and not in the dorsal one. Though unexpected, this result leads us to hypothesize a possible involvement also of this thin membranous flap in the dynamics of a discharge.

The structure of the system that received more attention over the past generations of scientists is by far the reaction chamber, also called vestibule (Schildknecht, 1970) or combustion chamber (Beheshti and McIntosh, 2007), where the explosive exothermic reaction takes place, and that represents the heart of the system. Different parts of the reaction chamber show a differential sclerotization of the integument, according to their specific functions. Due to its role in absorbing the shock of the explosion, the basal part is highly sclerotized and shows a multilayered cuticular wall. However, its sclerotization is not continuous, since a longitudinal membranous strip is present dorsally between the two lateral lobes. Arndt et al. (2015) in a recent paper dealing with the mechanism of brachinines’ spray pulsation demonstrated that this

fluorescence microscopy to show the presence of resilin on the ventral layer (light blue) of the valve. C. Dorsal view of the *B. sclopeta* reaction chamber, not digested by KOH, to show the arrangement of the valvular muscles. D. Same as C but after KOH digestion of the organic parts. E. Reaction chamber of *Pheropsophus occipitalis*, KOH digested and cut along a longitudinal plane to show the cuticular parts of the valve in section. F. Lateral view of the longitudinally sectioned reaction chamber of *B. sclopeta*, not digested by KOH to show the cuticular parts of the valve and the valvular muscle attachments on the dorsal valve layer. *AM* addressing muscles, *AF* alveolate floor, *AG* accessory glands, *DRE* dynamic reservoir, *HW* haired walls, *LL* lateral lobe, *ML* medial lobe, *MS* membranous strip, *PS* particulate secretion, *RC* reaction chamber, *RCL* reaction chamber lumen, *RE* reservoir, *SPL* spiny lobes, *TMS* turret membranous sheath, *TR* trachea, *TSP* turret sclerotized plate, *TU* turret, *VDL* valve dorsal layer, *VM* valvular muscles, *VVL* valve ventral layer. Scale bars: A = 150 μm; B = 150 μm; C = 100 μm; D = 100 μm; E = 500 μm; F = 100 μm.

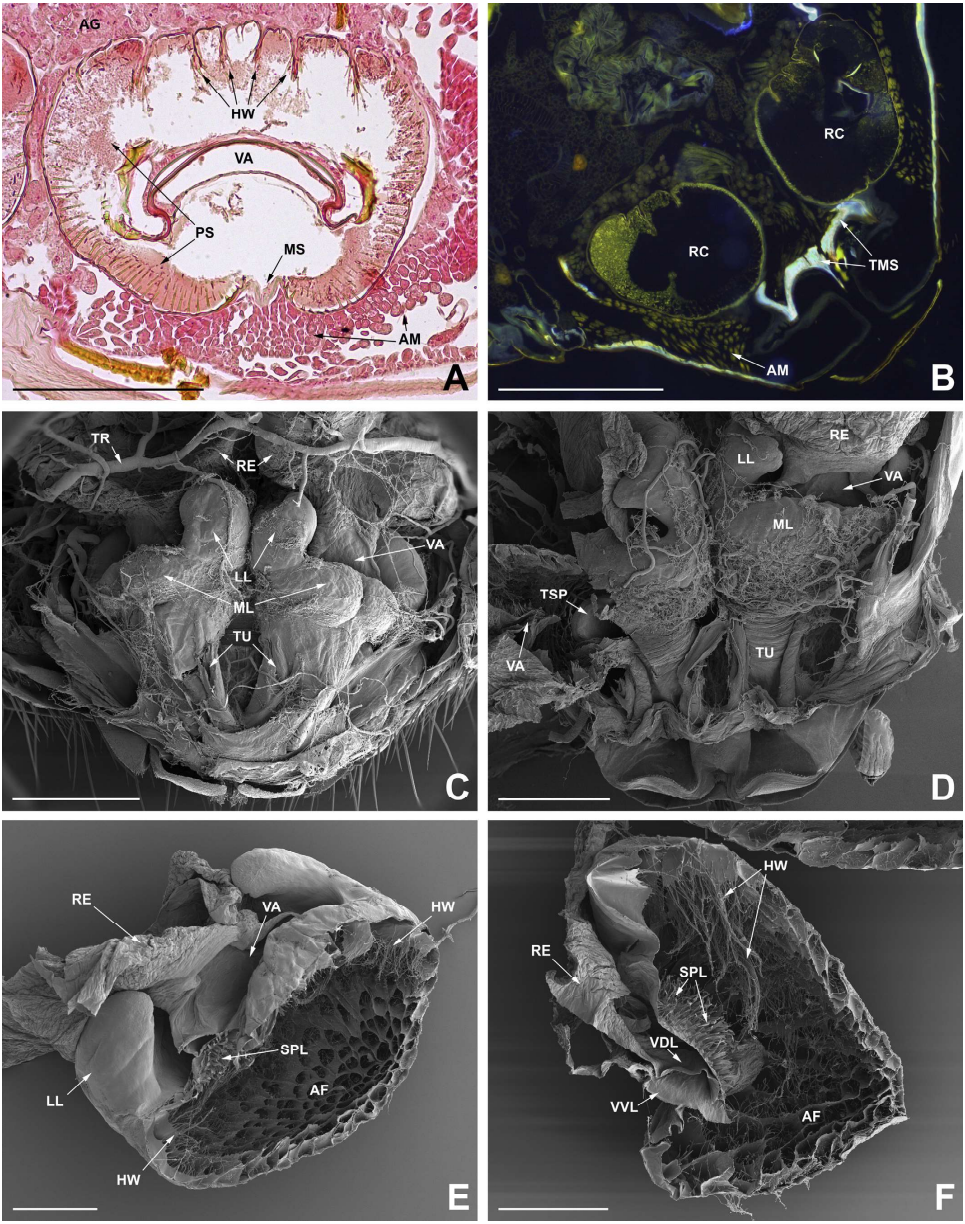

Fig. 9. Reaction chamber structure. A. Histological cross section of *Brachinus sclopeta* reaction chamber, showing the position of the different types of microsculpture and the presence of particulate secretion attached to the wall. B. Horizontal histological section of *B. sclopeta* abdominal apex observed by fluorescence microscopy, showing the presence of resilin (light blue) at the level of the turret membranous sheath. C—D. Dorsal view of reaction chambers in *B. sclopeta* (C) and *Pheropsophus occipitalis* (D); note that in D the left reaction chamber is longitudinally sectioned to show the turret sclerotized plate. E—F. Reaction chamber of *P. occipitalis* in cross (E) and longitudinal (F) section to show the position of the different types of microsculpture. *AF* alveolate floor, *AG* accessory gland, *AM* addressing muscles, *HW* haired walls, *LL* lateral lobe, *ML* medial lobe, *MS* membranous strip, *PS* particulate secretion, *RC* reaction chamber, *RE* reservoir, *TMS* turret membranous sheath, *TR* trachea, *TSP* turret sclerotized plate, *TU* turret, *SPL* spiny lobes, *VA* valve, *VDL* valve dorsal layer, *VVL* valve ventral layer. Scale bars: A = 200 μm; B = 400 μm; C = 400 μm; D = 500 μm; E = 250 μm; F = 250 μm.

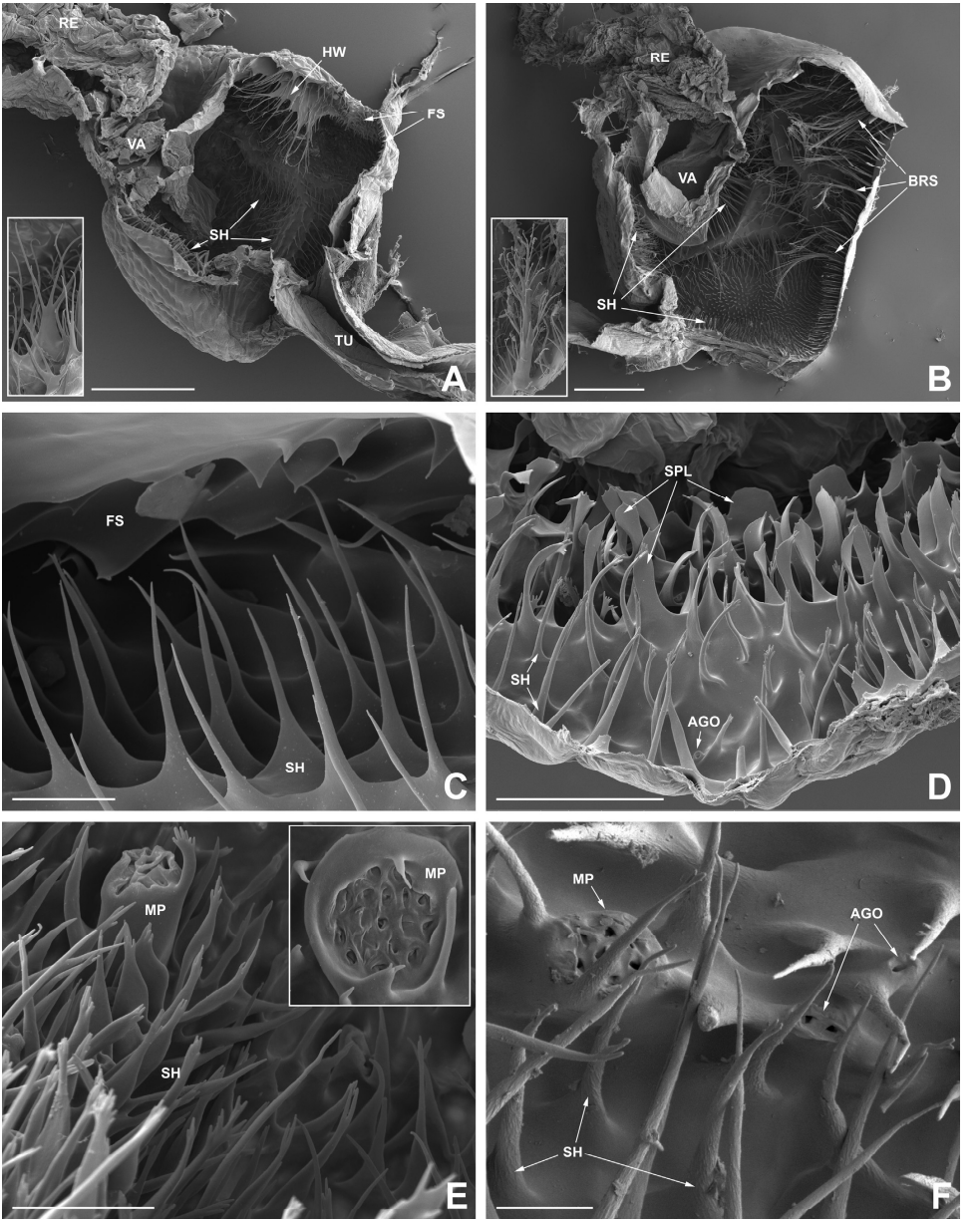

Fig. 10. Fine structure of the reaction chamber internal wall. A–B. Reaction chambers of *Brachinus sclopeta* (A) and *Aptinus creticus* (B) cut longitudinally to show the relative position of the microsculpture. C–F. Different types of microsculpture on the basal part of reaction chamber in *B. sclopeta*. *AGO* accessory gland opening, *BRS* branched spines, *FS* flattened spines, *HW* haired walls, *MP* multiperforated plate, *RE* reservoir, *SH* spiny hairs, *SPL* spiny lobes, *TU* turret, *VA* valve. Scale bars: Scale bars: A = 100 μm; B = 100 μm; C = 10 μm; D = 30 μm; E = 10 μm; F = 5 μm.

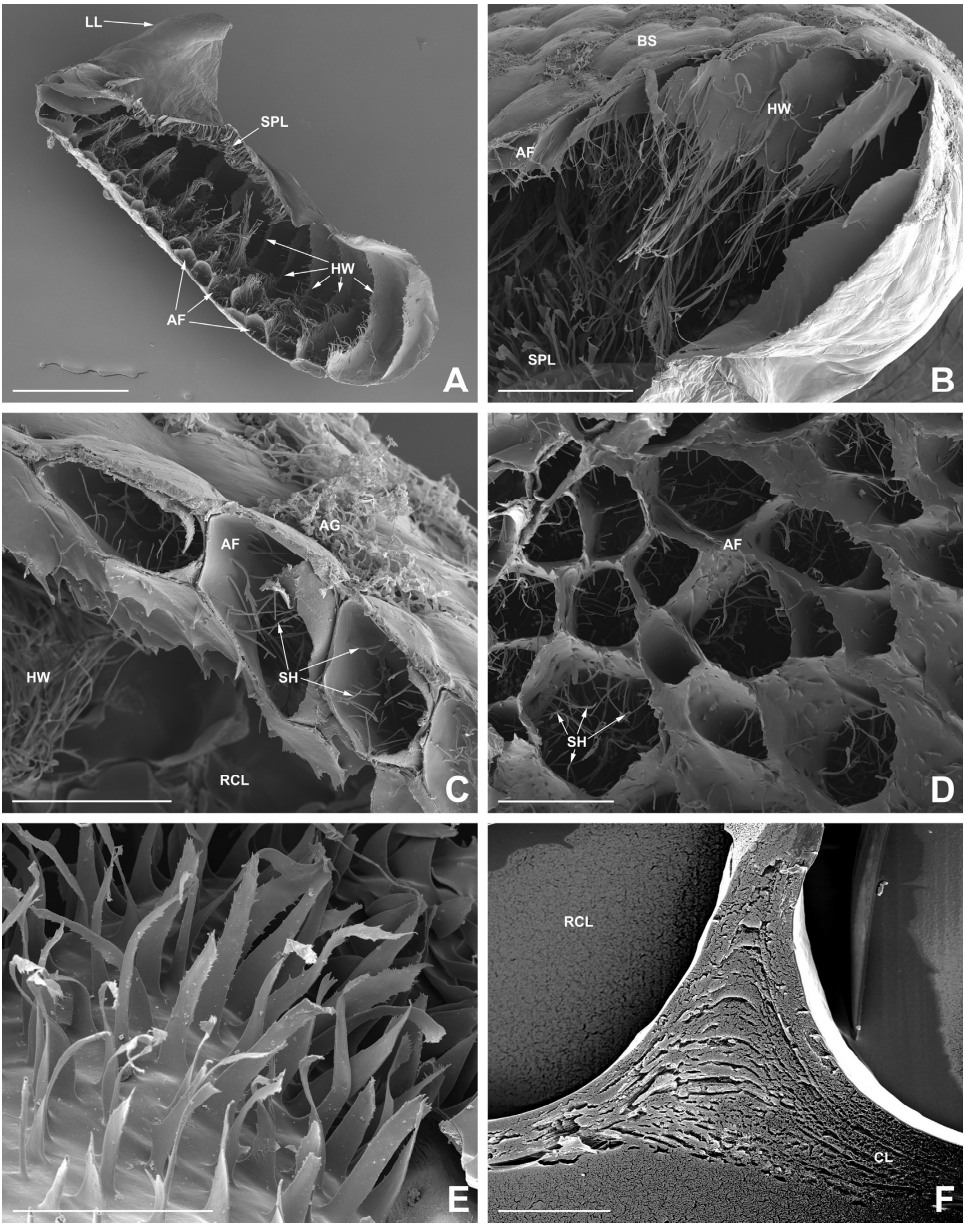

Fig. 11. Fine structure of the reaction chamber internal wall of *Pheropsophus occipitalis*. A. Internal structure of left lateral lobe; note the laminar subparallel structure of the haired walls along the ventrolateral part. B. Close-up of the haired walls showing the long hairs projecting into the reaction chamber lumen. C–D. Compartmented structure of the peculiar alveolate floor. E. Spiny lobes in the region close to the valve. F. Thick multi-layered cuticle of the reaction chamber wall. *AF* alveolate floor, *AG* accessory gland, *BS* bumped surface, *CL* cuticular layers, *HW* haired walls, *LL* lateral lobe, *RCL* reaction chamber lumen, *SH* spiny hairs, *SPL* spiny lobes. Scale bars: A = 250 μm; B = 100 μm; C = 50 μm; D = 50 μm; E = 50 μm; F = 10 μm.

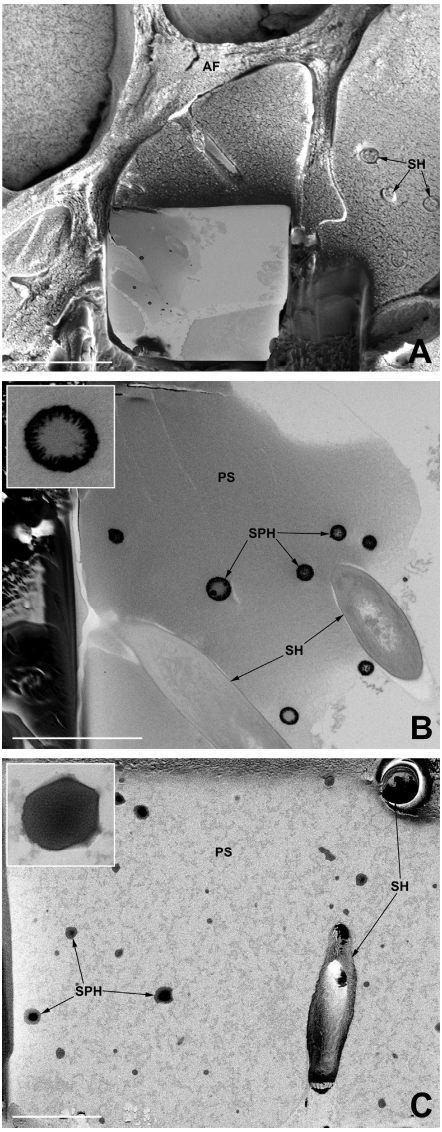

Fig. 12. Dark spherules embedded in the particulate catalytic secretion attached to the reaction chamber microsculpture. A. FIB/SEM cross section of a slice of reaction chamber wall of *Pheropsophus hispanus* embedded in epoxy resin, showing the position of the dark spherules. B–C. Different structure of dark spherules in *Pheropsophus hispanus* and *Brachinus elongatulus*; note in B the multi-layered structure and the different density of the secretion attached to the wall. *AF* alveolate floor, *PS* particulate secretion, *SH* spiny hairs, *SPH* spherule. Scale bars: A = 10 μm; B = 4 μm; C = 5 μm.

unsclerotized belt, named by the authors as "expansion membrane", plays a key role in the discharge mechanism. Indeed, increasing the elasticity of the basal part of the reaction chamber functions in metering out the micropulses of each discharge.

On the contrary, the turrets are mainly membranous structures, with an additional highly sclerotized, ventral, subrectangular plate, concave in the middle, extended up to the apex of the abdomen. It is remarkable that the fluorescence microscopy analysis outlined the presence of resilin at the level of the membranous part of the turrets. Insect resilin is usually present in membranous cuticular structures often subject to stretching (Michels and Gorb, 2012), and its presence in the turrets confirms the need of elasticity of this part to limit recoil during discharge. In fact, the cylindrical structure of the turrets is clearly functional to channel the products of the reactions outside the body and undergoes very high pressures during blasting. Precise aiming of the spray is mainly performed by the contraction of complex specific muscles that run obliquely around the reaction chambers and give a high mobility to the abdominal apex. The amazing ability of the brachinines in shooting precisely against predators, and in general against the source of the disturbance, has been widely studied (Eisner, 1958; Eisner and Aneshansley, 1999; Eisner et al., 2006).

The FIB/SEM analysis showed a great structural diversity of microsculpture on the basal part of the reaction chamber, where we could recognize six main types of microsculpture located in specific districts of the chamber. The presence of cuticular projections of very diverse shapes and dimensions suggests different functional roles for each type of sculpticle.

We hypothesize that the main function of the microsculpture is to keep the catalytic secretion attached to the wall of the reaction chamber. In fact the microsculpture is most developed near the glandular pores of the accessory glands. The histology of the reaction chamber confirms that a dense secretion produced by the accessory glands is encrusted on this highly sculptured basal part, especially inside the lobes. Additionally, both the histological and ultrastructural analyses show that multiple layers of this catalytic secretion are overlapped into an irregular stratification, with a distinct decreased density from the wall to the center of the lumen.

The problem of the multiple blasting, i.e. the ability of explosively discharge benzoquinones several times without consuming all catalyzers at once, has been object of discussion (Dean, 1979). Our results show that the density of the secretion and its sticky properties, combined with the presence of elongate microsculptures, act in combination to retain the catalytic secretion attached to the wall of the chamber. We predict that, during a blast, the amount of chemicals forced into the reaction chamber does not mix with all of the available catalytic secretion, since it is not liquid but dense and sticky. On the contrary the reactive liquid most likely comes into contact only with the superficial layer, which contains enough catalases and peroxidases to catalyze the exothermic reaction. The blast probably washes out only part of the secretion, while the internal layers, that become superficial after blasting, are ready to catalyze the subsequent reaction. The different densities of the observed layers of secretion could be the result of successive waves of secretion and washouts.

In the histological samples we observed that, while in some specimens both reaction chambers were similarly filled with catalytic secretion, others were very differently filled. This is in agreement with the recent findings by Arndt et al. (2015) showing that the two chambers could be used singularly by the beetle and not always in combination.

By using FIB/SEM microscopy it was possible to visualize the unexpected presence of a high number of electrondense spherules, regular in *Pheropsophus* and slightly irregular in *Brachinus*, immersed in the catalytic secretion. It is likely that these particles

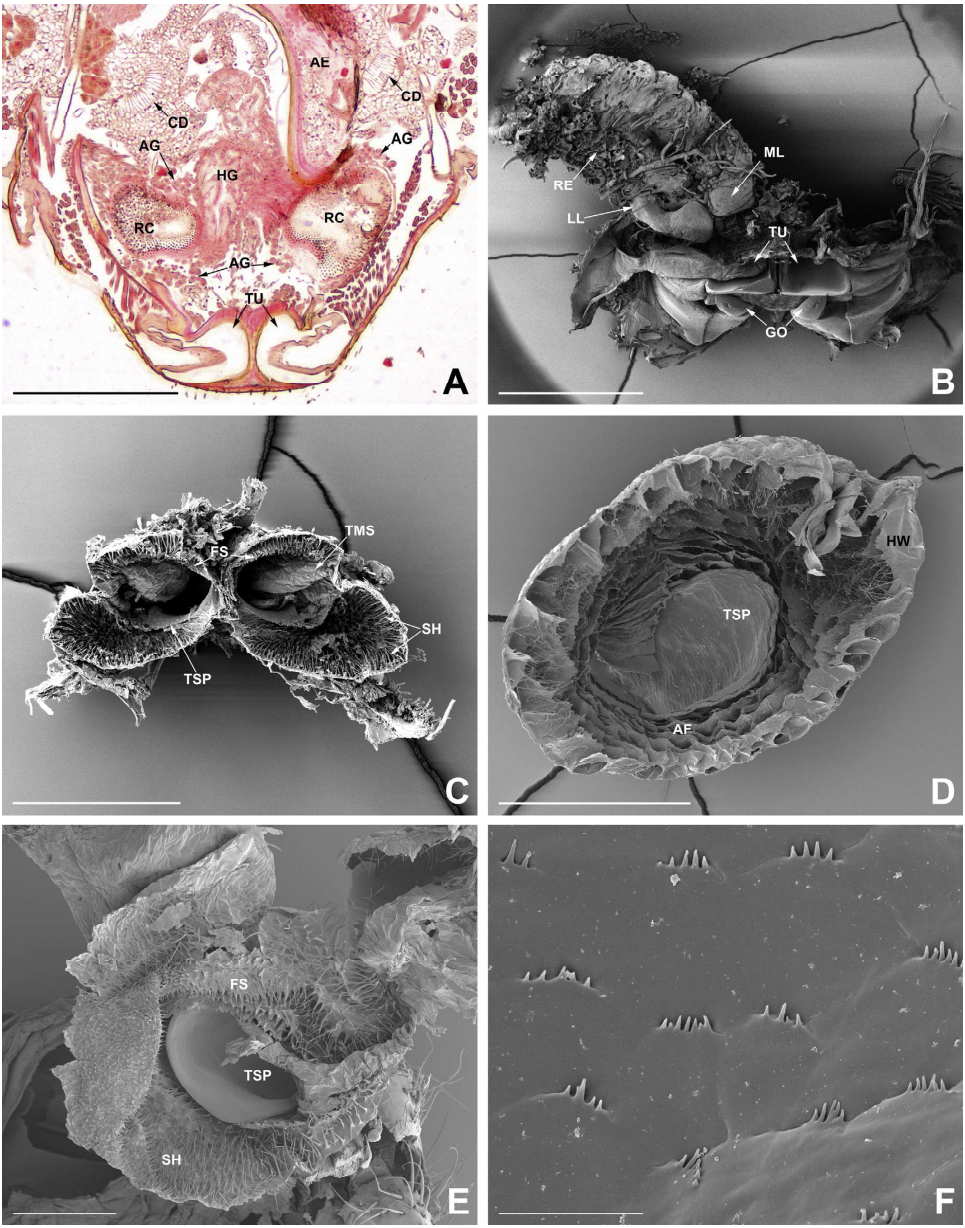

Fig. 13. Reaction chamber structure. A. Horizontal histological section of *Brachinus sclopeta* abdominal apex, showing the ventral part of the reaction chamber and the turrets. B. Abdominal apex with left system in dorsal view of *B. sclopeta*, showing the external part of the turrets. C. Reaction chambers of *B. sclopeta* medially cross sectioned, showing the turrets from anterior view. D–E. Cross sections of reaction chamber basal part in *Pheropsophus occipitalis* (D) and *B. sclopeta* (E) showing the turrets from anterior view. F. Spinules of microsculpture on turret sclerotized plate of *P. occipitalis*. *AE* aedeagus, *AF* alveolate floor, *AG* accessory gland, *CD* collecting duct, *FS* flattened spines, *GO* gonostyli, *HG* hindgut, *LL* lateral lobe, *ML* medial lobe, *RC* reaction chamber, *RE* reservoir, *SH* spiny hairs, *TMS* turret membranous sheath, *TSP* turret sclerotized plate, *TU* turret. Scale bars: A = 400 μm; B = 500 μm; C = 300 μm; D = 400 μm; E = 100 μm; F = 10 μm.

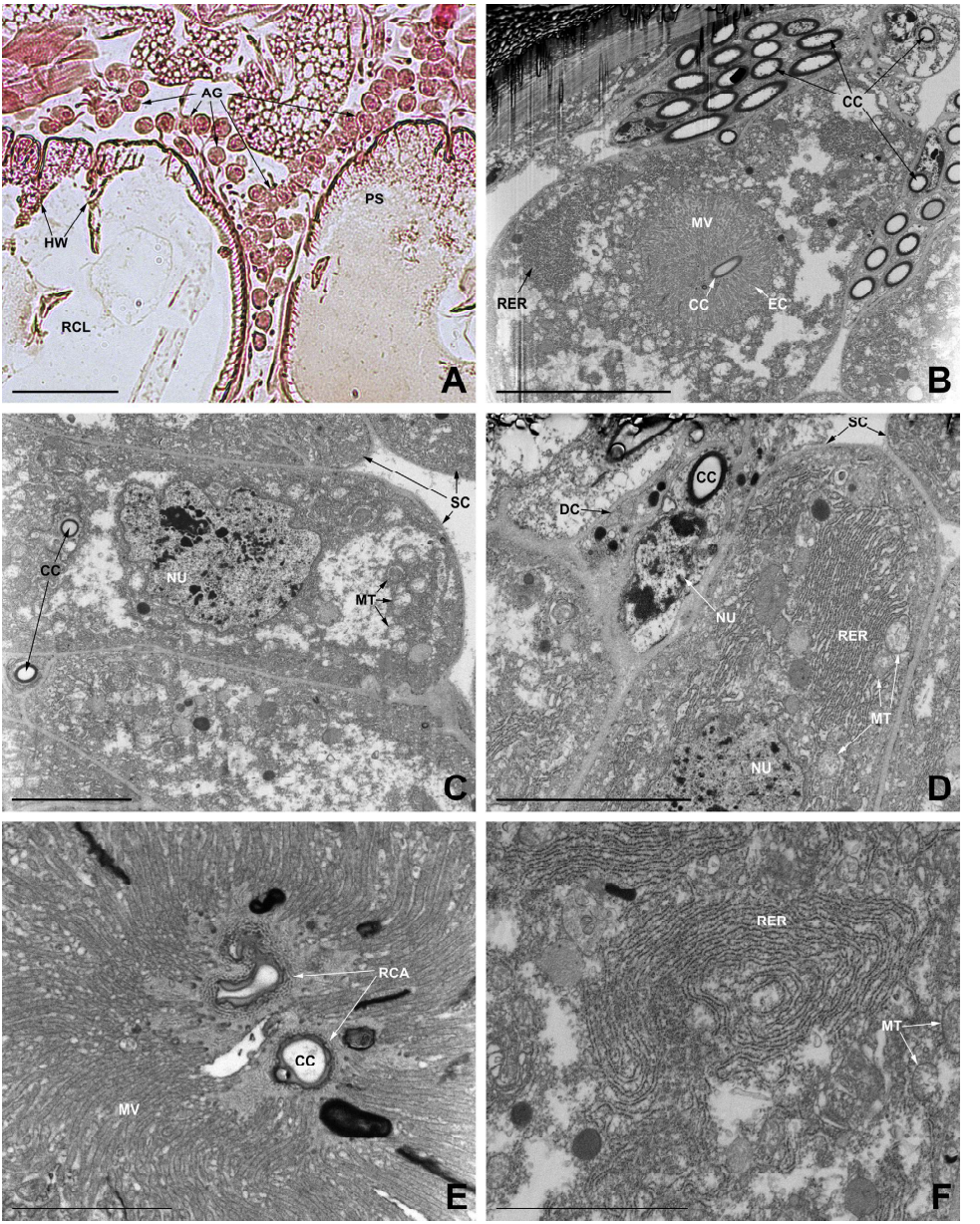

Fig. 14. Accessory gland anatomy. A. Horizontal histological sections of *Brachinus sclopeta* abdomen at the level of the reaction chambers, showing groups of accessory glands inserting in the lateral lobes. B–F. FIB/SEM sections of *B. elongatulus* accessory gland cells, both secretory and duct cells, showing several ultrastructural details; note the clustering of several conducting canals before entering the reaction chamber wall, the great amount of rough endoplasmic reticulum, and the complex multilobed structure of the receiving canal. *AG* accessory gland, *CC* conducting canal, *DC* duct cell, *EC* extracellular cavity, *HW* haired walls, *MT* mitochondrion, *MV* microvilli, *NU* nucleus, *PS* particulate secretion, *RCA* receiving canal, *RCL* reaction chamber lumen, *RER* rough endoplasmic reticulum, *SC* secretory cell. Scale bars: A = 50 μm; B = 10 μm; C = 5 μm; D = 5 μm; E = 2 μm; F = 3 μm.

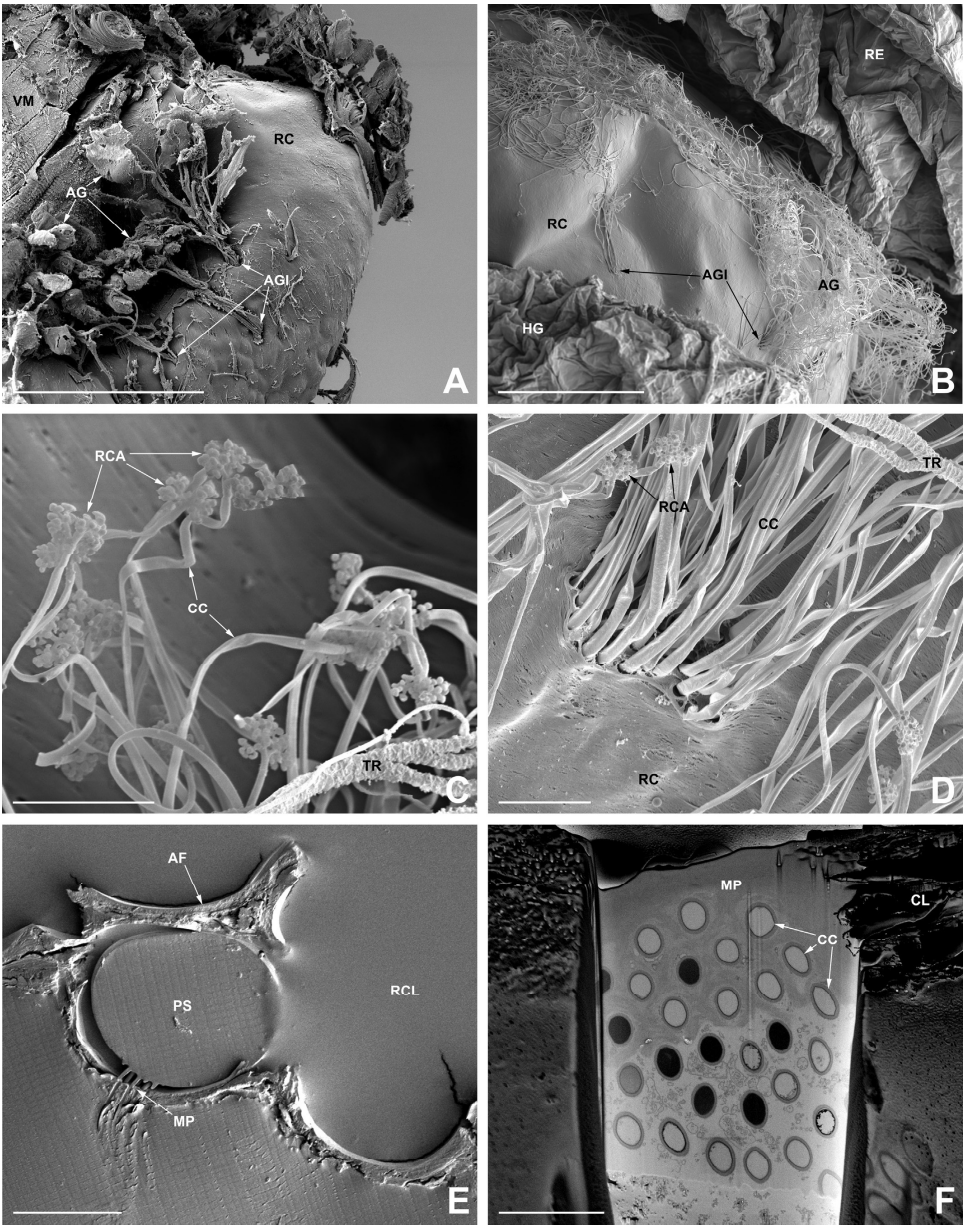

Fig. 15. Accessory gland fine structure. A. External surface of the reaction chamber of *B. sclopeta* showing the cuticular conducting canals knot before KOH digestion. B. Same as A but after KOH digestion. C. Receiving canals of the duct cells of *Pheropsophus occipitalis*, showing their multilobed structure. D. Cluster of conducting canals inserting inside the

in both genera are related to the catalytic activity, and are not secondary products of the explosion, since they are deeply embedded in the dense secretion, close to the walls of the reaction chamber and not on the external layers. The chemical nature of these globular structures is unknown and need to be investigated further.

In this paper the ultrastructure of the glandular cells producing catalase and peroxidase enzymes is analyzed for the first time. These are typical bicellular glands type III, composed of one secretory cell and a very long duct cell which is depleted of cytoplasm and most organelles. Several duct cells group together in bundles, opening in the reaction chamber at the level of multiperforated cuticular plates. Compared to the glands of the secretory lobes, characterized by a conical secretory cell and a very short duct cell, the accessory glands are spherical, freely floating into the hemolymph singly or in clusters thanks to their elongate duct cells.

Most of the descriptions reported in the results, refer to the system of the genus *Brachinus* that remains quite stable even in species of different size. However, in order to have a broader overview of the possible conditions of this system in the whole Brachinini, we comparatively analyzed the pygidial defensive systems in several specimens, both males and females, of various representative species, belonging to the genera *Brachinus* (Brachinina), *Pheropsophus* (Pheropsophina) and *Aptinus* (Aptinina). Though our results show a general similarity of the system in all brachinines, we found significant structural differences not only among genera but also among species of the same genus at the level of:

1. Collecting duct. The number of the collecting ducts varies among the examined species; it is single in the small *Brachinus*, single or double in the intermediate sized *Aptinus,* while in the large *Pheropsophus* ranges from 8 to 16. In all cases, each duct ends in a single multilobed glandular system, while all ducts (in species with multiple ducts) converge in only one short unique duct before entering the reservoir chamber. It is possible that the number of ducts and their length could be related to the body size while the diameter of each single duct remains very similar in all examined species, as if there are constraints for its functionality. Also the terminal part of each duct at the level of the secretory lobes is enlarged but simple in *Pheropsophus,* divided in two simple thin branches in *Brachinus*, divided in two thin branches each one distally bifurcate in *Aptinus*. These characters seem to be constant in each genus, at least in all examined species.
2. Reservoir chamber. The reservoir of *Pheropsophus* seems to be quite different from the structure shared by *Brachinus* and *Aptinus*. Besides the widely increased dimensions of the reservoirs of *Pheropsophus*, to store a higher volume of liquids, also the folding in this genus seems to be deeper, with a longer and more regularly structured distal dynamic part.
3. Reaction chamber. *Pheropsophus* seems to be unique compared to the others, showing a peculiar honeycomb-like, complex cuticular floor internally to its basal part. This multichambered cuticular floor replaces the carpet of spiny hairs typical of *Brachinus* and *Aptinus*. We can speculate that this complex structure can be functional to keep the dense increased amount of secretions better than other types of microsculptures in a reaction chamber much wider than those of the other genera.

It is worth noting that *Aptinus* shows a distinctive type of elongate arborescent microsculptures laying on the lateroventral part of the chambers and homologous to the haired walls of *Brachinus* and *Pheropsophus*.

Concerning the sexual dimorphism, we observed a different level of medial coalescence of the turrets, that appear completely fused medially in males and only apically in females. This is in agreement with the recent findings by Arndt et al. (2015) in *B. elongatulus*. Though apparently of minor significance, it is not excluded that this character could reflect functional differences in the discharge, since it seem to be constant in different genera.

Though not analyzed in the present work, it is worth to report that the Crepidogastrini, acknowledged sister group of Brachinini, show, according to Eisner et al. (2001) an explosive defensive system quite similar to that described above, except for a few remarkable differences: 1) structure of the secretory lobes, acinous (instead of digitiform); 2) receiving canals of the glands converging into the apex of short lateral ducts forming “florets” (*sensu* Eisner et al., 2001) (instead of inserting individually into ductules); 3) reservoirs showing a pre-valvular region with a plissé folding (instead of bellows-like folding); 4) reaction chambers with broad lateral lobes (instead of moderately bulged lobes). Whether these characters represent plesiomorphic or apomorphic conditions will be subject of further studies.

Only very few studies have tackled the morphology and ultrastructure of this system in “non-exploding” ground beetles (Forsyth, 1970, 1972; Balestrazzi et al., 1985; Eisner et al., 2000; Will et al., 2000), while most interest was paid to the different chemicals produced by the pygidial glands (Moore and Wallbank, 1968; Aneshansley et al., 1983; Dettner, 1987). The system of a generalized ground beetle is composed by a pair of glandular structures, each producing secretions by usually acinous glands; one single collecting duct, laterally inserting into a rounded unfolded reservoir chamber; a moderately thin and simple efferent duct from each reservoir; a cuticular valve at the end of the efferent duct, positioned immediately anterior to the external opening.

The explosive pygidial defensive system of bombardier beetles is clearly derived from this basic model, with the different components specialized according to the ability of explosively produced quinones.

The pygidial explosive system of brachinines and paussines shows chemical and morphological similarities. From the chemical point of view, paussines show only subtle differences while the explosive reaction is basically identical. From a structural point of view is remarkable in both groups the presence of a strikingly long collecting duct, a widened reservoir chamber and a sclerotized reaction chamber. However, according to the available literature (Forsyth, 1972; Eisner et al., 1989, 1991, 2000, 2001), paussines show substantial differences: multilobed glands with an acinous glandular structure (instead of digitiform); rounded (instead of funnel-shaped) reaction chambers, lateral (instead of terminal) in position; spray addressing performed by using the Coanda effect through distinctive elytral flanges (except *Metrius*, see Eisner et al., 2000) (instead of moving the abdominal tip).

reaction chamber wall of *P. occipitalis*. E. Reaction chamber wall of *P. hispanus* reaction chamber embedded in epoxy resin sectioned at the level of a multiperforated plate; note the density of the secretion emerging from the accessory gland openings. F. FIB/SEM cross sectioning of a multiperforated plate of *P. hispanicus* showing the regular spacing of the conducting canal openings at the level of the cuticular wall of the reaction chamber; note the different filling of the conducting canal lumen, and the electron density of the secretion. *AF* alveolate floor, *AG* accessory gland, *AGI* accessory gland insertion, *CC* conducting canal, *CL* cuticular layers, *HG* hindgut, *MP* multiperforated plate, *PS* particulate secretion, *RC* reaction chamber, *RCA* receiving canal, *RCL* reaction chamber lumen, *RE* reservoir, *TR* tracheae, *VM* valvular muscles. Scale bars: A = 100 μm; B = 100 μm; C = 10 μm; D = 10 μm; E = 25 μm; F = 5 μm.

Over the past 50 years several scientists have greatly emphasized the strong similarities between the two explosive defensive systems, mostly giving a crucial importance to the chemical part of the explosive reactions (Eisner et al., 1977; Roach et al., 1979; Aneshansley et al., 1983) and underestimating the structural differences of the components. Unfortunately, phylogenetic analyses based on both morphological and molecular characters, which mirror the problem of independent or share derived evolution of the two explosive pygidial defensive systems, gave contrasting and non-conclusive results. While morphological characters based on both larval (Beutel, 1992, 1993; Arndt, 1998) and adult (Deuve, 1993; Liebherr and Will, 1998) stages outlined a parallel and independent evolution of the two taxa (and of the two systems), with paussine as basal and brachinine as derived lineages within Carabidae, the molecular analyses showed some intrinsic analytic problems (i.e. long branch attraction, see Maddison et al., 1999) that hampered a reliable, definitive result. In order to contribute to this discussion, this paper is aimed to give a solid anatomic overview of the most popular bombarding system, contributing to the debate on its evolution within the Carabidae and in view of broader future comparative research.

Acknowledgments

We are particularly grateful to Manfred Egger, Wendy Moore and Claudio Ghittino for their help in finding part of the studied material. Wendy Moore is also acknowledged for the continuous discussions on the functional morphology of the system and for the deep review of the manuscript from both linguistic and scientific points of views. We are indebted to Marco Valerio Rossi Stacconi and Sandra Moreno for their valuable technical support and availability, and Luigi Presutti (Italian Ministry of Health) for his precious help in facilitating the exchange of live material between USA and Italy. We thank three anonymous reviewers for their helpful suggestions that improved the manuscript.

References

Álvarez-Padilla, F., Hormiga, G., 2007. A protocol for digesting internal soft tissues and mounting spiders for scanning electron microscopy. J. Arachnol. 35, 538–542.

Aneshansley, D.J., Eisner, T., Widom, J.M., Widom, B., 1969. Biochemistry at 100°C: explosive secretory discharge of bombardier beetles (*Brachinus*). Science 165, 61–63.

Aneshansley, D.J., Jones, T.H., Alsop, D., Meinwald, J., Eisner, T., 1983. Thermal concomitants and biochemistry of the explosive discharge mechanism of some little known bombardier beetles. Experientia 39, 366–368.

Arndt, E., 1998. Phylogenetic investigation of Carabidae (Coleoptera) using larval characters. Phylogeny and classification of Caraboidea (Coleoptera: Adephaga). In: Ball, G.E., Casale, A., Taglianti, A.V. (Eds.), International Congress of Entomology, Phylogeny and Classification of Caraboidea (Coleoptera:Adephaga): Proceedings of a Symposium, 28 August 1996, Florence, Italy: XX International Congress of Entomology. Museo regionale di scienze naturali, Torino, pp. 171–190.

Arndt, E.M., Moore, W., Lee, W.K., Ortiz, C., 2015. Mechanistic origins of bombardier beetle (Brachinini) explosion-induced defensive spray pulsation. Science 348, 563–567.

Balestrazzi, E., Valcurone Dazzini, M.L., Bernardi, M.D., Vidari, G., Vita-Finzi, P., Mellerio, G., 1985. Morphological and chemical studies on the pygidial defence glands of some Carabidae (Coleoptera). Naturwissenschaften 72, 482–484.

Beheshti, N., McIntosh, A.C., 2007. A biomimetic study of the explosive discharge of the bombardier beetle. Int. J. Des. Nat. Ecodyn. 1, 61–69.

Beutel, R.G., 1992. Study on the systematic position of Metriini based on characters of the larval head (Coleoptera: Carabidae). Syst. Entomol. 17, 207–218.

Beutel, R.G., 1993. Phylogenetic analysis of Adephaga (Coleoptera) based on characters of the larval head. Syst. Entomol. 18, 12–147.

Bonacci, T., Brandmayr, P., Zetto, T., Perrotta, I.D., Guarino, S., Peri, E., Colazza, S., 2011. Volatile compounds released by disturbed and undisturbed adults of *Anchomenus dorsalis* (Coleoptera, Carabidae, Platynini) and structure of the pygidial gland. ZooKeys 81, 13–25.

Booth, A., McIntosh, A.C., Beheshti, N., Walker, R., Larsson, L.U., Copestake, A., 2012. Spray technologies inspired by bombardier beetle. In: Bhushan, Bharat (Ed.), Encyclopedia of Nanotechnology. Springer, Heidelberg, New-York, pp. 2495–2503.

Dean, J., 1979. Defensive reaction time of bombardier beetles. J. Chem. Ecol. 5, 691–701.

Dean, J., 1980a. Effect of thermal and chemical components of bombardier beetle chemical defense: glossopharyngeal response in two species of toads (*Bufo americanus, B. marinus*). J. Comp. Physiol. 135, 51–59.

Dean, J., 1980b. Encounters between bombardier beetles and two species of toads (*Bufo americanus, B. marinus*): speed of prey-capture does not determine success. J. Comp. Physiol. 135, 41–50.

Dettner, K., 1987. Chemosystematics and evolution of beetle chemical defenses. Annu. Rev. Entomol. 32, 17–48.

Deuve, T., 1993. L'abdomen et les genitalia des femelles de Coléoptères Adephaga. Mémoires du Muséum national d'histoire naturelle. Editions du Muséum, Paris.

Di Giulio, A., Maurizi, E., Stacconi, M.V.R., Romani, R., 2012. Functional structure of antennal sensilla in the myrmecophilous beetle *Paussus favieri* (Coleoptera, Carabidae, Paussini). Micron 43, 705–719.

Dierckx, F., 1899. Étude comparée des glandes pygidiennes chez les carabides et les dytiscides avec quelques rémarques sur le classement des carabides. La Cell. 16, 63–176.

Eisner, T., 1958. The protective role of the spray mechanism of the bombardier beetle, *Brachynus ballistarius* Lec. J. Insect Physiol. 2, 215–220.

Eisner, T., Aneshansley, D.J., 1999. Spray aiming in the bombardier beetle: photographic evidence. P. Natl. Acad. Sci. U.S.A. 96, 9705–9709.

Eisner, T., Aneshansley, D.J., 1982. Spray aiming in bombardier beetles: jet deflection by Coanda effect. Science 215, 83–85.

Eisner, T., Aneshansley, D.J., Eisner, M., Attygalle, A.B., Alsop, D.W., Meinwald, J., 2000. Spray mechanism of the most primitive bombardier beetle (*Metrius contractus*). J. Exp. Biol. 203, 1265–1275.

Eisner, T., Aneshansley, D.J., Yack, J., Attygalle, A.B., Eisner, M., 2001. Spray mechanism of crepidogastrine bombardier beetles (Carabidae: Crepidogastrini). Chemoecology 11, 209–219.

Eisner, T., Aneshansley, D.J., del Campo, M.L., Eisner, M., Frank, J.H., Deyrup, M., 2006. Effect of bombardier beetle spray on a wolf spider: repellency and leg autotomy. Chemoecology 16, 185–189.

Eisner, T., Attygalle, A.B., Eisner, M., Aneshansley, D.J., Meinwald, J., 1991. Chemical defense of a primitive Australian bombardier beetle (Carabidae): *Mystropomus regularis*. Chemoecology 2, 29–34.

Eisner, T., Ball, G.E., Roach, B., Aneshansley, D.J., Eisner, M., Blankespoor, C.L., Meinwald, J., 1989. Chemical defense of an ozaenine bombardier beetle from New Guinea. Psyche 96, 153–160.

Eisner, T., Jones, T.H., Aneshansley, D.J., Tschinkel, W.R., Silberglied, R.E., Meinwald, J., 1977. Chemistry of defensive secretions of bombardier beetles (Brachinini, Metriini, Ozaenini, Paussini). J. Insect Physiol. 23, 1383–1386.

Forsyth, D.J., 1968. The structure of the defence glands in the Dytiscidae, Noteridae, Haliplidae and Gyrinidae (Coleoptera). Trans. Zool. Soc. Lond. 120, 159–181.

Forsyth, D.J., 1970. The ultrastructure of the pygidial defence glands of the carabid *Pterostichus madidus* F. J. Morphol. 131, 397–415.

Forsyth, D.J., 1972. The structure of the pygidial defence glands of Carabidae (Coleoptera). Trans. Zool. Soc. Lond. 32, 249–309.

Lai, C., 2010. Potential Applications of the Natural Design of Internal Explosion Chambers in the Bombardier Beetle (Carabidae, *Brachinus*) (Doctoral dissertation). Massachusetts Institute of Technology.

Liebherr, J.K., Will, K.W., 1998. Inferring phylogenetic relationships within Carabidae (Insecta, Coleoptera) from characters of the female reproductive tract. Phylogeny and classification of Caraboidea (Coleoptera: Adephaga). In: Ball, G.E., Casale, A., Taglianti, A.V. (Eds.), International Congress of Entomology, Phylogeny and Classification of Caraboidea (Coleoptera:Adephaga): Proceedings of a Symposium, 28 August 1996, Florence, Italy : XX International Congress of Entomology. Museo regionale di scienze naturali, Torino, pp. 107–170.

Maddison, D.R., Baker, M.D., Ober, K.A., 1999. Phylogeny of carabid beetles as inferred from 18S ribosomal DNA (Coleoptera: Carabidae). Syst. Entomol. 24, 103–138.

Michels, J., Gorb, S.N., 2012. Detailed three-dimensional visualization of resilin in the exoskeleton of arthropods using confocal laser scanning microscopy. J. Microsc. 245, 1–16.

Moore, B.P., Wallbank, B.E., 1968. Chemical composition of the defensive secretion in carabid beetles and its importance as a taxonomic character. Proc. R. Entomol. Soc. Lond. Ser. B 37, 62–72.

Neff, D., Frazier, S.F., Quimby, L., Wang, R.T., Zill, S., 2000. Identification of resilin in the leg of cockroach, *Periplaneta americana*: confirmation by a simple method using pH dependence of UV fluorescence. Arthropod Struct. Dev. 29, 75–83.

Noirot, C., Quennedey, A., 1974. Fine structure of insect epidermal glands. Annu. Rev. Entomol. 19, 61–80.

Noirot, C., Quennedey, A., 1991. Glands, gland cells, glandular units: some comment on terminology and classification. Ann. Soc. Entomol. Fr. 27, 123–128.

Quennedey, A., 1998. Insect epidermal gland cells: ultrastructure and morphogenesis. In: Harrison, F.W., Locke, M. (Eds.), Microscopic Anatomy of Invertebrates: Insecta, vol. 11A. Wiley-Liss, New York, pp. 177–207.

Roach, B., Dodge, K.R., Aneshansley, D.J., Wiemer, D., Meinwald, J., Eisner, T., 1979. Chemistry of defensive secretions of ozaenine and paussine bombardier beetles (Coleoptera: Carabidae). Coleopts. Bull. 33, 17–19.

Schildknecht, H., Holoubek, K., 1961. Die Bombardierkäfer und ihre Explosionschemie V. Mitteilung über Insekten-Abwehrstoffe. Angew. Chem. Ger. Ed. 73, 1–7.

Schildknecht, H., Maschwitz, E., Maschwitz, U., 1968. Die Explosionschemie der Bombardierkäfer (Coleoptera, Carabidae) III. Mitt.: Isolierung und Charakterisierung der Explosionskatalysatoren. Z. Naturforsch. B 23, 1213–1218.

Schildknecht, H., 1970. The defensive chemistry of land and water beetles. Angew. Chem. Int. Ed. 9, 1–9.

Schildknecht, H., Maschwitz, E., Maschwitz, U., 1970. Die Explosionschemie der Bombardierkäfer: Struktur und Eigenschaften der Brennkammerenzyme. J. Insect Physiol. 16, 749–789.

Schnepf, E., Wenneis, W., Schildknecht, H., 1969. Über Arthropoden-Abwehrstoffe XLI. Zur Explosionschemie der Bombardierkäfer (Coleoptera, Carabidae). Z. Zellforsch. Mikrosk. Anat. 96, 582–599.

Will, K.W., Attygalle, A., Herath, K., 2000. New defensive chemical data for ground beetles (Coleoptera: Carabidae): interpretations in a phylogenetic framework. Biol. J. Linn. Soc. 71, 459–481.

Micron 119 (2019) 24–38

Contents lists available at ScienceDirect

Micron

journal homepage: www.elsevier.com/locate/micron

Tutorial

Morpho-functional analysis of the explosive defensive system of basal bombardier beetles (Carabidae: Paussinae: Metriini)

Maurizio Muzzi[a,b], Wendy Moore[c], Andrea Di Giulio[a,b,*]

[a] Department of Science, University Roma Tre, Viale G. Marconi, 446, 00146 Rome, Italy
[b] Laboratorio Interdipartimentale di Microscopia Elettronica (LIME), University Roma Tre, Rome, Italy
[c] Department of Entomology, University of Arizona, Tucson, AZ, United States

ARTICLE INFO

Keywords:
Carabidae
Paussinae
Brachininae
Pygidial glands
FIB/SEM
Ultrastructure

ABSTRACT

Bombardier beetles, belonging to the carabid subfamilies Paussinae and Brachininae, are famous for their unique ability to explosively discharge a hot spray of quinones from their pygidial glands when threatened. The paussine tribe Metriini is broadly acknowledged as the most basal group of bombardiers. In order to complement the available information on the chemical substances and the primitive discharging mechanism of Metriini, we provide a detailed morpho-functional analysis of the explosive defensive system of *Metrius contractus* Eschscholtz, 1829 and *Sinometrius turnai* Wrase and J. Schmidt, 2006, representatives of the two genera in this tribe. We use dissections, histology, scanning electron microscopy (SEM), and focused ion beam microscopy (FIB/SEM) to describe and illustrate various levels of anatomical complexity. FIB/SEM microscopy is used to analyse ultrastructural features of the cellular regions, replacing the classical transmission electron microscopy (TEM). Compared to other Paussinae tribes, Metriini lacks the typical flange of Coanda, the elytral fold used to direct the defensive secretions forward, but has a similar arrangement of internal components. We find that the internal components of the explosive defensive system, including the secretory lobes, collecting duct, reservoir chamber, valve, reaction chamber, accessory chamber and accessory glands, are only slightly different between *Metrius* Eschscholtz, 1829 and *Sinometrius* Wrase and J. Schmidt, 2006. The accessory chamber to the reaction chamber is a unique, derived character state common to all Paussinae examined and therefore represents a clear apomorphy of the Paussinae. We use the same microscopy techniques as used in a recent publication on the Brachininae, to compare the defensive systems of Metriini and Brachininae. We find a lack of morphological similarity at the ultrastructural level, suggesting that the bombarding mechanism may have evolved independently in the Paussinae and the Brachininae, perhaps in response to different ecological pressures.

1. Introduction

Bombardier beetles possess one of the most extraordinary examples of defensive strategies to have evolved in animals: when disturbed, they abruptly produce hot quinones and release them as a caustic spray against offenders and potential predators (Eisner, 1958; Dean, 1980a, b; Eisner et al., 2006). This unique ability is found only in the ground beetle subfamilies Brachininae and Paussinae. Whether the bombarding mechanism evolved once or twice in the history of carabid beetles has been a subject of controversy. Some authors emphasize the astonishing chemical and functional similarities of the two explosive defensive systems and favor a hypothesis that Paussinae and Brachininae are sister groups, and therefore the bombarding mechanism evolved only once (Eisner et al., 1977, 2000, 2001; Aneshansley et al., 1983; Erwin and Sims, 1984; Bousquet, 1986). However, analyses of adult (Forsyth, 1972; Ball and McCleve, 1990; Deuve, 1993; Liebherr and Will, 1998) and larval morphological characters (Beutel, 1992, 1993; Arndt, 1998), have led other authors to hypothesize that Paussinae and Brachininae are more distantly related, and therefore the bombarding mechanism evolved independently. Molecular phylogenetic work has not yet resolved this question, largely because the subfamily Paussinae is subtended by a long branch in trees inferred by molecular sequence data and therefore is prone to long branch attraction issues, and the phylogenetic placement of this subfamily relative to all other carabids is uncertain (Maddison et al., 2009).

The tribe Metriini was finally proven to belong to the subfamily Paussinae only after the discovery of the first instar larva of *Metrius contractus* Eschscholtz, 1829 (Bousquet, 1986). Now it is broadly acknowledged as the most basal group within the Paussinae (Beutel, 1992, 1993; Beutel and Haas, 1996; Di Giulio et al., 2003; Moore,

* Corresponding author at: Department of Science, University Roma Tre, Viale G. Marconi, 446, 00146 Rome, Italy.
E-mail address: andrea.digiulio@uniroma3.it (A. Di Giulio).

https://doi.org/10.1016/j.micron.2019.01.003
Received 29 October 2018; Received in revised form 7 January 2019; Accepted 8 January 2019
Available online 08 January 2019
0968-4328/

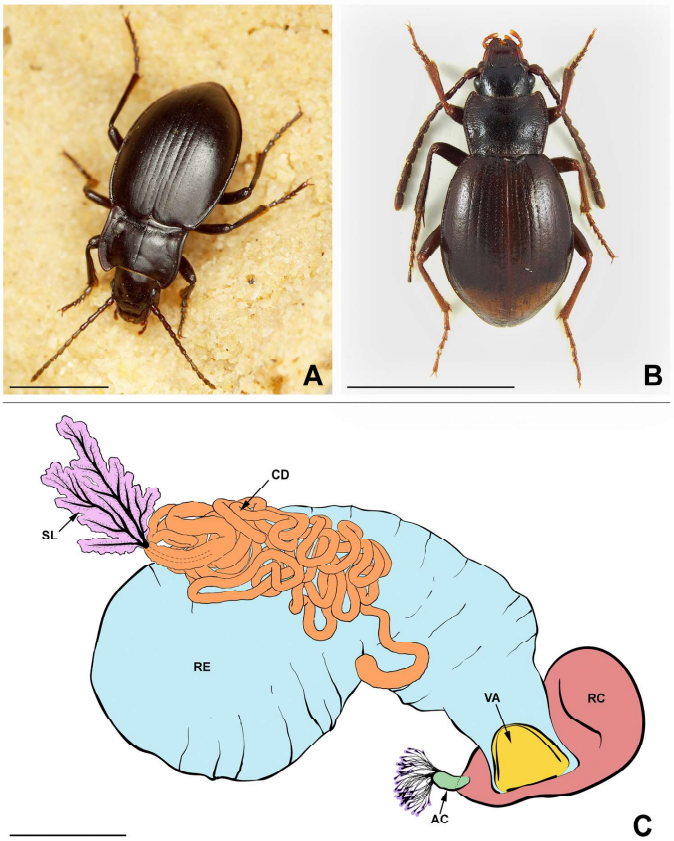

Fig. 1. A. A live specimens of *M. contractus*. B. A dried specimens of *S. turnai*, note the smaller dimension of this species compared to *M. contractus*. C. Schematic drawing of a generalized explosive defensive system of Metriini; different components are highlighted by different colors. AC accessory chamber (green), CD collecting duct (orange), RC reaction chamber (red), RE reservoir chamber (light blue), SL secretory lobe (purple). Scale bars: A = 0.5 cm; B = 0.5 cm; C = 0.5 mm.

2006). Metriini has an amphi-Pacific distribution and is represented by only three extant species classified in two genera: *M. contractus* and *M. explodens* Bousquet and Goulet, 1990 from western North America, and *Sinometrius turnai* Wrase and J. Schmidt, 2006 from China (Wrase and Schmidt, 2006). The peculiar tenebrioid habitus of these species, the fact that they do not have a distinctive cuticular fold along the postero-lateral region of their elytra, and their distribution in the temperate regions of the Northern Hemisphere long concealed that the Metriini belong to the Paussinae (about 800 species).

All other species in this subfamily are found in tropical and sub-tropical regions and are characterized by having a distinctive flange of Coanda, a subapical elytral fold used to precisely aim the hot quinones after they are ejected from their pygidial glands. Eisner and Aneshansley (1982) demonstrated that the elytral flange exploits the Coanda effect, to forwardly aim and channel the ejected chemicals, thereby allowing them to more precisely reach their targets. In contrast, the Metriini release their defensive substances as a froth that clings to a lateral groove on the elytra and the insect's body (Eisner et al., 2000).

While the pygidial defensive system of Metriini has been investigated from chemical and functional aspects, the anatomy has only been studied using optical microscopy on dried dissected specimens (Forsyth, 1972; Deuve, 1993; Eisner et al., 2000; Wrase and Schmidt, 2006). In this paper, we analyse the fine morphology and ultrastructure of the explosive defensive system of *M. contractus* and *S. turnai* using optical, electron and ion beam microscopy. Metriini is acknowledged to be the sister group of the remaining Paussinae, thus comparing their

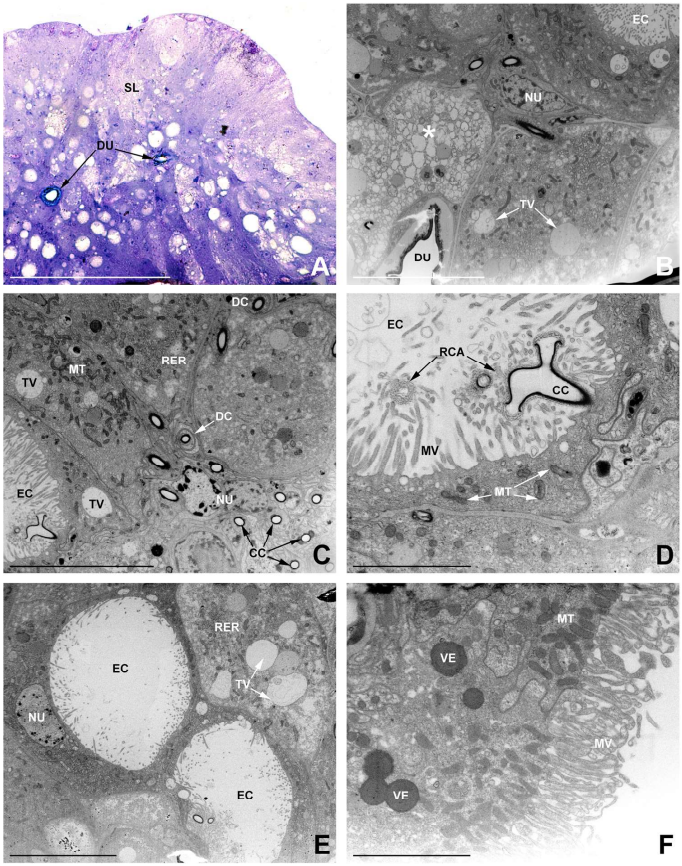

Fig. 2. Secretory lobes anatomy of *M. contractus*. A. Histological section showing the disposition of the secretory cells around ductules. B–F. FIB/SEM analysis of cross sectioned secretory lobe, showing the anatomy of secretory cells, duct cells and ductules at different magnifications. The asterisk (*) in B indicates a degenerating cell. CC conducting canal, DC duct cell, DU ductule, EC extracellular cavity, MT mitochondria, MV microvilli, NU nucleus, SL secretory lobe, RCA receiving canal, RER rough endoplasmic reticulum, TV translucent vesicle, VE vesicle. Scale bars: A = 100 µm; B = 10 µm; C = 10 µm; D = 3 µm; E = 10 µm F = 4 µm.

defensive system with the one of Brachininae, recently described by Di Giulio et al. (2015), is critical to obtain information about the evolution of explosive defensive systems in beetles.

2. Material and methods

Adults of *M. contractus* (Fig. 1A) were hand collected at night from Blodgett Forest Research Station, El Dorado County, California, in September 2012 by Kipling Will. Adults of *S. turnai* (Fig. 1B) were collected by pitfall traps in China, W Hubei Province, in May 2005 by Jaroslav Turna.

Samples were analysed with a Dual Beam (FIB/SEM) Helios Nanolab 600 (FEI Company, Hillsboro, USA) at the electron microscopy laboratory of Roma Tre University (LIME, Rome, Italy). FIB/SEM is an integrated instrument that combines a field emission Scanning Electron Microscope column (SEM) with a Focused Ion Beam column (FIB). The two columns are oriented at 52° and focused on the same point of the sample allowing one to selectively ablate specific regions of the sample. FIB/SEM was used to analyse both the fine morphology of the cuticular regions and the ultrastructure of the explosive defensive system.

For the analysis of the cuticular structures of the defensive system, four abdomens of *M. contractus* (2 males and 2 females) and two of *S.*

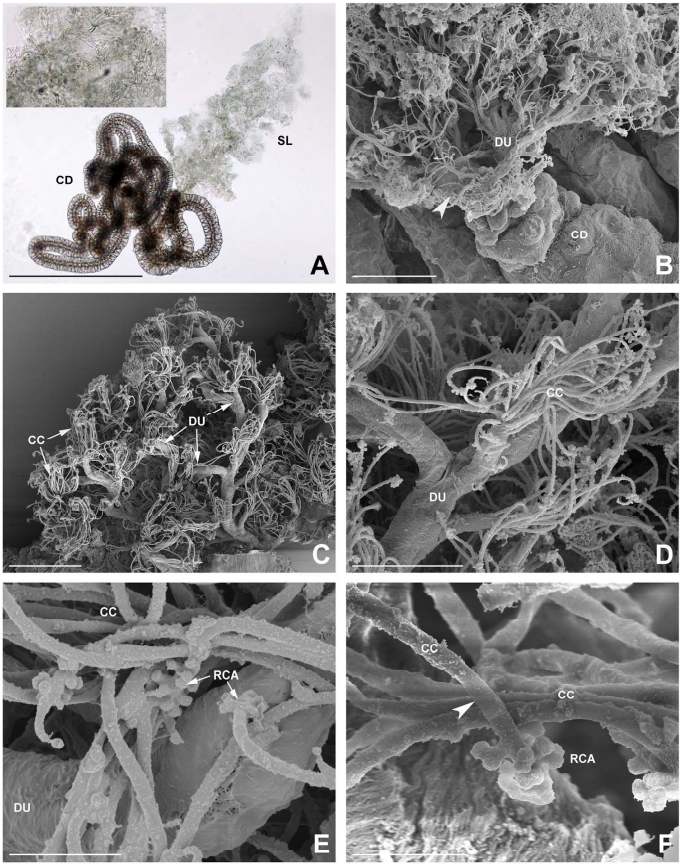

Fig. 3. Secretory lobes structure in *M. contractus*. A. Dissected system after KOH digestion showing the general structure of the secretory lobes and close up of the same (upper-left window), observed at optical microscope. B. Insertion of the ductules in the collecting duct; arrowhead indicates the basal expanded region of the ductule (trunk). C. Apical part of the secretory lobes. D. Close up of C showing the converging conducting canals entering a lateral branch of the ductule. E–F. Close ups of conducting canals and receiving canals, note the smooth transition zone (arrowhead) on the apical part of the conducting canal, just below the receiving canal. CC conducting canals, CD collecting duct, DU ductule, RCA receiving canal, SL secretory lobe. Scale bars: A = 200 µm; B = 50 µm; C = 50 µm; D = 20 µm; E = 5 µm F = 3 µm.

turnai (1 male and 1 female) were detached and treated with an aqueous solution of 10% KOH (at 50 °C) for sufficient time to digest the tissues. After rinsing in distilled water, the different parts of the system were isolated and dehydrated in a graded ethanol series, critical point dried in a CPD 030 unit (BalTec, Balzers, Liechtenstein), and secured to aluminium stubs using conductive adhesive carbon discs. Subsequently, the samples were sputter coated with a thin layer (30 nm) of gold, using a K550 sputter coater (Emithech, Kent, UK) and examined with the SEM column.

For the ultrastructural analysis, four *M. contractus* (2 males and 2 females) were euthanized with CO_2, abdomens were removed from the specimens, submerged in cacodylate buffer 0.1 M and dissected in order to isolate the different components of the system (to facilitate fixation and staining processes). Subsequently, the samples were immersed in Karnovsky's solution for 2 h at 4 °C, post-fixed in 1% osmium tetroxide for 1 h at 4 °C, en bloc stained with 2% aqueous uranyl acetate, dehydrated in a graded ethanol series, and embedded in epoxy resin. Thick sequential slices of about 15–20 µm were obtained with a glass knife on an Ultracut T ultramicrotome (Leica Microsystems, Vienna, Austria) and analysed following the "Slice&Mill" method (Di Giulio and Muzzi, 2018).

Serial semi-thin sections of 1 µm were stained with toluidine blue, viewed with a BX51 light microscope (Olympus, Tokyo, Japan), and photographed with an OM-D E-M5 digital camera (Olympus, Tokyo, Japan).

3. Results

3.1. General structure of the defensive system of Metriini

The explosive defensive system (Fig. 1C) is composed of two symmetrical glandular systems, located dorso-laterally in the posterior part of the abdomen, laying above the reproductive organs and flanking the hindgut. Each system is independent from the other. Each is composed

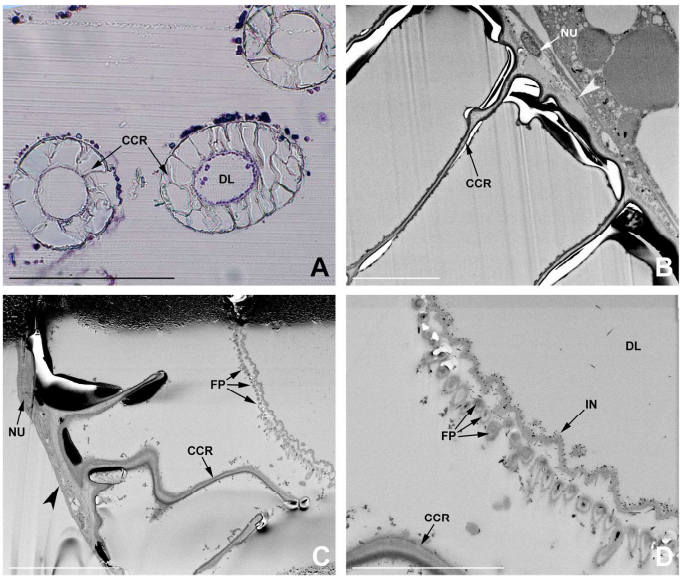

Fig. 4. Collecting duct anatomy of *M. contractus*. A. Histological slice showing different cross sections of the collecting duct. B. Detail of duct in cross section, showing duct cells (arrowhead) and cuticular cristae. C. Detail of the duct showing duct cells (arrowhead), cuticular cristae and medial fringed projections. D. Close up of C, showing the cuticular intima adhering to the fringed cuticular projections. CCR cuticular crista, DL duct lumen, FP fringed projections, IN intima, NU nucleus. Scale bars: A = 100 μm; B = 5 μm; C = 10 μm; D = 4 μm.

of a multilobed secretory tissue that directs secretions into a long coiled collecting duct, which attaches to a sac-like reservoir chamber. A cuticular valve separates the reservoir chamber from a reaction chamber, which is a smaller and more sclerotized compartment with an associated accessory chamber (represented by a minute cuticular sac). The reaction chamber thus receives secretions stored in the reservoir chamber, as well as other secretions produced by numerous accessory glands via the accessory chamber. Each reaction chamber is posteroventrally fused to the ninth latero-tergite and has a lateral opening from which the hot defensive substances are released to the outside via an exit pore. Associated with each exit pore, the grooved elytral epipleuron creates a channel used to forwardly project the substances. In the following, we describe in detail the components of *M. contractus* system, and in subsection 3.8 we compare it to the system of *S. turnai*.

3.2. Secretory lobes

Each secretory system is made of two secretory lobes producing chemical precursors and discharging their secretions into the long collecting duct (Fig. 3A-B). SEM analysis of KOH treated tissues reveals that each secretory lobe, which appears as a cluster of twisted cuticular tubes of various length and diameters, is made of a single cuticular ductule that undergoes many irregular ramifications (Fig. 3A-D). This arborescent ductule includes a moderately short but enlarged area (roughly 25 μm long and 25 μm in diameter) where it inserts into the collecting duct (Fig. 3B). In the secretory lobe, this basal trunk branches out into 2 or 3 long (up to 200 μm) branches of reduced diameter (7–10 μm), which in turn, can split and which leads to branches of similar or slightly reduced diameters (usually ranging between 5 and 7 μm). Both the trunk and the long branches are subdivided into short and fine lateral branches (3–4 μm in diameter and 8–10 μm long). These are the narrowest branches of the ductules and receive in their apical part the secretions produced by groups of 8–20 secretory units (Fig. 3C-D). Each secretory unit, assignable to class III glands cells according to Noirot and Quenneday (1974, 1991), is composed of two cells: a distal secretory cell and a medial duct cell (Fig. 2B-F).

Secretory cells are arranged in a compact glandular tissue, irregular in shape (Fig. 2A); they are almost exclusively located near the smallest branches of the ductule and only a few of them are positioned near the ductule trunk. Secretory cells present a big spherical extracellular cavity (10–15 μm in diameter) with several microvilli and have a peripheral and oval nucleus of approximately 5 × 7 μm (Fig. 2E). Slender mitochondria are abundant and evenly distributed within the cytoplasm and many are often found encircling the outer limits of the extracellular cavity (Fig. 2F). The cytoplasm shows abundant stacks of rough endoplasmic reticulum and many vesicles of various dimensions (ranging from 0.7 to 3 μm in diameter); some of them contain electron dense secretions while others appear filled by an electron lucent content (Fig. 2B-F). Some secretory cells of the examined specimens appear in a degenerative phase, showing altered and disorganized organelles (Fig. 2B).

Duct cells produce conducting canals, thin cuticular ducts receiving and draining the secretions that the secretory cells release in the extracellular cavity. Duct cells are thin and characterized by a strongly diminished cytoplasm, which includes almost exclusively the conducting canal and a heterochromatic nucleus (Fig. 2C). Conducting canals are 20–30 μm long and have a more or less constant diameter (0.6–0.7 μm). All conducting canals enter inside the extracellular cavity of the secretory cells to collect the secretions through a permeable receiving canal, a multi-perforated and porous cuticular structure with a variable number of spherical evaginations (Figs. 2D; 3E-F). The surface of the conducting canals appears moderately rough with the exception

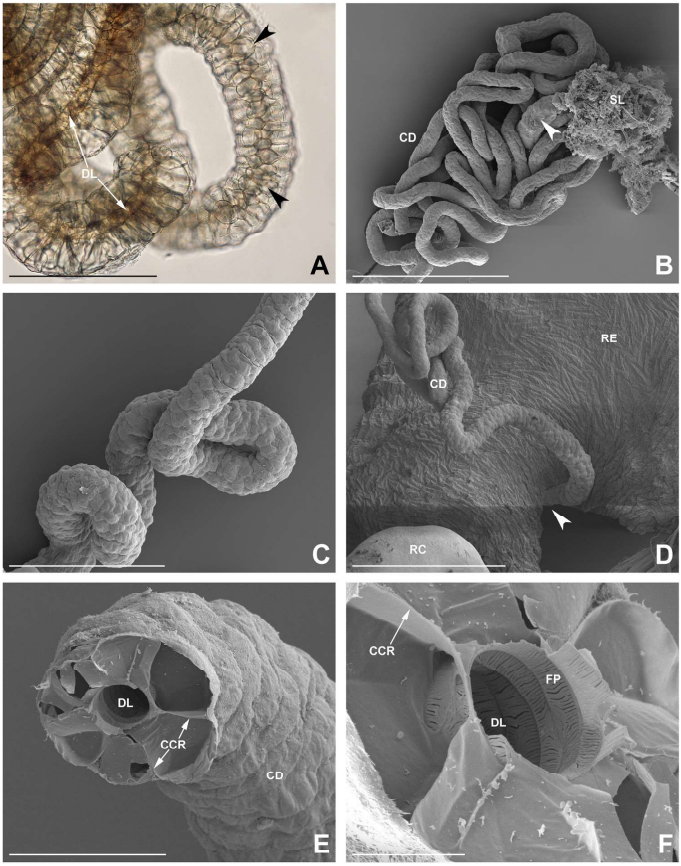

Fig. 5. Fine structure of *M. contractus* collecting duct. A. Dissected system after KOH digestion showing part of the collecting duct; note the bubble-like appearance of the duct wall (arrowheads) and its inner lumen. B. General view of the collecting duct and secretory lobe showing the complex tangled arrangement and the length of the collecting duct; note the augmented diameter of the apical region (arrowhead). C. Loops of the medial part of the collecting duct. D. Basal part of the collecting duct inserting in the reservoir chamber (arrowhead); note the increased diameter and bubble-like appearance of the basal part compared to the rest of the duct. E. Cross-section of the medial part of the collecting duct showing cuticular cristae and the small size of the duct lumen compared to the diameter of the collecting duct. F. Close-up of the duct lumen showing cuticular cristae and the internal fringed projections; the thin cuticular intima was lost after KOH treatment. CCR cuticular crista, CD collecting duct, DL duct lumen, FP fringed projections, RC reaction chamber, RE reservoir chamber, SL secretory lobe. Scale bars: A = 100 μm; B = 500 μm; C = 200 μm; D = 400 μm; E = 40 μm F = 10 μm.

of a small apical transitional area 1 μm long, that is located just prior to the receiving canal (Fig. 3F). Collecting canals of different secretory units converge conveying the carried secretions inside the apex of the small ductule branches (Figs. 2B; 3C-D).

3.3. Collecting duct

The collecting duct (Figs. 4 and 5) is an extremely long cuticular canal (up to 5 times the length of the whole beetle) that coils and tangles on itself for most of its length (Figs. 3A; 5A-B). It is attached apically to the secretory lobes (Figs. 3A; 5B) and basally to the reservoir chamber (Fig. 5D), allowing the transport of the secretions produced by the secretory lobes to the reservoir chamber, where they are stored. The surface of the collecting duct is characterized by a "bubble-like" appearance (Fig. 5A,C) that is particularly pronounced towards the basal and apical regions. The diameter of the duct is 40–45 μm for most of its length with the exception of the basal and apical regions. The basal region is 60 μm in diameter (Fig. 5D), and the apical region 80 μm in diameter, followed by a rapid constriction near the secretory lobes insertion (Fig. 5B). The external diameter of the duct mirrors the diameter of the internal lumen which is 10–12 μm for most of the duct length, roughly 20 μm towards the expanded region near the reservoir chamber and approximately 30 μm at the most expanded apical part.

The collecting duct is formed by a single layer of specific epidermal cells characterized by a strong reduction of cytoplasm, which is mainly filled with a depressed heterochromatic nucleus (Fig. 4B–C). These epidermal cells create epicuticular walls (cristae) that circumscribe bubble-like empty chambers (Figs. 4A-C; 5E-F), which separate the collecting duct from the haemolymph. The arrangement of the epidermal cells and cuticular cristae indicate that the cells form a continuous, radially arranged ring which spirals around the lumen of the collecting duct (Fig. 5E). The internal lumen of the collecting duct is

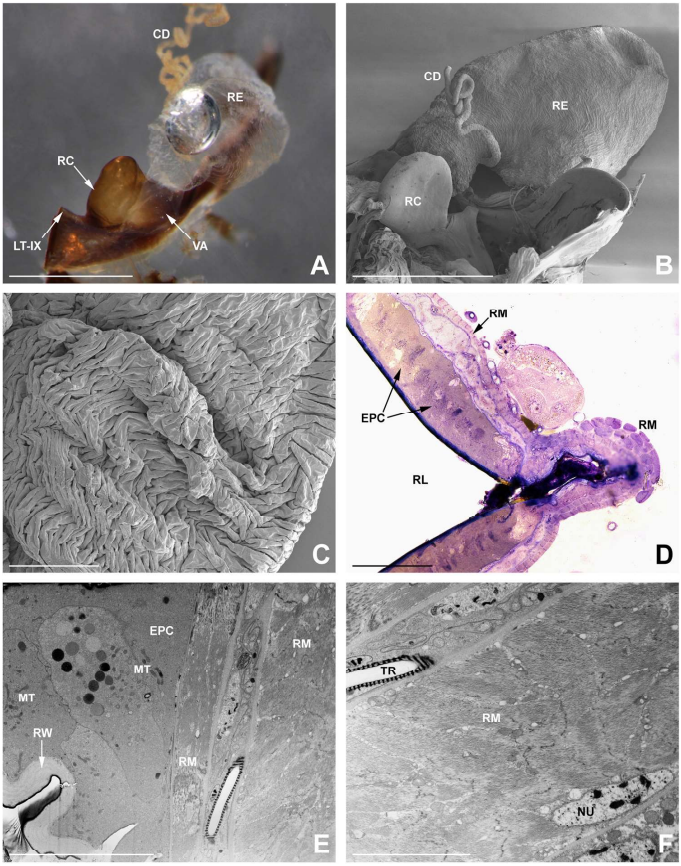

Fig. 6. Fine structure and anatomy of *M. contractus* reservoir chamber. A. Dissected system after KOH digestion showing the light sclerotization of the reservoir compared to the reaction chamber. B. Latero-ventral view of the reservoir. C. Wrinkled surface of an empty reservoir. D. Histological section showing the thick layer of epidermal cells and muscles enclosing the reservoir. E–F. Ultrastructure of epidermal cells and differently oriented muscles. CD collecting duct, EPC epidermal cell, LT-IX ninth laterotergite, MT mitochondria, NU nucleus, RC reaction chamber, RE reservoir chamber, RL reservoir lumen, RM reservoir muscles, RW reservoir wall, TR tracheae, VA valve. Scale bars: A = 1 mm; B = 1 mm; C = 100 µm; D = 20 µm; E = 10 µm F = 5 µm.

surrounded by a thin epicuticular intima (Fig. 4C-D) that prevents the secretions, flowing in the duct lumen, from leaking into the neighbouring bubble-like chambers. The thin layer of intima lays on a scaffold made of parallel cuticular fringes, longitudinally oriented, resulting from cuticular projections of the duct cells (Figs. 4D; 5F).

3.4. Reservoir chamber and valve

The reservoir chamber (Fig. 6) is a pear-shaped compartment with an apical expanded region, gradually tapering toward a shorter tubular area located before the cuticular valve (Fig. 6A-B). The collecting duct enters in the reservoir chamber wall ventrally, between the expanded and tubular regions (Fig. 6B). The reservoir chamber is a cuticular sac, surrounded by a sheath of differently oriented muscles (Fig. 6D-F) and a dense net of tracheal branches. The cuticular lining of the reservoir has two layers (Fig. 6E): the inner layer, in contact with the reservoir lumen, is made of a thin (50–100 nm) electrondense epicuticule; the second layer, in contact with the epidermal cells, is composed of a thick (1–1.3 µm) pale procuticle. The epidermal cells (Fig. 6D-E) are columnar in shape and their cytoplasm contains several mitochondria and inclusions. When the reservoir is emptied, the external surface of its wall appears wrinkled and finely creased (Fig. 6C).

The valve (Fig. 7) is a U-shaped cuticular structure that separates the reservoir chamber from the reaction chamber (Fig. 7A-C); it appears continuous with the reservoir (Fig. 7A-B) and consists of two lightly sclerotized layers of cuticle, one dorsal and one ventral (Fig. 7D-F). The opening of the valve is regulated by muscles, which control the raising and lowering of the dorsal layer.

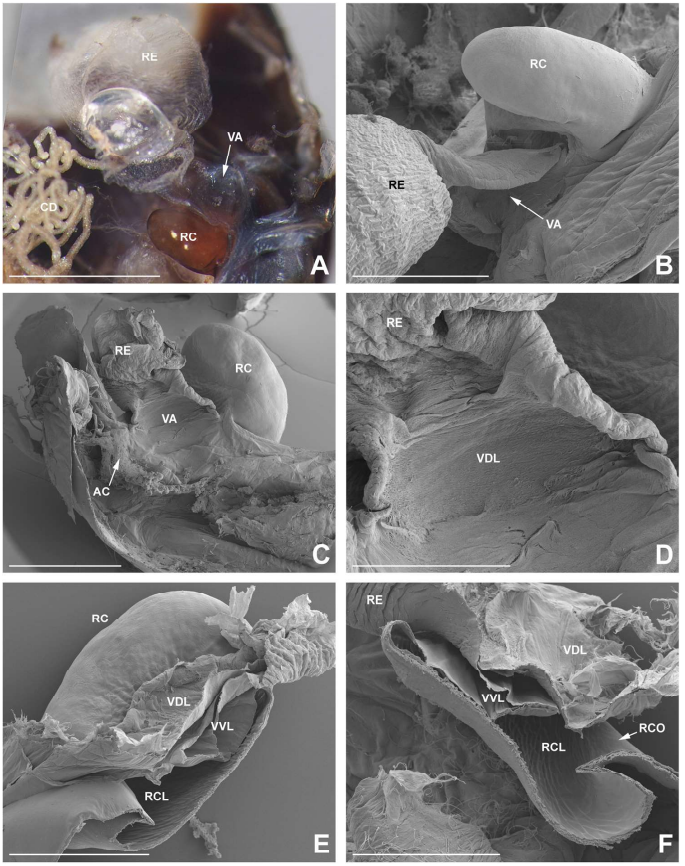

Fig. 7. Fine structure of *M. contractus* valve. A. Dissected system after KOH digestion showing the relative position of the valve between reservoir and reaction chamber. B. Latero-ventral view of the valve. C–D. Dorsal view of the valve. E–F. Cross section of valve and reaction chamber, showing the thickness of the ventral and dorsal layer of the valve; note also the diminished thickness of the reaction chamber, near the valve insertion. AC accessory chamber, CD collecting duct, RC reaction chamber, RCL reaction chamber lumen, RCO reaction chamber opening, RE reservoir chamber, VA valve, VDL valve dorsal layer, VVL valve ventral layer. Scale bars: A = 1 mm; B = 400 μm; C = 500 μm; D = 200 μm; E = 300; F = 200.

3.5. Accessory chamber and accessory glands

The accessory glands are composed of bicellular units discharging their secretions into the accessory chamber (Fig. 8), a cylindrical, blind-ended cuticular outgrowth, dorso-laterally connected directly to the reaction chamber without a valve (Figs. 7C; 8A). Each secretory unit of the accessory glands, composed of a secretory cell and a duct cell, hangs freely in the haemolymph, without forming a true tissue (Fig. 8D-F). Drop-shaped secretory cells present an eccentric ellipsoidal nucleus (roughly 10 x 5 μm) and show a rounded extracellular cavity (approximately 8–12 μm in diameter). The extracellular cavities are lined with microvilli and filled with an electron-dense secretion that is also found inside the conducting canals (Fig. 8E). The cytoplasm of the secretory cells contains abundant stacks of rough endoplasmic reticulum and many slender mitochondria, which are evenly distributed throughout the cell (Fig. 8F).

Duct cells (Fig. 8E, DC) exhibit a marked reduction of cytoplasm and organelles and contain extremely long conducting canals (60–100 μm long; 0.5–0.6 μm diameter) (Fig. 8A-B, CC). Each conducting canal is apically connected to a multi-lobed receiving canal (RCA), an irregular and elongated permeable structure bearing minute spherical evaginations (Fig. 8C). Conducting canals exhibit a rough surface except for a short (0.8 μm long) and smooth transition area that is located just before the receiving canal (Fig. 8C, arrowhead).

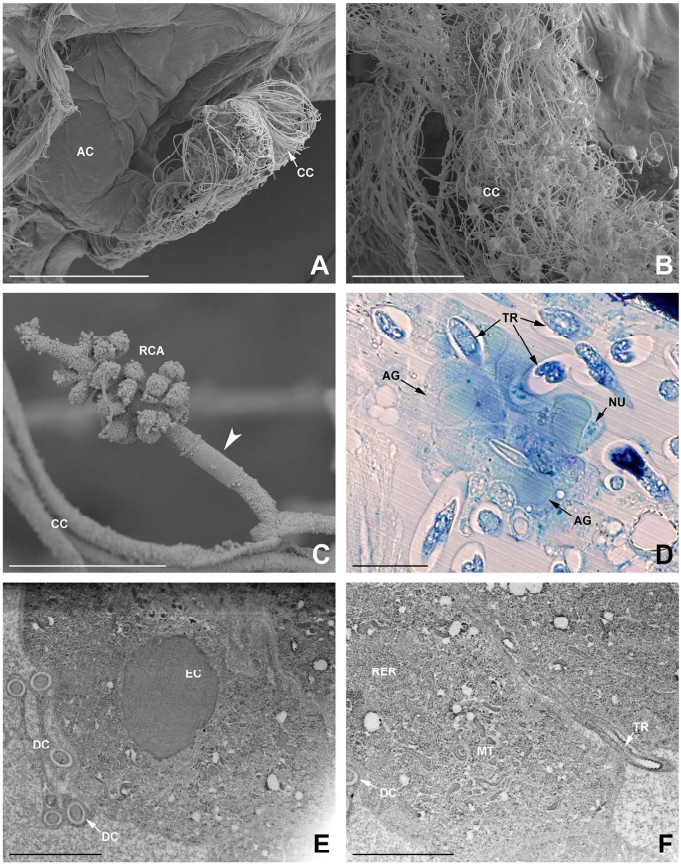

Fig. 8. Fine structure and anatomy of the accessory chamber and related glands in *M. contractus*. A. Lateral view of the accessory chamber showing its cylindrical shape and the apical insertion of the conducting canals of the accessory glands. B. Tangled conducting canals after mild KOH maceration. C. Detail of the multi-lobed receiving canal; note the smooth transition zone (arrowhead) between the conducting canal and the receiving canal. D. Histological section of accessory glands. E–F. Ultrastructure of secretory cells and duct cells. AC accessory chamber, AG accessory glands, CC conducting canal, DC duct cell, EC extracellular cavity, MT mitochondria, NU nucleus, RCA receiving canal, RER rough endoplasmic reticulum, TR tracheae. Scale bars: A = 100 μm; B = 50 μm; C = 4 μm; D = 20 μm; E = 5 μm F = 5 μm.

3.6. Reaction chamber

The reaction chamber (Fig. 9) is a thick-walled reniform pocket, rounded postero-ventrally and slightly tapering anteriorly (Fig. 9A-C). The reaction chamber has an antero-dorsal concavity where the valve inserts (Figs. 7B; 9B). The lateral region of the chamber, instead, is oriented toward a cuticular invagination of the abdomen, visible from outside as a lateral exit pore (Fig. 10B,D). The opening of the reaction chamber is a wide, transverse slot 500 μm long (Fig. 9B) coupled with a curved cuticular margin characterized by fine digitiform microsculpture (Fig. 9D, window). The outer wall of the reaction chamber is smooth (Fig. 9A-D) while the internal surface is covered with wrinkled microsculpture (Fig. 9E-F). The wall of the reaction chamber is evenly thick (7–9 μm), with the exception of a thinner area of 1.5–2 μm located near the valve (Fig. 7E-F).

3.7. Delivery system

Metriini, unlike other Paussinae, do not possess a noticeable flange of Coanda but they still use their elytra to forwardly direct the defensive secretions released from lateral abdominal exit pores (Fig. 10). The elytra have a concave epipleuron (Fig. 10A-B) used to guide the defensive substances forward. This hollowed stripe is narrow near the elytral apex and widens anteriorly. Each elytron and its marginal band is distinctly constricted in the area that corresponds with the exit pore of the internal defensive system (Fig. 10B–C). Near this constricted area, the edge of the marginal band has a small fold (Fig. 10E-F). Each elytron also has a lateral longitudinal groove on the ventral surface (Fig. 10G-I). The groove is flanked by an elongate crista that bears spinulate sculpticels (Fig. 10I).

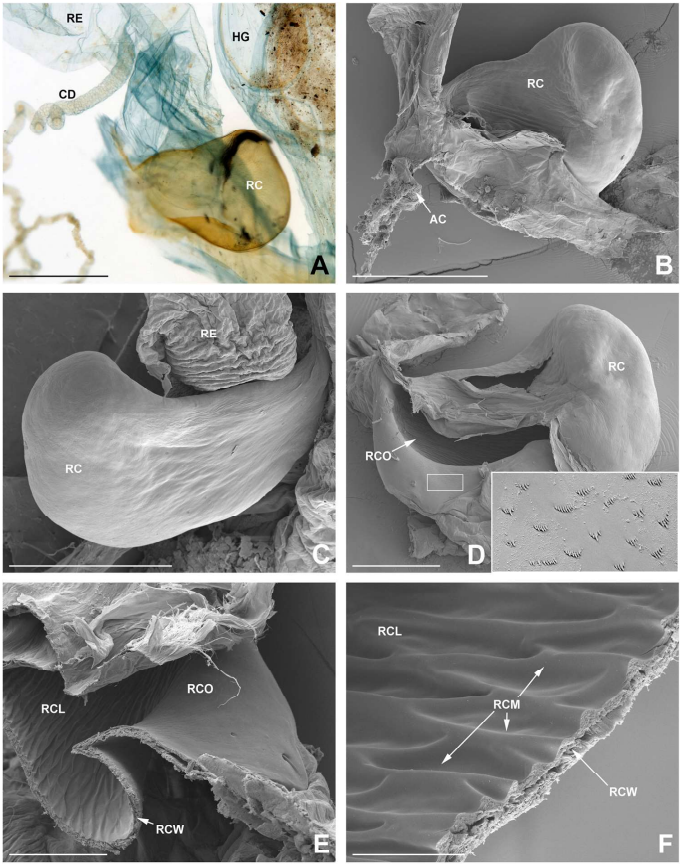

Fig. 9. Anatomy and fine structure of *M.contractus* reaction chamber. A. Dissected system after KOH digestion showing the sclerotization of the reaction chamber compared to the other parts of the system. B. Dorsal view of reaction chamber (valve removed). C. Ventral view of the reaction chamber. D. Dorsal view of the reaction chamber showing the reaction chamber opening; note the fine digitiform microsculpture present on the curved margin (bottom-right window). E. Cross section of the reaction chamber at the level of the opening. F. Cuticular reaction chamber wall showing the thickness of the wall and the wrinkled internal microsculpture. AC accessory chamber, CD collecting duct, HG hindgut, RC reaction chamber, RCL reaction chamber lumen, RCM reaction chamber microsculpture, RCO reaction chamber opening, RCW reaction chamber wall, RE reservoir chamber. Scale bars: A = 500 μm; B = 500 μm; C = 400 μm; D = 250 μm; E = 100 μm F = 20 μm.

3.8. *Pygidial defensive system of S. turnai*

While the overall body size of *S. turnai* is much smaller than *M. contractus* (Fig. 1A-B), the dimensions of each component of their defensive systems (Fig. 11) are almost identical. The general organization of the system is the same for both species, however, there are a few noticeable differences, associated with the collecting duct and reaction chamber. In the following, we briefly compare the two genera.

Secretory lobes. We found no significant differences between the two genera.

Collecting duct. In *S. turnai*, the extremities of the collecting duct (Fig. 11A-D) show loose and distinctly separated cuticular chambers that are not as crowded and appressed to one another as in the rest of the duct. In *M. contractus*, instead, the cuticular chambers of these regions appear more fused and compact.

Reservoir chamber. In *S. turnai* the blind-ended apical region of the reservoir chamber (Fig. 11A) is slender and not as expanded as in *M. contractus*.

Cuticular valve. We found no significant differences between the two genera.

Accessory chambers and accessory glands. We found no significant differences between the two genera.

Reaction chamber. In *S. turnai* the reaction chamber (Fig. 11E-F) is a sub-oval structure, more flattened and less restricted anteriorly compared to *M. contractus*. In addition, the bottom of the reaction chamber of *S. turnai* is longitudinally deeply wrinkled, with the internal surface

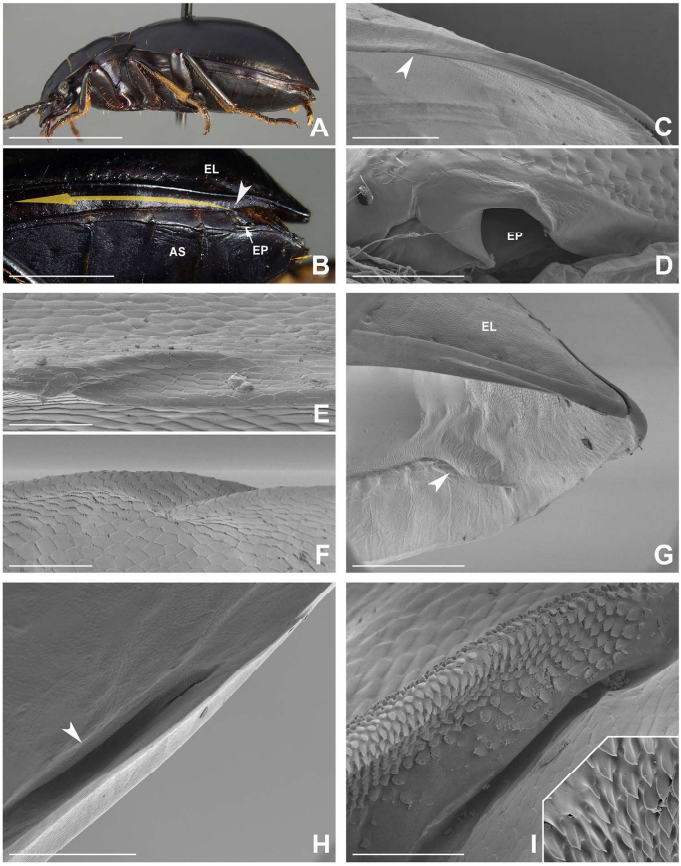

Fig. 10. Fine structure of the delivery system of the defensive spray in *M. contractus*. A. Lateral view of *M. contractus*. B Close up of A, showing the exit pore and the elytral margin, acting as a track for the secretions (yellow arrow); arrowhead indicates the approximate position of the small fold. C. Sub apical margin of elytron in ventro-lateral view; arrowhead indicates the position of the small fold. D. Lateral exit pore. E–F. Ventral (E) and inner (F) view of the small elytral fold. G. Ventro-lateral view of elytra; arrowhead shows spinulated crista. H. Ventral view of the spinulated crista and groove; arrowhead indicates spinulated crista. I. Detail of crista microsculpture; higher magnification in the bottom right window. AS abdominal sternum, EL Elytra, EP exit pore. Scale bars: A = 0.5 cm; B = 0.2 cm; C = 500 μm; D = 500 μm; E = 50 μm F = 50 μm; G = 500 μm; H = 500 μm; I = 50 μm.

bearing sub-parallel cuticular cristae, visible from the external surface as longitudinal furrows.

Delivery system. It is noteworthy that, contrary to *M. contractus*, *S. turnai* does not have the small fold along the elytral epipleuron (Fig. 12); while the longitudinal fold on the ventral surface is shallow.

4. Discussion

The explosive defensive system of Metriini is analysed in detail by using different microscopy techniques and providing for the first time a comprehensive view of the fine morphological and ultrastructural details of representative species of the two genera of this tribe. *M. contractus* and *S. turnai* appear very similar. In fact, the explosive defensive systems of the two genera differ only slightly for the shape of reservoir, reaction chamber and apical region of the duct. However, the simpler structure of the elytra of *S. turnai* is noteworthy, in that it lacks the small fold on the edge and shows only a shallow ventral longitudinal furrow with a small associated crista. We hypothesize that the small fold could be useful to keep the elytra in place during discharge, providing a tighter fit between elytra and abdomen. Alternatively, despite the reduced dimension, the fold could have a role in facilitating the passage of the defensive secretions from the exit pore towards the elytral marginal band. In this respect, it could be considered as an ancestral and incipient flange of Coanda. The spinulated crista, instead, could have an important role in directing the defensive substances towards the marginal band, as it may block the flow of these secretions

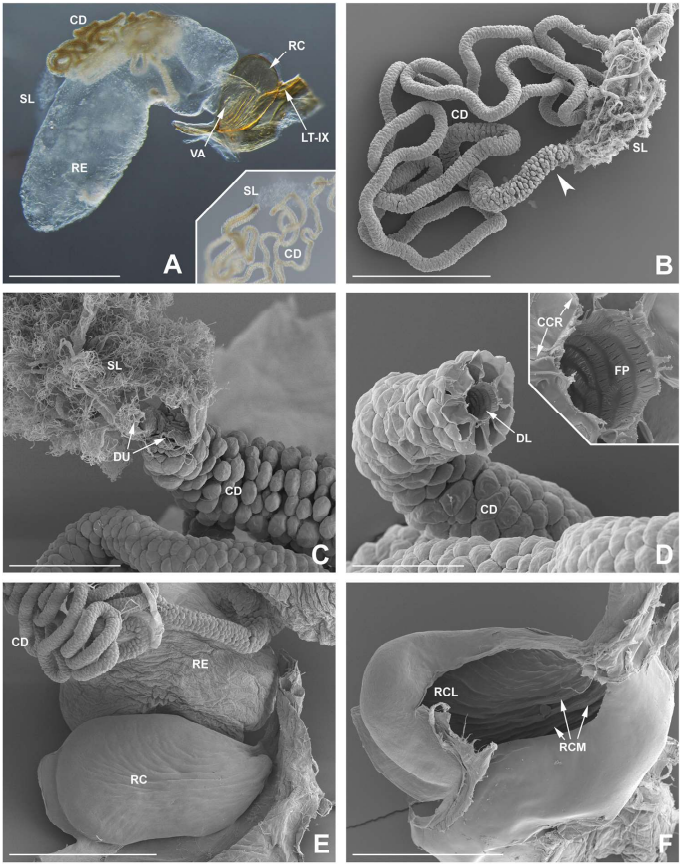

Fig. 11. Fine structure of *S. turnai* explosive defensive system. A. Dissected system after KOH digestion observed at optical microscope, showing the differential sclerotization of the components; the bottom right window shows the secretory lobes and the collecting duct. B. General view of secretory lobes and collecting duct; arrowhead indicates the extreme bubble-like appearance of the apex of duct. C. Insertion of the basal trunk of the ductules in the expanded apical region of the collecting duct. D. Cross-section of the medial part of the collecting duct showing cuticular cristae and the small size of the duct lumen compared to the diameter of the collecting duct; in the upper right window a close-up of the duct lumen showing cuticular cristae and the internal fringed projections, the thin cuticular intima was lost after KOH treatment. E. Ventral view of the reaction chamber. F. Dorsal view of the reaction chamber; valve and reservoir removed to show the internal microsculpture of the reaction chamber. CCR cuticular crista, CD collecting duct, DU ductule, FP fringed projections, LT-IX ninth laterotergite, RC reaction chamber, RCL reaction chamber lumen, RCM reaction chamber microsculpture, SL secretory lobes, VA valve. Scale bars: A = 1 mm; B = 500 μm; C = 100 μm; D = 50 μm; E = 500 μm F = 400 μm.

towards the back of the beetle. The defensive system of *S. turnai* seems to be less refined than that of *M. contractus*, and this is in accordance with other plesiomorphic characters of the adults (pubescence of antennae and abdominal sternum) that suggest a basal phylogenetic condition of *S. turnai* inside Metriini (Wrase and Schmidt, 2006).

Despite broad interest in the explosive defensive system of Paussinae bombardier beetles, very little attention has been paid to their morphology. In fact, the vast majority of studies have focused almost exclusively on the chemical composition of the defensive secretions and the functional aspects of their discharge (Moore and Wallbank, 1968; Eisner et al., 1977, 1989, 1991, 2000; Eisner and Aneshansley, 1982; Aneshansley et al., 1983). Currently, morphological data on the Paussinae explosive defensive system are still surprisingly few, restricted to a reduced number of species (far from being representative of the subfamily diversity) and usually limited to gross morphological information concerning the cuticular part of the system (Raffray, 1892; Escherich, 1898, 1899; Dierckx, 1901; Forsyth, 1972; Eisner et al., 1989, 1991). Some SEM micrographs have been published, but not discussed, in papers dealing with chemistry or functional aspects of the explosive defensive system (Eisner et al., 2000, 2001). The accessory chamber associated with the reaction chamber is missing from most illustrations of the gross anatomy of the paussine defensive system (Eisner et al., 1989, 1991, 2000, 2001; Deuve, 1993). Its presence seems to have been largely forgotten since it was first described and illustrated by Forsyth (1972). This is perhaps due to the very fragile connection between this lightly sclerotized accessory chamber and the

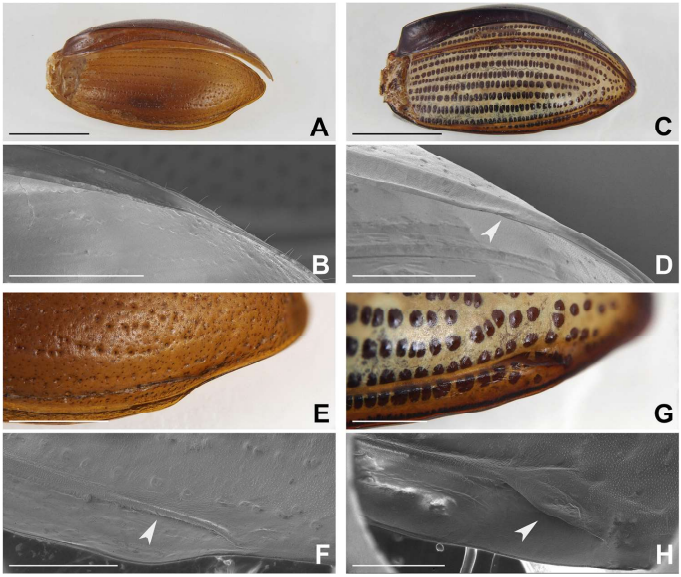

Fig. 12. Comparative morphology of elytra of *S. turnai* and *M. contractus*. A. Elytra of *S. turnai* observed at optical microscope. B. Lateral band of *S. turnai* elytron, note the lack of lateral folding. C. Elytra of *M. contractus* observed at optical microscope. D. Epipleuron of *M. contractus* showing the presence of a small fold (arrowhead). E. Ventral view of *S. turnai* elytron observed at optical microscope. F. Detail of the shallow ventral groove (arrowhead) at SEM. G. Ventral view of *M. contractus* elytron observed at optical microscope. H. Detail of the deep ventral fold (arrowhead) at SEM. A = 0.3 cm; B = 1 cm; C = 0.3 cm ; D = 1 cm; E = 1 cm F = 0.5 cm; G = 1 cm; H = 0.5 cm.

heavily sclerotized reaction chamber which is easily broken during dissections. The accessory chamber to the reaction chamber is a unique, derived character state common to all Paussinae examined and therefore represents a clear apomorphy of the Paussinae. We also note that the defensive systems of Metriini and *Mystropomus* Chaudoir, 1848 are particularly similar, especially with respect to the shape of the reservoirs and reaction chambers (Eisner et al., 1991). Whereas, all other Ozaenini and Paussini are different in that they have bilobed reservoirs and asymmetrical reaction chambers (Forsyth, 1972; Eisner et al., 1989). Ultrastructural and anatomical information at cellular and subcellular levels are completely absent for other species of Paussinae and therefore it is not yet possible to adequately compare ultrastructural features and fine cuticular morphology of the Metriini with those of other paussines.

The results of this work contributes to the debate concerning the evolution of the explosive defensive system in carabid beetles, supplying additional fine morphological and ultrastructural data on the pygidial glands of Metriini and comparing them to the Brachininae defensive system, recently explored in detail by using the same microscopy techniques (Di Giulio et al., 2015). In Table 1 we report the main differences between the two systems, based on the present study and on previously published information (Forsyth, 1972; Deuve, 1993; Eisner et al., 1989, 1991, 2000, 2001).

Our comparative analysis reveals that the systems of Metriini and Brachininae differ in many ways, not only in their position, gross morphology and delivery system, but also in fine cuticular morphology and ultrastructure. Despite the remarkable similarity of the chemical composition of their defensive spray, the lack of morphological similarity between the explosive defensive systems supports the hypothesis that Brachininae and Paussinae independently evolved a bombarding mechanism. Undoubtedly, explosive defensive systems represent a big step forward in efficiency compared to the non-explosive glands of all other adephagan beetles; a distinct advantage that comes at a cost linked to a higher structural complexity and to the production of an increased number of toxic chemicals (including the cytotoxic hydrogen peroxide). We suppose that the evolution of this peculiar strategy might represent a response to an increased predatory pressure. In fact, Brachininae are opportunistic predators or scavengers on organic matter that inhabit riparian zones, areas where they are particularly subject to a vast array of predators such as birds, amphibians, reptiles and small mammals (Eisner, 1958; Dean, 1980a, b; Eisner et al., 2005, 2006; Schaller et al., 2018). On the contrary, it has been demonstrated that *Metrius* is facultatively myrmecophagous (Moore and Di Giulio, 2008), and also *Sinometrius* is partially feeding on ants (Di Giulio and Muzzi, personal observations, gut analysis). Ants are abundant in all terrestrial ecosystems, and they represent a potential source of rich food; nevertheless myrmecophagy is definitively uncommon in beetles since ants are protected by both chemical and behavioural strategies. The ability to feed on ants represents a great advantage for predators but it must be accompanied by defensive strategies that allow them to overcome the aggressiveness of ants and by metabolic pathways aimed at neutralizing their toxicity. We hypothesize that the tenebrioid shape of Metriini and the extreme sclerotization of their bodies may function to protect them from ant attacks during incursions inside ant nests. Similarly, the evolution of an effective explosive defensive strategy could have been very advantageous to escape from the massive attacks of ants.

Table 1
Main differences between Metriini and Brachininae explosive defensive systems based on the present work and previous publications (Forsyth, 1972; Eisner et al., 1989, 1991, 2000, 2001; Deuve, 1993; Di Giulio et al., 2015).

	Metriini Figure numbers refer to the present paper	**Brachininae** Figure numbers refer to Di Giulio et al. (2015)
Secretory Lobes		
glandular tissue shape	compact (neither digitiform nor acinous), with secretory cells irregularly arranged (Fig. 2A)	digitiform, with secretory cells regularly arranged (Fig. 3A-B)
receiving canal shape	multilobed (Figs. 2D; 3E-F)	ovoid (Figs. 3D; 4F)
conducting canals	converging in clusters before entering in the ductules (Fig. 3D)	entering individually without forming clusters (Fig. 4B,D,E)
ductules	arborescent and ramified (Fig. 3A-C)	elongated, without branching or ramification (Fig. 4C,F)
ductules surface	smooth (Fig. 3D)	rough (Fig. 4F)
Collecting Duct		
surface	irregularly swollen with "bubble-like" appearance (Fig. 5A,C)	corrugated (Fig. 6A-B)
intima	laying on numerous cuticular fringes (Fig. 4D)	secured by a reduced number of "match-like" cuticular projections (Figs. 5B-D,F; 6D)
branching	unbranched (Fig. 5B,D)	branched (up to 16 branches) (Fig. 6E)
diameter	widens near the apical and basal regions (Fig. 5D)	constant (for every branch) (Fig. 6A,B,E)
Reservoir Chamber		
shape	piriform (Fig. 6A-B)	bellows like (Fig. 7)
internal cristae	absent (Fig. 6A,D)	present (Fig. 7F)
Valve		
shape	U-shaped made of two thin cuticular layers (Fig. 7E-F)	V-shaped made of two thin cuticular layers (Fig. 8E-F)
Reaction Chamber		
position	lateral (Fig. 6A)	medial (Figs. 1; 2)
shape	asymmetrical, slender, reniform, without a "turret" (Fig. 9A-C)	symmetrical, funnel-shaped, basally cordiform, with an apical turret (Fig. 9B-D)
internal microsculpture	wrinkled and uniform (Fig. 9F)	spiny, complex and variable (Figs. 9A,E-F; 10; 11)
opening shape and position	broad and lateral (Fig. 9D)	relatively small and apical (Fig. 13)
Accessory Chamber		
chamber	present (Fig. 9)	absent (Fig. 9C-D)
Catalase Glands		
shape	drop-shaped (Fig. 8D)	rounded (Fig. 14A)
insertion	inside the accessory chamber (Fig. 8A-B)	inside the reaction chamber (Fig. 15)
Spray Delivery		
method of forward projection of spray	using elytral margin (Fig. 10)	revolving the abdominal tip (Fig. 13)

Acknowledgements

We are grateful to Richard C. Brusca for the helpful comments and suggestions; we thank Roberto Romani for his kind help in preparing some of the samples for electron microscopy and Kipling Will for collecting some of the specimens. We appreciated the comments of three reviewers that improved the manuscript. The research was possible thanks to research grants to A. Di Giulio (CAL, University Roma Tre, Rome, IT) and the co-funding of the Department of Science of Roma Tre University for the use of LIME electron microscopy facilities.

References

Aneshansley, D.J., Jones, T.H., Alsop, D., Meinwald, J., Eisner, T., 1983. Thermal concomitants and biochemistry of the explosive discharge mechanism of some little known bombardier beetles. Experientia 39, 366–368.
Arndt, E., 1998. Phylogenetic investigation of Carabidae (Coleoptera) using larval characters. Phylogeny and classification of Caraboidea (Coleoptera: Adephaga). In: Ball, G.E., Casale, A., Taglianti, A.V. (Eds.), International Congress of Entomology, Phylogeny and Classification of Caraboidea (Coleoptera:Adephaga): Proceedings of a Symposium, 28 August 1996, Florence, Italy: XX International Congress of Entomology. Museo regionale di scienze naturali, Torino. pp. 171–190.
Ball, G.E., McCleve, S., 1990. The middle American genera of the tribe Ozaenini, with notes about the species in southwestern United States and selected species from Mexico. Quest. Ent. 26, 30–116.
Beutel, R.G., 1992. Study on the systematic position of Metriini based on characters of the larval head (Coleoptera: Carabidae). Syst. Entomol. 17, 207–218.
Beutel, R.G., 1993. Phylogenetic analysis of Adephaga (Coleoptera) based on characters of the larval head. Syst. Entomol. 18, 127–147.
Beutel, R.G., Haas, A., 1996. Phylogenetic analysis of larval and adult characters of Adephaga (Coleoptera) using cladistic computer programs. Insect Syst. Evol. 27, 197–205.
Bousquet, Y., 1986. Description of first-instar larva of *Metrius contractus* Eschscholtz (Coleoptera: Carabidae) with remarks about phylogenetic relationships and ranking of the genus Metrius Eschscholtz. Can. Entomol. 118, 373–388.
Dean, J., 1980a. Effect of thermal and chemical components of bombardier beetle chemical defense: glossopharyngeal response in two species of toads (*Bufo americanus, B. marinus*). J. Comp. Physiol. 135, 51–59.
Dean, J., 1980b. Encounters between bombardier beetles and two species of toads (*Bufo americanus, B. marinus*): speed of prey-capture does not determine success. J. Comp. Physiol. 135, 41–50.
Deuve, T., 1993. L'abdomen et les genitalia des femelles de Coléoptères Adephaga. Mémoires du Muséum national d'histoire naturelle. Editions du Muséum, Paris.
Di Giulio, A., Muzzi, M., 2018. Two novel approaches to study arthropod anatomy by using dualbeam FIB/SEM. Micron 106, 21–26.
Di Giulio, A., Fattorini, S., Kaupp, A., Taglianti, A.V., Nagel, P., 2003. Review of competing hypotheses of phylogenetic relationships of Paussinae (Coleoptera: Carabidae) based on larval characters. Syst. Entomol. 28, 509–537.
Di Giulio, A., Muzzi, M., Romani, R., 2015. Functional anatomy of the explosive defensive system of bombardier beetles (Coleoptera, Carabidae, Brachininae). Arthropod Struct. Dev. 44, 468–490.
Dierckx, F., 1901. Les Glandes pygidiennes des Coléoptères. La Cellule 18, 255–310.
Eisner, T., 1958. The protective role of the spray mechanism of the bombardier beetle, *Brachynus ballistarius* Lec. J. Insect Physiol. 2, 215–220.
Eisner, T., Aneshansley, D.J., 1982. Spray aiming in bombardier beetles: jet deflection by Coanda effect. Science 215, 83–85.
Eisner, T., Jones, T.H., Aneshansley, D.J., Tschinkel, W.R., Silberglied, R.E., Meinwald, J., 1977. Chemistry of defensive secretions of bombardier beetles (Brachinini, Metriini, Ozaenini, Paussini). J. Insect Physiol. 23, 1383–1386.
Eisner, T., Ball, G.E., Roach, B., Aneshansley, D.J., Eisner, M., Blankespoor, C.L., Meinwald, J., 1989. Chemical defense of an ozaenine bombardier beetle from New Guinea. Psyche 96, 153–160.
Eisner, T., Attygalle, A.B., Eisner, M., Aneshansley, D.J., Meinwald, J., 1991. Chemical defense of a primitive Australian bombardier beetle (Carabidae): Mystropomus regularis. Chemoecology 2, 29–34.
Eisner, T., Aneshansley, D.J., Eisner, M., Attygalle, A.B., Alsop, D.W., Meinwald, J., 2000. Spray mechanism of the most primitive bombardier beetle (*Metrius contractus*). J. Exp. Biol. 203, 1265–1275.

Eisner, T., Aneshansley, D.J., Yack, J., Attygalle, A.B., Eisner, M., 2001. Spray mechanism of crepidogastrine bombardier beetles (Carabidae: Crepidogastrini). Chemoecology 11, 209–219.
Eisner, T., Eisner, M., Aneshansley, D., 2005. Pre-ingestive treatment of bombardier beetles by jays: food preparation by "anting" and "sand-wiping". Chemoecology 15, 227–233.
Eisner, T., Aneshansley, D.J., del Campo, M.L., Eisner, M., Frank, J.H., Deyrup, M., 2006. Effect of bombardier beetle spray on a wolf spider: repellency and leg autotomy. Chemoecology 16, 185–189.
Erwin, T.L., Sims, L.L., 1984. Carabid beetles of the West Indies (Insects: Coleoptera): a synopsis of the genera and checklists of tribes of Caraboidea, and of the West Indian species. Quaest. ent. 20, 351–466.
Escherich, K., 1898. Zur anatomie und biologie von *Paussus turcicus* Friv.: zugleich ein beitrag zur kenntnis der myrmecophilie. Zoologische Jahrbücher 12, 27–70.
Escherich, K., 1899. Zur Naturgeschichte von *Paussus favieri* Fairm. Verhandlungen der kaiserlich-königlichen zoologisch-botanischen Gesellschaft in Wien 49. pp. 278–283.
Forsyth, D.J., 1972. The structure of the pygidial defence glands of Carabidae (Coleoptera). Trans. Zool. Soc. Lond. 32, 249–309.
Liebherr, J.K., Will, K.W., 1998. Inferring phylogenetic relationships within Carabidae (Insecta, Coleoptera) from characters of the female reproductive tract. Phylogeny and classification of Caraboidea (Coleoptera: Adephaga). In: Ball, G.E., Casale, A., Taglianti, A.V. (Eds.), International Congress of Entomology, Phylogeny and Classification of Caraboidea (Coleoptera:Adephaga): Proceedings of a Symposium, 28 August 1996, Florence, Italy : XX International Congress of Entomology. Museo regionale di scienze naturali, Torino. pp. 107–170.
Maddison, D.R., Moore, W., Baker, M.D., Ellis, T.M., Ober, K.A., Cannone, J.J., Gutell, R.R., 2009. Monophyly of terrestrial adephagan beetles as indicated by three nuclear genes (Coleoptera: Carabidae and Trachypachidae). Zool. Scr. 38, 43–62.
Moore, W., 2006. Molecular Phylogenetics, Systematics, and Natural History of the Flanged Bombardier Beetles (Coleoptera: Adephaga: Carabidae: Paussinae) (PhD Thesis). University of Arizona, Tucson.
Moore, W., Di Giulio, A., 2008. *Metrius* Eschscholtz (Carabidae: Paussinae) is not a millipede specialist. Pan-Pac. Entomol. 84, 33–34.
Moore, B.P., Wallbank, B.E., 1968. Chemical composition of the defensive secretion in carabid beetles and its importance as a taxonomic character. Proc. R. Entomol. Soc. Lond. Ser. B 37, 62–72.
Noirot, C., Quennedey, A., 1974. Fine structure of insect epidermal glands. Annu. Rev. Entomol. 19, 61–80.
Noirot, C., Quennedey, A., 1991. Glands, gland cells, glandular units: some comment on terminology and classification. Ann. Soc. Entomol. Fr. 27, 123–128.
Raffray, A., 1892. Recherches anatomiques sur le *Pentaplatarthrus paussoides* Coléoptère de la famille des Paussides. Nouvelles Archives du Muséum d'histoire naturelle, 3 Série. pp. 91–102.
Schaller, J.C., Davidowitz, G., Papaj, D.R., Smith, R.L., Carrière, Y., Moore, W., 2018. Molecular phylogeny, ecology and multispecies aggregation behaviour of bombardier beetles in Arizona. PLoS One 13, e0205192.
Wrase, D.W., Schmidt, J., 2006. A first representative of the tribe Metriini in the Palaearctic: *Sinometrius turnai* gen. nov., spec. nov. Insecta: Coleoptera: Carabidae: Metriini). In: Hartmann, M., Weipert, J. (Eds.), Biodiversity and Natural Heritage of the Himalaya II. Verein der Freunde und Förderer des Naturkundemuseums Erfurt eV, Erfurt, pp. 315–324.

Chapter 4

The ant nest "bomber": explosive defensive system of the flanged bombardier beetle *Paussus favieri* (Coleoptera, Carabidae)

Maurizio Muzzi[a,b] & Andrea Di Giulio[a,b,*]

[a]. Department of Science, University Roma Tre, Viale G. Marconi, 446, 00146 – Rome, Italy
[b]. Laboratorio Interdipartimentale di Microscopia Elettronica (LIME), University Roma Tre, Rome, Italy
[*]. Corresponding author. Email: andrea.digiulio@uniroma3.it

Keywords: Carabidae, FIB/SEM, Myrmecophily, Paussinae, Pygidial glands, Ultrastructure

Abstract

Bombardier beetles are famous for their unique ability to explosively discharge hot quinones from their pygidial glands when threatened. Here we provide the first detailed description of the ultrastructure of the defensive gland system of the genus *Paussus*, the most speciose genus in the ground beetle subfamily Paussinae. Paussine beetles are commonly known as "flanged bombardier beetles" due to the presence of a flange on their elytra that assists in directing their defensive chemicals toward the front of their bodies. In this paper, we use optical, fluorescence and focused ion beam (FIB/SEM) microscopy to analyse and illustrate anatomy and ultrastructure of the explosive defensive system of *Paussus favieri*, a charismatic myrmecophilous species. The defensive system of this species consists of two independent, symmetrical glands each composed of secretory lobes, a long collecting duct, a bilobed reservoir chamber, a cuticular valve, a sclerotized reaction chamber, and an accessory chamber, associated with the reaction chamber, that is surrounded by several isolated glandular cells. Differences between the pygidial defensive systems of *Paussus favieri* and those of Brachininae are discussed.

1. Introduction

"*...I saw two rare beetles, and seized one in each hand; then I saw a third and new kind, which I could not bear to lose, so that I popped the one which I held in my right hand into my mouth. Alas! it ejected some intensely acrid fluid, which burnt my tongue so that I was forced to spit the beetle out, which was lost, as was the third one.*" Charles Darwin

Bombardier beetles, the only animals capable of sustaining hot explosions inside their bodies (Aneshansley et al., 1969; Arndt et al., 2015), are commonly recognized as having one of the most sophisticated defensive mechanisms documented to date. Each blast is accompanied by an audible "pop", heat, and a fine aerosolized spray resembling swirling smoke, all reminiscent of small cannons, which they aim at their enemies with astonishing accuracy (Eisner and Aneshansley, 1982, 1999).

Since the beginning of the 19th century, this explosive defensive system has attracted the attention of generations of scientists and has been studied as a biomimetic model for several human applications (Beheshti and McIntosh, 2007; Lai, 2010; Booth et al., 2012; Schroeder et al. 2018). Scientists have most thoroughly investigated this system from chemical and functional points of view (Eisner, 1958; Schildknecht and Holoubek, 1961; Moore and Wallbank, 1968; Schildknecht et al., 1968, 1970; Aneshansley et al., 1969, 1983; Schildknecht, 1970; Eisner et al., 1977, 1989, 1991, 2000, 2001; Eisner and Aneshansley, 1982, 1999; Arndt et al., 2015). Most recently, the defensive systems of several genera within the subfamily Brachininae were investigated in detail (Di Giulio et al. 2015b) building upon previous work at a gross morphological level (Forsyth, 1972; Deuve, 1993).

Members of the subfamily Brachininae are the most famous bombardier beetles, but a similar explosive defensive system is also found in all members of the ground beetle subfamily Paussinae. Paussine beetles are commonly known as "flanged bombardier beetles" (Moore, 2006) due to the presence of a unique subapical fold on their elytra which they use to direct the spray toward the front of their bodies (Eisner and Aneshansley, 1982). There are approximately 800 species of Paussinae classified in 4 tribes. The tribe Paussini is the most speciose (with about 600 described species) and contains species that live obligately with ants and contain many highly derived and

bizarre adaptations for this extreme lifestyle (Di Giulio et al., 2009, 2012, 2014, 2015a; Moore and Robertson, 2014; Robertson and Moore, 2017).

The unique similarities between the defensive systems of Brachininae and Paussinae, including the gross structure of the defensive system (especially the unique presence of the reaction chamber in both lineages of bombardier beetles) and the ejected chemicals (mainly benzoquinones, hydrogen peroxide and various hydrocarbons such as alkanes, alkenes and alkadienes) have been stressed in the past as evidence that paussines and brachinines are sister groups (Eisner et al., 1977, 1989, 1991, 2000). However, the phylogenetic relationship between Brachininae and Paussinae remains unclear (Maddison et al., 1999, 2009; Eisner et al., 2000, 2001), and some authors regard the similarities in the defensive systems of the bombardier beetles as products of convergent evolution (Forsyth, 1972; Ball and McCleve, 1990; Beutel, 1993; Arndt, 1998; Liebherr and Will, 1998).

In this paper we use optical, fluorescence and focused ion beam (FIB/SEM) microscopy to analyse the explosive defensive system of the flanged bombardier beetle *Paussus favieri*, a social parasite of *Pheidole pallidula* Forel, and one of the most charismatic beetles in Europe (Fig. 1A). In order to facilitate comparisons between the defensive systems of paussines and brachinines, we followed the same methods and techniques used in our recently published work on Brachininae genera *Brachinus*, *Pheropsophus* and *Aptinus* (Di Giulio et al., 2015b) and on Paussinae genera *Metrius* and *Sinometrius* (Muzzi et al., 2019).

2 Material and Methods

2.1 Material examined

Twelve adults of *Paussus favieri* (6 females and 6 males) were collected in 2010 from nests of *Pheidole pallidula* found under stones in a Mediterranean garigue on the High Atlas Mountains (Tizi-n-Test, about 3 km N to pass, 2063 m elevation, 30.87288° N– 8.36204° W).

2.2. Histology

Two specimens of *Paussus favieri* were anesthetized with CO_2, fixed with Bouin's solution, dehydrated in a graded ethanol series, and embedded in paraffin. Serial sections were cut at 5-7 µm with a rotary microtome CUT 6062 (SLEE, Mainz, Germany) and stained with haematoxylin and eosin. Serial sections were observed and photographed using a BX51 light microscope (Olympus, Tokyo, Japan) equipped with an OM-D E-M5 digital camera (Olympus, Tokyo, Japan).

2.3. Fluorescence microscopy

The presence of resilin, an elastomeric protein that autofluoresces at wavelengths of 420 nm (Neff et al., 2000; Michels and Gorb, 2012), was assessed using fluorescence microscopy. The same slide mounted slices used for the histological analysis were exposed to UV light and observed with an Axio Zoom V16 microscope (Carl Zeiss AG; Oberkochen, Germany) using a DAPI filter. Cuticular regions containing resilin appeared blue under UV excitation. Pictures of the slides were acquired using an Axiocam 503 (Carl Zeiss MicroImaging GmbH, Jena, Germany).

2.4. Focused ion beam/scanning electron microscope (FIB/SEM)

The defensive system of *Paussus favieri* was analysed with a Dual Beam (FIB/SEM) Helios Nanolab 600 (FEI Company, Hillsboro, USA) at the electron microscopy laboratory of Roma Tre University (LIME, Rome, Italy). FIB/SEM is an integrated instrument that combines a field emission Scanning Electron Microscope column (SEM) with a Focused Ion Beam column (FIB). The two columns are oriented at 52° and focused on the same point of the sample allowing us to precisely ablate distinct regions of the sample. FIB/SEM was used to analyse the explosive defensive system of both cleared and uncleared specimens, allowing us to examine the fine morphology of the cuticular regions and the ultrastructure of cellular regions.

For the analysis of the cuticular regions, 4 abdomens of naturally dead beetles were detached and treated with an aqueous solution of 10% KOH (at 50 °C) or a Pancreatin solution (at 36 °C, see Álvarez-Padilla and Hormiga, 2007) for sufficient time to digest the tissues. After rinsing in distilled water, parts of the system were isolated and dehydrated in a graded ethanol series, critical point dried in a CPD 030 unit (BalTec, Balzers, Liechtenstein) and secured to aluminium stubs using conductive adhesive carbon discs. Subsequently the samples were sputter coated with a thin layer (30 nm) of gold, using a K550 sputter coater (Emithech, Kent, UK), and examined with FIB/SEM. FIB milling was used to reveal hidden cuticular region while the SEM column was used to acquire micrographs detecting secondary electrons.

For the ultrastructural analysis, 6 beetles were euthanized with CO_2 prior to dissection. Abdomens were removed, submerged in cacodylate buffer 0.1 M, cut in half (to facilitate fixation and staining processes), immersed in Karnovsky's solution for 2h at 4 °C, post-fixed in 1% Osmium tetroxide for 1h at 4 °C, en bloc stained with 2% aqueous Uranyl acetate, dehydrated in a graded ethanol series and embedded in epoxy resin. Thick sequential slices of about 15-20 µm were obtained with a glass knife on an Ultracut T ultramicrotome (Leica Microsystems, Vienna, Austria) and analysed following the “Slice&Mill” method (Di Giulio and Muzzi, 2018).

3 Results

3.1 General structure of the defensive system

As in all adephagan beetles, the defensive system of *Paussus favieri* (Fig. 1B-C) comprises two symmetrical glandular systems located in the apical part of the abdomen, between the sixth and ninth abdominal segments, dorsal to the reproductive organs and adjacent to the hindgut. Each glandular system is physically and functionally independent of the other. Secretory lobes discharge chemical precursors into a collecting duct, which empties into a voluminous reservoir chamber. A cuticular valve separates the reservoir chamber from the reaction chamber. The reaction chamber is strongly sclerotized and associated with an accessory chamber, a cuticular sac lined by many accessory glands. The reaction chamber is ventrally fused to the lateral margin of the ninth tergite. The exit pore of the defensive system opens near the flange of Coanda, a subapical cuticular fold on each elytron that, exploiting the Coanda's effect, allows the beetle to direct its defensive spray toward the front of its body.

3.2 Secretory lobes

Each secretory system (Figs. 2-3) is made of two secretory lobes, which discharge chemical precursors into the collecting duct (Figs. 2A; 3A-B). SEM analysis of cleared tissues shows that each secretory lobe, appearing as a group of interconnected tubes of different sizes, consists of a single cuticular ductule that undergoes multiple dichotomous splitting and lateral ramification (Figs. 2B-C; 3B-C,E). A first dichotomous division occurs at the base of the ductule, near the insertion in the collecting duct; this division is accompanied by the halving of the ductule diameter that is reduced from 12 to 6 μm (Fig. 3B). The two resulting branches are subjected to other bifurcations that create second and third order branches with an unchanged or slightly reduced calibre (5 μm). All the ductule branches resulting from dichotomous splitting undergo multiple lateral ramifications that lead to a strong reduction of the new branch diameter (Fig. 3C). Usually, for every lateral ramification the diameter is reduced at least by half, leading to the

creation of minute branches with a diameter of 2-3 μm and a length of 5-10 μm. These are the narrowest branches of the ductules and receive in their apical part the secretions produced by groups of 8-20 secretory units (Fig. 3C-D). Each secretory unit, assignable to class III glands cells according to Noirot and Quennedey (1974, 1991) and Quennedey (1998), is composed of two cells, a distal secretory cell (Fig. 2B-F) and a medial duct cell (Fig. 2D).

Secretory cells have a globose shape and create a compact and uniform glandular tissue that is arranged in irregular shaped aggregates (Fig. 2A). Each secretory cell exhibits an ovoidal and elongated extracellular cavity, 5-10 μm in diameter and extending for a length of at least 15 μm. These structures, acting as extracellular reservoirs for the secretions, appear usually filled with microvilli (Fig. 2B,E-F). A big and rounded nucleus, 5-7 μm in diameter, is usually located at the cell base (Fig. 2B). The cytoplasm of these cells contains many electron lucent vesicles, several regions of rough endoplasmic reticulum and abundant mitochondria (Fig. 2B-F). These latter are randomly distributed and have different shapes showing various degrees of elongation and curvature.

Duct cells support the conducting canals, thin cuticular ducts that receive and conduct the secretions released in the extracellular cavity by the secretory cells. Duct cells have a reduced cytoplasm that contains almost exclusively the conducting canal and a heterochromatic and ovoid nucleus, approximately 5 μm in diameter (Fig. 2C). As a result, duct cells appear thin and elongated and are only slightly longer and larger than the canal itself (Fig. 2D). Conducting canals are roughly 15-20 μm long and have a more or less constant diameter of 0,45-0,60 μm; the thickness of the conducting canal cuticle is roughly 100 nm. Each conducting canal penetrates inside the extracellular cavity where its inner part changes into a rounded receiving canal made of several layers of porous epicuticle and usually surrounded by many microvilli (Fig. 2E). Receiving canals are often lost after KOH treatment, but a milder maceration avoided their loss and allowed to confirm the rounded/ellipsoidal shape observed in the ultrastructural analysis (Fig. 3F). Conducting canals are linear isodiametric structures, with a slightly rough and uneven surface. The roughness of cuticle extends the whole length of the conducting canal with the exception of a small apical transitional area of 3 μm, found just before the receiving canal (Fig. 3D). Conducting canals

of different secretory units converge, right before discharging their content, inside the apex of the small ductule branches.

3.3 Collecting duct

Collecting duct (Figs. 4-5) connects the secretory lobes with the reservoir, allowing the transport of the secretions from the secretory lobes to the reservoir, where they are stored. Collecting duct is coiled and its length easily exceeds 4-5cm (Fig. 5A): ten times the length of the whole beetle. Duct is characterized by an irregularly swollen surface, with very pronounced bulges (Figs. 2A; 5B,D), and attaches basally to the reservoir (Figs. 4A; 5C) and apically to the base of the ductules (Fig. 3B). Near these two attachment points, the collecting duct appears noticeably expanded (Figs. 4A; 5A-B): in fact, while its diameter ranges between 20 and 25 μm for most of the length, its cross section doubles at the reservoir insertion (40-45 μm) and triples at the secretory glands level (60 μm). Despite the different external diameter, the calibre of the internal lumen is almost constant (7-9 μm) for the entire duct length, showing only a slight increase at the level of the secretory lobes.

This complex duct is produced by a single layer of modified epidermal cells that, after the completion of the duct, appear depleted of cytoplasm (Fig. 4B). Most of this latter is filled by a flattened irregular nucleus, which contains electron-dense clumps of heterochromatin and appears quite large relative to the size of the cell. Disposition of epidermal cells and analysis of the cuticular part of the duct suggest that the cells form a continuous, radially arranged ring, which spirals around the lumen of the collecting duct (Fig. 5E).

Duct cells produce epicuticular walls (cristae) that circumscribe bubble-like empty chambers (Figs. 4 A-D; 5D-E,G) that insulate the collecting duct from the hemolymph. The internal lumen of the collecting duct is surrounded by a thin epicuticular intima (Fig. 4D-F), separating the lumen from the bubble-like chambers. The epicuticular intima lays on a cuticular scaffold produced by parallel fringes, longitudinally oriented, resulting from cuticular projections of the duct cells (Figs. 4D-F; 5E-G). Some of these projections penetrate inside the intima, securing this latter to the scaffold (Fig. 4E).

3.4 Reservoir chamber

Reservoir chamber is a bilobed compartment (Fig. 6), restricted at the insertion of the collecting duct (Figs. 5C; 6E-F). It is composed by a single cuticular sac, encased in a sheath of differently oriented muscles (Figs. 6A-C; 7A). A dense net of fine tracheal branches penetrates inside the muscular sheath (Fig. 6C). The cuticular lining of the convoluted reservoir shows a double arrangement (Fig. 6B,D). The first layer, in contact with the reservoir lumen, is made of a thin (50-100nm) electrondense epicuticule; the second layer, in contact with the epidermal cells membrane, is made of a thick (300-400 nm) pale procuticle. The epidermal cells (Fig. 6D), flattened and irregular in shape, are characterized by diminished cytoplasm, large depressed nuclei, scarce endoplasmic reticulum and few mitochondria. Although the reservoir may show irregular and moderate folds, its wall does not show projections towards the lumen or septa. The internal surface of the reservoir lacks microsculpture and appears always smooth.

3.5 Valve

The valve (Fig. 7) is a broad cuticular structure that separates the reservoir chamber from the reaction chamber, regulating the entering of reservoir content inside the reaction chamber. The valve appears as an extension of the reservoir (Fig. 7A) and is composed of two strongly sclerotized layers of cuticle, one dorsal and one ventral, tapering towards the reaction chamber (Fig. 7A,C-D). Valve cuticle is thicker compared to the other districts of the glandular system (Fig. 7A), including the reaction chamber. The opening of the valve is due to the raising of the dorsal layer, markedly thicker (3-5 μm) than the ventral one (1,5-3 μm) (Fig. 7C-D), and is controlled by different muscles. A first group of muscles (Fig. 7A), arising from the muscle coat of the reservoir, attaches to the antero-dorsal layer of the valve, while other bundles of tergal muscles connect the postero-dorsal region of the valve with the tergite.

3.6 Accessory chamber

The accessory glands are bi-cellular units discharging their secretions in an accessory chamber (Figs. 8-9), a small bota bag-like pocket (Fig. 9A-B) directly connected dorso-laterally to the reaction chamber without any cuticular valve. The wall of the accessory chamber is much thicker (0,75-1,5 μm) than the reservoir chamber wall (Fig. 8E-F), but similarly composed of two layers: a dark electron-dense epicuticular layer (0,25-0,50 μm) and a pale procuticular layer (0,5-1 μm). The surface of the wall appears smooth and shows an irregular and fine folding (Fig.9 B-C), where most of the glandular units insert (Fig. 9B-C,E). Unlike the reservoir chamber, the external surface of the wall is not directly associated with any muscle (Fig. 8A), but only flattened epidermal cells are present (Fig. 8E-F). However, abdominal muscles are present near the accessory chamber (Fig. 8A,E). Each secretory unit, composed of a secretory cell and a duct cell, hangs freely in the hemolymph, without forming a true tissue (Fig. 8A-C). The spheroidal secretory cells (Fig. 8A-C) show an eccentric and irregular nucleus of conspicuous dimensions (up to 10 μm) and a wide (7-15 μm) and well-developed extracellular cavity (Fig. 8C-D). This latter is filled with a homogeneous electron-dense secretion and is lined by many microvilli. The blind ends of the microvilli converge towards a multi-lobed receiving canal (Figs. 8D; 9D); an irregular and elongated permeable structure, bearing minute spherical evaginations and appearing strongly different from the unbranched and rounded receiving canals of the secretory lobes. The cytoplasm of the secretory cells contains abundant stacks of rough endoplasmic reticulum, several electron dense vesicles and many slightly slender mitochondria that are evenly distributed throughout the cell (Fig. 8B-C). Duct cells (Fig. 8C,E-F), appearing depleted of cytoplasm and organelles, support long and rough surfaced conducting canals (50-120 μm long; 0,5-0,6 μm diameter) (Fig. 9C) that are apically connected to the multilobed receiving canals by a short (0,8 μm) and smooth transition area (Fig. 9D, arrowhead), having the same diameter of the conducting canals. Conducting canals enter individually into the accessory chamber wall (Fig. 9C,E) without forming clusters before the insertion, where the last 3 μm of the conducting canal appears annulated and slightly enlarged. Most of the conducting canals insert in the wider distal part of the accessory chamber (Fig. 9B-C). In correspondence to the insertion of the conducting canal, the smooth internal

surface of the accessory chamber shows pores (Figs. 8E; 9F). Ultrastructural and histological analyses revealed the constant presence of dense and compact secretions inside the accessory chamber (Fig. 8A,E).

3.7 Reaction chamber

The reaction chambers (Figs. 7A; 10-11) are the compartments where the secretions coming from the reservoir chambers are mixed with the secretions stored in the accessory chambers. Each reaction chamber is a thick-walled (Fig.11C-D), drop-like container, composed of a postero-ventral hemispherical region regularly tapering anteriorly (Fig. 10C-D). The whole structure appears curved and shows an anterior concavity where the valve inserts (Fig. 10C). The insertion of the valve, appearing as a thin and curved opening, is located above an area bearing a strong indentation towards the lumen of the reaction chamber (Figs. 7A; 10C). The region of the chamber responsible for spraying outside the defensive secretions is laterally oriented towards a cuticular invagination of the abdomen, visible from outside as a lateral exit pore. The opening of the reaction chamber is represented by a thin, transverse slot 120 µm long (Fig. 10B). The outer wall of the reaction chamber is smooth (Figs. 10C-E; 11C-D) while the internal surface exhibits subtle microsculptures, cuticular cristae and invaginations, defining different functional areas (Figs. 10E; 11C): 1) a dorsal anterior crista creates a slope that lays dorso-laterally, close to the insertion of the accessory chamber, and possibly guides the secretions (of the accessory chambers), from the latero-dorsal opening towards the postero-ventral expanded region of the reaction chamber; 2) an invagination, located just below the entrance of the valve, is probably involved in directing the hot defensive spray towards the slotted opening. These functional areas are both characterized by an irregularly furrowed microsculpture. The area located near the accessory chamber opening shows only a subtle furrowing while the one located below the valve shows a more pronounced, wrinkled and almost alveolate microscluplture.

As illustrated by the histological sections (Fig. 10A), reaction chambers are often filled with a well-stained substance matching the one stored in the accessory chamber. This substance appears particularly condensed and thickened in the most expanded region of the chamber. Samples prepared for

SEM analysis show that this substance can (at least partly) survive a mild KOH treatment, appearing as a dense net of thin filaments that create a spongy and porous matrix crowding the expanded hemi-spherical region of the reaction chamber (Figs. 7C-D; 10F).

The wall of the reaction chamber shows variable thickness ranging from 0,5 to 3 μm. The thinner areas (0,5-1,5 μm) are confined dorso-anteriorly, especially in correspondence to the insertion of the valve, while the thicker regions are localized postero-ventrally at the level of the expanded hemi-spherical region (Fig. 6A). Histological and ultrastructural analyses show that several bundles of tergal muscles connect the expanded region of the reaction chamber to the tergite.

Fluorescence analysis (Fig. 11A-B) highlighted the exceptional presence of resilin throughout the whole reaction chamber wall and, at the same time, showed no evidence of resilin at the level of the valve.

3.8 Flange of Coanda

In *Paussus favieri*, as in most Paussinae, the addressing of the defensive spray, discharged from the lateral slots of the reaction chamber, is achieved thanks to the coupling of an abdominal lateral opening with a sub apical fold of the sclerotized forewings (flange of Coanda) (Fig. 12). The curved flange (Fig. 12A) is characterized by sharp margins and a faint grooved microsculpture (Fig. 12C,E-F). The lightly sclerotized elytra of this species are thin and exhibit a remarkable flexibility that allows them to tightly adhere dorsally, latero-ventrally and posteriorly to the underlying abdomen (Fig. 12A,D). Posteriorly to the flange there is small orifice created by the elytral folding (Fig. 12E-F). The lateral abdominal opening (Fig. 12G), created by the juxtaposition of tergal and sternal folds, underlays that elytral orifice (Fig. 12F, window).

4. Discussion

Paussus favieri is a West-mediterranean species emerging as a model for the entire tribe Paussini, thanks to the recent studies dealing with larval development (Di Giulio et al., 2011), behaviour (Le Masne, 1961; Maurizi et al., 2012), parasitic strategies (Cammaerts, 1990; Di Giulio et al., 2014, 2015a), sensorial organs (Di Giulio et al., 2012) and glandular anatomy (Di Giulio et al., 2009). Below we compare the fine morphology and anatomy of the different components of the explosive defensive system of *P. favieri* with the information available in the literature (Forsyth, 1972; Deuve, 1993; Eisner et al., 1989, 1991, 2000, 2001), especially with those of Paussinae tribe Metriini (Muzzi et al., 2019) and Brachininae (Di Giulio et al., 2015b), that we recently analysed in detail.

Secretory lobes. The arrangement of the secretory cells in *P. favieri* is similar to the one observed in Metriini species *Metrius contractus* as in both cases the glandular tissues are markedly compact and consist of rounded and condensed elements, creating irregular aggregates that greatly differ from the typical elongated lobes or spherical acini found in many carabid beetles (Forsyth, 1972; Giglio et al., 2011). Each element is made of globose cells that irregularly surround the smaller branches of the two ramified ductules. Analogous structures of Brachininae are notably different as the glandular tissue consists of digitiform elements, made up of conical cells that are neatly arranged around multiple unbranched ductules. The nuclei and extracellular cavities of the secretory cells are irregularly distributed within the cytoplasm, while in Brachininae they are always distributed near the basal periphery of the cell. The conducting canals of *P. favieri* and *M. contractus* (respectively a derived and basal Paussinae species) are equally arranged in converging clusters (called “florets” by Eisner et al., 2001), suggesting that this configuration occurs throughout the whole subfamily. The conducting canal arrangement found in *P. favieri* and in other paussines belonging to the Metriini tribe is notably different from the one characterizing Brachininae (except Crepidogastrini), where the conducting canals insert in the ductule lumen individually and without clustering.

Collecting duct. As assessed in previous studies (Eisner et al., 2001; Muzzi et al., 2019), the bulged and swollen surface characterizing the outer wall of *P. favieri* duct is also present in *M. contractus* and *Sinometrius turnai*. Moreover, as observed by Forsyth (1972), the duct of *M. contractus* has a fringed internal region similar to that of *P. favieri*; unfortunately, due to the mere use of an optical microscope, the author was not able to detect the thin cuticular intima of the duct and misinterpreted the fringed area as an inner-coaxial tube in direct contact with the secretions.

We recognized many differences between Paussinae and Brachininae. Paussinae have a single collecting duct and the diameter of the duct is variable along its length (Forsyth, 1972; Eisner et al., 1989, 1991, 2000; Muzzi et al., 2019); whereas Brachininae have either one, two or multiple ducts of constant diameter (Forsyth, 1972; Di Giulio et al., 2015b). Brachininae ducts are proportionally shorter and less tangled than Paussinae where the duct reaches up to ten times the length of the entire beetle. Among the possible explanations of this exaggerated length have been proposed the maturation of the secretions, along with preventing the backflow of the secretions towards the secretory lobes (Forsyth, 1970). In addition, we hypothesize that the extended length could enable the duct to act as a reserve for secretions, allowing a prompt refilling of the reservoir after relaxation of muscles.

Finally, brachinines ducts appear regularly corrugated, instead of swollen as in Paussinae, and the inner cuticular intima, in which secretions flow, is secured by individual match-like cuticular projections instead of a complex fringed cuticular scaffold like the one observed in *P. favieri* and in Metriini beetles.

Reservoir chamber. The reservoir chamber in *P. favieri* and most other Paussinae examined (personal observation) is distinctly bilobous while in *M. contractus* and *S. turnai* appears as a single ovoid chamber (Forsyth, 1972; Eisner et al., 2000; Muzzi et al., 2019). On the contrary, Brachininae display a completely different reservoir: a curved and tubular multi-folded chamber. Our findings in *P. favieri* uncover that the reservoir cuticle does not show pronounced folds or internal incomplete septa (as seen in Brachininae).

Similarly to Brachininae, the muscles encasing the reservoir show different orientation and create 2-3 continuous layers; nevertheless Brachininae demonstrate an increased level of complexity exhibiting also longitudinal strands of muscles that connect adjacent folds of the bellows-like reservoir.

Valve. The valve of *P. favieri* is similar to the one observed in Metriini beetles and significantly different compared to the one of Brachininae. While in *P. favieri, M. contractus* and *S. turnai* the valve is a broad structure that tapers towards the reaction chamber; in Brachininae the valve is narrower near the reservoir and enlarges towards the reaction chamber. In the aforementioned Paussinae beetles the opening of the valve is operated by two different groups of muscles, the first connects the dorsal layer of the valve with the reservoir musculature and the second couples the same valvular district with the tergite of the beetle. Conversely, in Brachininae the opening of the valve relies only on the curved muscles that arise from the reservoir and attach to the dorsal layer of the valve. Additionally, in Paussinae the valve consists of extremely thick layers while in Brachininae the layers are very thin, presenting only small curved region of increased thickness and sclerotization. Another important dissimilarity concerns the presence of resilin in the valve: Brachininae show this protein in the ventral layer while in Paussinae there is no sign of resilin throughout the valve. The exclusive presence of resilin in the Brachininae valve is in line with their unique ejection mechanism that, contrary to Paussinae, allows an extremely fast and repeated pulsed ejection of the spray (Dean et al., 1990; Arndt et al., 2015).

Accessory chamber. The accessory chamber associated with the reaction chamber is missing from most illustrations of the gross anatomy of the paussine defensive system (Eisner et al., 1989, 1991). Its presence seems to have been largely forgotten since it was first described and illustrated by Forsyth (1972). This is perhaps due to the very fragile connection between this lightly sclerotized accessory chamber and the heavily sclerotized reaction chamber which is easily broken during dissections.

P. favieri has an accessory chamber, a cuticular pocket that collects the secretions, likely catalytic enzymes, produced by the accessory glands, so that they can be stored inside this compartment before reaching the reaction chamber. Accessory chamber does not have muscles surrounding it and it does not have a valve separating it from the reaction chamber, so we hypothesize that secretions from this chamber continually pours into the reaction chamber. It might be possible that contraction of the pygidial muscles exerts pressure on this chamber, squeezing the catalytic secretion into the reaction chamber. Forsyth (1972) described a similar sac-like chamber in a dried specimen of *Heteropaussus jeanneli* but did not detect similar structures in other analysed species of dried paussines. Nevertheless also the basal Paussinae species *M. contratus* and *S. turnai*, show a pair of accessory chambers albeit their relative size appears smaller compared to the one of *P. favieri*. Brachininae do not exhibit an accessory chamber as the accessory glands discharge their secretion directly inside the reaction chamber, where the enzymes are gathered in specific regions.

Reaction chamber. The lateral position of the reaction chambers in *P. favieri* is in accordance with the typical arrangement observed in the entire Paussinae subfamily and appears completely different from the medial, apical position characterizing Brachininae. Except for the ovoid chamber of *Metrius* and *Mystropomus* (Eisner et al., 1991, 2000; Muzzi et al., 2019) the shape of the reaction chamber in Paussinae is generally compressed, slender and curved, posteriorly expanded. In brachinines the inner surface of the reaction chamber is covered with complex patterns of cuticular microscuplture which helps maintain the catalytic enzymes inside. Other than the presence of several longitudinal carinae, this surface is smooth in *P. favieri*, this is likely related to the presence of the accessory chamber that stores the enzymatic secretions.

Fluorescence microscopy analysis revealed the presence of resilin throughout the entire sclerotized wall of *P. favieri* reaction chamber. Resilin is an elastic protein that could be of paramount importance to reduce the mechanical stress caused by the internal explosive reactions. On the contrary, the presence of resilin in Brachininae is limited to the apical unsclerotized part of the reaction chamber known as turret (Di Giulio et al., 2015b).

Flange of Coanda. *P. favieri* has a peculiar subapical elytral fold that is found in all Paussinae except for Metriini and it is known as "flange of Coanda". This fold allows the beetle to anteriorly direct the defensive spray due to the Coanda effect, the tendency of moving fluids to cling to curved surfaces and move along them. The position and shape of the flange of Coanda of *P. favieri* differs from that of Ozaenini in that it is not positioned anterior to the exit pore (Eisner and Aneshansley, 1982), but rather overlays the exit pore and has a small orifice which likely funnels the spray into the rest of the flange. The elytral orifice may also prevent dispersion and scattering of the defensive secretions (as it happens in Ozaenini), and is a refinement of the Ozaenini elytral flange which, in turn, represents an effective enhancement compared to the basal non flanged condition of *Metrius* and *Sinometrius* (Eisner et al., 2000; Muzzi et al., 2019).

During the manipulation of living specimens of *P. favieri* we observed that the beetles, when disturbed from one side, spray defensive secretions only from that side, confirming their ability to use the two symmetrical defensive gland systems independently. Nevertheless, when disturbed on the head, the beetles use the right and left explosive defensive glands at the same time.

P. favieri, as all Paussini, is an obligate myrmecophile that spends most of its life inside the ant nest of *Pheidole pallidula*, which is a very well protected environment. Despite this, *P. favieri* not only retains the explosive glands but shows one the most refined explosive defensive system in Paussinae. Crowson (1981) considered the presence of efficient pygidial glands as an essential preadaptation for the evolution of myrmecophily in Paussini. Similarly, the presence of tergal glands has been considered one of the primary preadaptations promoting colony exploitation in aleocharines (Staphylinoidea), one of the most successful groups of myrmecophilous beetles (Parker, 2016). The retention of defensive glands even in myrmecophiles that are highly integrated into the social structure of their host ant colonies has been interpreted as a "backup" mechanism in rare cases when they are detected as foreigners by hosts, and for defense during host colony switches and nest migration (Hölldolber et al., 1981). The presence of explosive defensive glands in Paussinae could represent a preadaptation for the evolution of myrmecophily, which has occurred multiple times within this subfamily (Di Giulio et al., 2003; Moore, 2008; Moore et al., 2011).

Acknowledgements

We are grateful to Prof. Sandra Moreno (University Roma Tre, Rome, Italy) for the help in preparing the biological samples, and Eng. Daniele De Felicis (University Roma Tre, Rome, Italy) for the kind availability and technical assistance in the LIME lab. We thank Prof. Ahmed El Hassani (Institut Scientifique, Université Mohammed V Agdal, Rabat, Morocco) for granting us the permit to collect *Paussus favieri* specimens. The research was possible thanks to the A. Di Giulio research grants (CAL, University Roma Tre, Rome, Italy) and the co-funding of the Department of Science of Roma Tre University for the use of LIME electron microscopy facilities.

References

Alvarez-Padilla, F. and Hormiga, G., 2007. A protocol for digesting internal soft tissues and mounting spiders for scanning electron microscopy. J. Arachnol. 35, 538-542.

Aneshansley, D.J., Eisner, T., Widom, J.M. and Widom, B., 1969. Biochemistry at 100°C: explosive secretory discharge of bombardier beetles (*Brachinus*). Science 165, 61-63.

Aneshansley, D.J., Jones, T.H., Alsop, D., Meinwald, J. and Eisner, T., 1983. Thermal concomitants and biochemistry of the explosive discharge mechanism of some little known bombardier beetles. Experientia 39, 366-368.

Arndt, E., 1998. Phylogenetic investigation of Carabidae (Coleoptera) using larval characters. Phylogeny and classification of Caraboidea (Coleoptera: Adephaga). In: Ball, G.E., Casale, A., Taglianti, A.V. (Eds.), International Congress of Entomology, Phylogeny and Classification of Caraboidea (Coleoptera:Adephaga): Proceedings of a Symposium, 28 August 1996, Florence, Italy: XX International Congress of Entomology. Museo regionale di scienze naturali, Torino, pp. 171-190.

Arndt, E.M., Moore, W., Lee, W.K. and Ortiz, C., 2015. Mechanistic origins of bombardier beetle (Brachinini) explosion-induced defensive spray pulsation. Science 348, 563-567.

Ball, G.E. and McCleve, S., 1990. The middle American genera of the tribe Ozaenini, with notes about the species in southwestern United States and selected species from Mexico. Quest. Ent. 26, 30-116.

Beheshti, N. and McIntosh, A.C., 2007. A biomimetic study of the explosive discharge of the bombardier beetle. Int. J. Des. Nat. Ecodyn. 1, 61-69.

Beutel, R.G., 1993. Phylogenetic analysis of Adephaga (Coleoptera) based on characters of the larval head. Syst. Entomol. 18, 127–147.

Booth, A., McIntosh, A.C., Beheshti, N., Walker, R., Larsson, L.U. and Copestake, A., 2012. Spray technologies inspired by bombardier beetle. In:

Bhushan, Bharat (Ed.), Encyclopedia of Nanotechnology. Springer, Heidelberg, New-York, pp. 2495-2503.

Cammaerts, R., Detrain, C. and Cammaerts, M. C., 1990. Host trail following by the myrmecophilous beetle *Edaphopaussus favieri* (Fairmaire)(Carabidae Paussinae). Insectes Soc. 37, 200-211.

Casale, A., Sturani, M. and Vigna Taglianti, A., 1982. Coleoptera, Carabidae. I. Introduzione, Paussinae, Carabinae. Fauna d'Italia, vol.18. Edizione Calderini, Bologna.

Crowson, R.A., 1981. The Biology of the Coleoptera. Academic Press, London

Dean, J., 1980a. Effect of thermal and chemical components of bombardier beetle chemical defense: glossopharyngeal response in two species of toads (*Bufo americanus*, *B. marinus*). J. Comp. Physiol. 135, 51-59.

Dean, J., 1980b. Encounters between bombardier beetles and two species of toads (*Bufo americanus*, *B. marinus*): speed of prey-capture does not determine success. J. Comp. Physiol. 135, 41-50.

Dean, J., Aneshansley, D.J., Edgerton, H.E. and Eisner, T., 1990. Defensive spray of the bombardier beetle: a biological pulse jet. Science 248, 1219-1221.

Deuve, T., 1993. L'abdomen et les genitalia des femelles de Coléoptères Adephaga. Mémoires du Muséum national d'histoire naturelle. Editions du Muséum, Paris.

Di Giulio, A., Fattorini, S., Kaupp, A., Taglianti, A.V. and Nagel, P., 2003. Review of competing hypotheses of phylogenetic relationships of Paussinae (Coleoptera: Carabidae) based on larval characters. Syst. Entomol. 28, 509-537.

Di Giulio, A., Stacconi, M.V.R. and Romani, R., 2009. Fine structure of the antennal glands of the ant nest beetle *Paussus favieri* (Coleoptera, Carabidae, Paussini). Arthropod Struct. Dev. 38, 293-302.

Di Giulio, A., Maurizi, E., Hlavac, P. and Moore, W., 2011. The long-awaited first instar larva of *Paussus favieri* (Coleoptera: Carabidae: Paussini). Eur. J. Entomol. 108, 127.

Di Giulio, A., Maurizi, E., Stacconi, M.V.R. and Romani, R., 2012. Functional structure of antennal sensilla in the myrmecophilous beetle *Paussus favieri* (Coleoptera, Carabidae, Paussini). Micron 43, 705-719.

Di Giulio, A., Fattorini, S., Moore, W., Robertson, J. and Maurizi, E., 2014. Form, function and evolutionary significance of stridulatory organs in ant nest beetles (Coleoptera: Carabidae: Paussini). Eur. J. Entomol. 111, 692.

Di Giulio, A., Maurizi, E., Barbero, F., Sala, M., Fattorini, S., Balletto, E. and Bonelli, S., 2015a. The pied piper: a parasitic beetle's melodies modulate ant behaviours. Plos one 10 e0130541.

Di Giulio, A., Muzzi, M. and Romani, R., 2015b. Functional anatomy of the explosive defensive system of bombardier beetles (Coleoptera, Carabidae, Brachininae). Arthropod Struct. Dev. 44, 468-490.

Di Giulio, A. and Muzzi, M., 2018. Two novel approaches to study arthropod anatomy by using dualbeam FIB/SEM. Micron, 106, 21-26.

Eisner, T., 1958. The protective role of the spray mechanism of the bombardier beetle, *Brachynus ballistarius* Lec. J. Insect Physiol. 2, 215-220.

Eisner, T., Jones, T.H., Aneshansley, D.J., Tschinkel, W.R., Silberglied, R.E. and Meinwald, J., 1977. Chemistry of defensive secretions of bombardier beetles (Brachinini, Metriini, Ozaenini, Paussini). J. Insect Physiol. 23, 1383-1386.

Eisner, T. and Aneshansley, D.J.,1982. Spray aiming in bombardier beetles: jet deflection by Coanda effect. Science 215, 83-85.

Eisner, T., Ball, G.E., Roach, B., Aneshansley, D.J., Eisner, M., Blankespoor, C.L. and Meinwald, J., 1989. Chemical defense of an ozaenine bombardier beetle from New Guinea. Psyche 96, 153-160.

Eisner, T., Attygalle, A.B., Eisner, M., Aneshansley, D.J. and Meinwald, J., 1991. Chemical defense of a primitive Australian bombardier beetle (Carabidae): *Mystropomus regularis*. Chemoecology 2, 29-34.

Eisner T. and Aneshansley, D.J., 1999. Spray aiming in the bombardier beetle: photographic evidence. P. Natl. Acad. Sci. U.S.A. 96, 9705-9709.

Eisner, T., Aneshansley, D.J., Eisner, M., Attygalle, A.B., Alsop, D.W. and Meinwald, J., 2000. Spray mechanism of the most primitive bombardier beetle (*Metrius contractus*). J. Exp. Biol. 203, 1265-1275.

Eisner, T., Aneshansley, D.J., Yack, J., Attygalle, A.B. and Eisner, M., 2001. Spray mechanism of crepidogastrine bombardier beetles (Carabidae: Crepidogastrini). Chemoecology 11, 209-219.

Eisner, T., Aneshansley, D.J., del Campo, M.L., Eisner, M., Frank, J.H. and Deyrup, M., 2006. Effect of bombardier beetle spray on a wolf spider: repellency and leg autotomy. Chemoecology 16, 185-189.

Forsyth, D.J., 1970. The ultrastructure of the pygidial defence glands of the carabid *Pterostichus madidus* F. J. Morphol. 131, 397-415.

Forsyth, D.J., 1972. The structure of the pygidial defence glands of Carabidae (Coleoptera). Trans. Zool. Soc. Lond. 32, 249-309.

Giglio, A., Brandmayr, P., Talarico, F. and Brandmayr, T.Z., 2011. Current knowledge on exocrine glands in carabid beetles: structure, function and chemical compounds. ZooKeys 193.

Hölldolber, B., Möglich, M. and Maschwitz, U., 1981. Myrmecophilic relationship of *Pella* (Coleoptera: Staphylinidae) to *Lasius fuliginosus* (Hymenoptera: Formicidae). Psyche 88, 347-374.

Lai, C., 2010. Potential Applications of the Natural Design of Internal Explosion Chambers in the Bombardier Beetle (Carabidae, *Brachinus*) (Doctoral dissertation). Massachusetts Institute of Technology.

Le Masne, G., 1961. “Recherches sur la biologie des animaux myrmécophiles IV: observations sur le comportement de *Paussus favieri* Fairm., hôte de la fourmi *Pheidole pallidula* Nyl.,”. Ann. Fac. Sci. Marseille 31, 111-130.

Liebherr, J.K., Will, K.W., 1998. Inferring phylogenetic relationships within Carabidae (Insecta, Coleoptera) from characters of the female reproductive tract. Phylogeny and classification of Caraboidea (Coleoptera: Adephaga). In: Ball, G.E., Casale, A., Taglianti, A.V. (Eds.), International Congress of Entomology, Phylogeny and Classification of Caraboidea (Coleoptera:Adephaga): Proceedings of a Symposium, 28 August 1996, Florence, Italy : XX International Congress of Entomology. Museo regionale di scienze naturali, Torino, pp. 107-170.

Maddison, D.R., Baker, M.D. and Ober, K.A., 1999. Phylogeny of carabid beetles as inferred from 18S ribosomal DNA (Coleoptera: Carabidae). Syst. Entomol. 24, 103-138.

Maddison, D.R., W. Moore, M.D. Baker, T.M. Ellis, K.A. Ober, J.J. Cannone, and R.R. Gutell. 2009. Monophyly of terrestrial adephagan beetles as indicated by three nuclear genes (Coleoptera: Carabidae and Trachypachidae). Zool. Scr. 38, 43–62.

Maurizi, E., Fattorini, S., Moore, W. and Di Giulio, A., 2012. Behavior of *Paussus favieri* (Coleoptera, Carabidae, Paussini): a myrmecophilous beetle associated with *Pheidole pallidula* (Hymenoptera, Formicidae). Psyche.

Michels, J. and Gorb, S.N., 2012. Detailed three-dimensional visualization of resilin in the exoskeleton of arthropods using confocal laser scanning microscopy. J. Microsc. 245, 1-16.

Moore, B.P. and Wallbank, B.E., 1968. Chemical composition of the defensive secretion in carabid beetles and its importance as a taxonomic character. Proc. R. Entomol. Soc. Lond. Ser. B 37, 62-72.

Moore, W., 2006. Molecular phylogenetics, systematics, and natural history of the flanged bombardier beetles (Coleoptera: Adephaga: Carabidae: Paussinae) (PhD thesis). Tucson: University of Arizona.

Moore, W., 2008. Phylogeny of the western Hemisphere Ozaenini (Coleoptera: Carabidae: Paussinae) based on DNA sequence data. Ann. Carnegie Mus. 77, 79-92.

Moore, W., Song, X. B. and Di Giulio, A., 2011. The larva of *Eustra* (Coleoptera, Paussinae, Ozaenini): a facultative associate of ants. ZooKeys 90, 63-82.

Moore, W. and Robertson, J.A., 2014. Explosive adaptive radiation and extreme phenotypic diversity within ant-nest beetles. Curr. Biol., 24, 2435-2439.

Muzzi, M., Moore, W. and Di Giulio, A., 2019. Morpho-functional analysis of the explosive defensive system of basal bombardier beetles (Carabidae: Paussinae: Metriini). Micron 119, 24-38.

Neff, D., Frazier, S.F., Quimby, L., Wang, R.T. and Zill, S., 2000. Identification of resilin in the leg of cockroach, *Periplaneta americana*: confirmation by a simple method using pH dependence of UV fluorescence. Arthropod Struct. Dev. 29, 75-83.

Noirot, C. and Quennedey, A., 1974. Fine structure of insect epidermal glands. Annu. Rev. Entomol. 19, 61-80.

Noirot, C. and Quennedey, A., 1991. Glands, gland cells, glandular units: some comment on terminology and classification. Ann. Soc. Entomol. Fr. 27, 123-128.

Parker, J., 2016. Myrmecophily in beetles (Coleoptera): evolutionary patterns and biological mechanisms. Myrmecol. News 22, 65-108.

Quennedey, A., 1998. Insect epidermal gland cells: Ultrastructure and morphogenesis. In: Harrison, F.E., Locke, M. (eds.), Microscopic Anatomy of Invertebrates, Vol. 11A, Insects. Wiley-Liss, New York, pp. 177-207.

Roach, B., Dodge, K.R., Aneshansley, D.J., Wiemer, D., Meinwald, J. and Eisner, T., 1979. Chemistry of defensive secretions of ozaenine and paussine bombardier beetles (Coleoptera: Carabidae). Coleopts. Bull. 33, 17-19.

Robertson, J.A. and Moore, W., 2017. Phylogeny of *Paussus* L. (Carabidae: Paussinae): unravelling morphological convergence associated with myrmecophilous life histories. Syst. Entomol. 42, 134-170.

Schildknecht, H. and Holoubek, K., 1961. Die Bombardierkäfer und ihre Explosionschemie V. Mitteilung über Insekten-Abwehrstoffe. Angew. Chem. Ger. Ed. 73, 1-7.

Schildknecht, H., Maschwitz, E. and Maschwitz, U., 1968. Die Explosionschemie der Bombardierkäfer (Coleoptera, Carabidae) III. Mitt.: Isolierung und Charakterisierung der Explosionskatalysatoren. Z. Naturforsch. B 23, 1213-1218.

Schildknecht, H., 1970. The defensive chemistry of land and water beetles. Angew. Chem. Int. Ed. 9, 1-9.

Schildknecht, H., Maschwitz, E. and Maschwitz, U., 1970. Die Explosionschemie der Bombardierkäfer: Struktur und Eigenschaften der Brennkammerenzyme. J. Insect Physiol. 16, 749-789

Schroeder, T.B., Houghtaling, J., Wilts, B.D. and Mayer, M., 2018. It's Not a Bug, It's a Feature: Functional Materials in Insects. Advanced Materials, 30, 1705322.

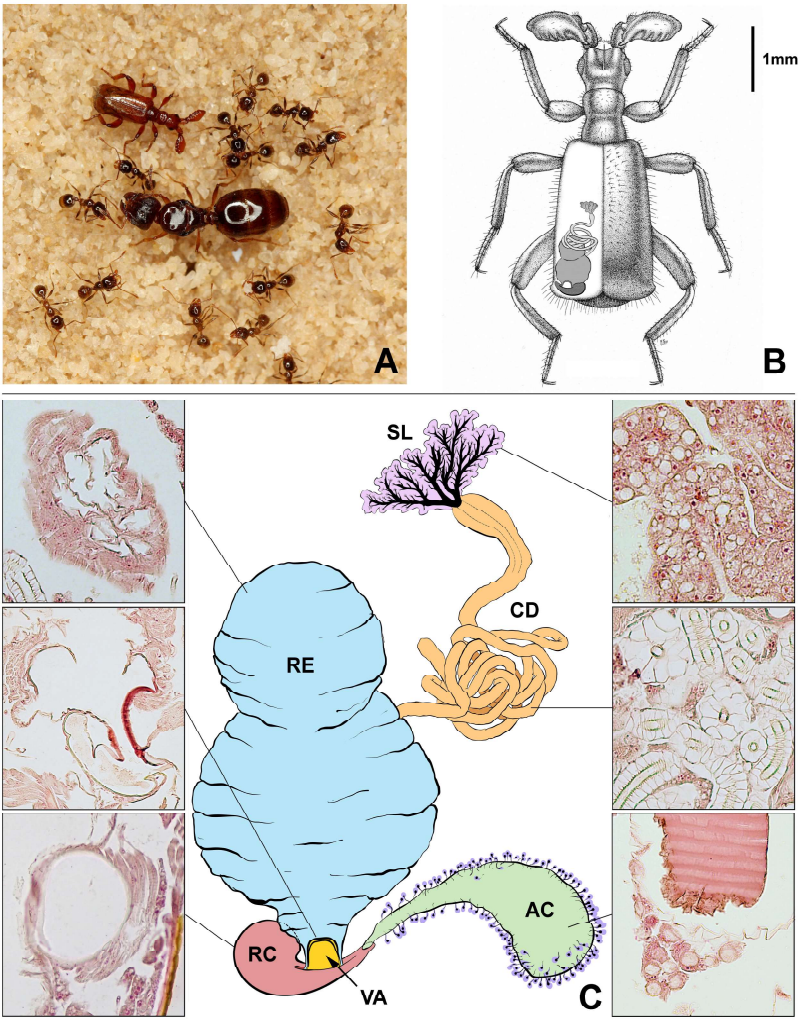

Figure 1

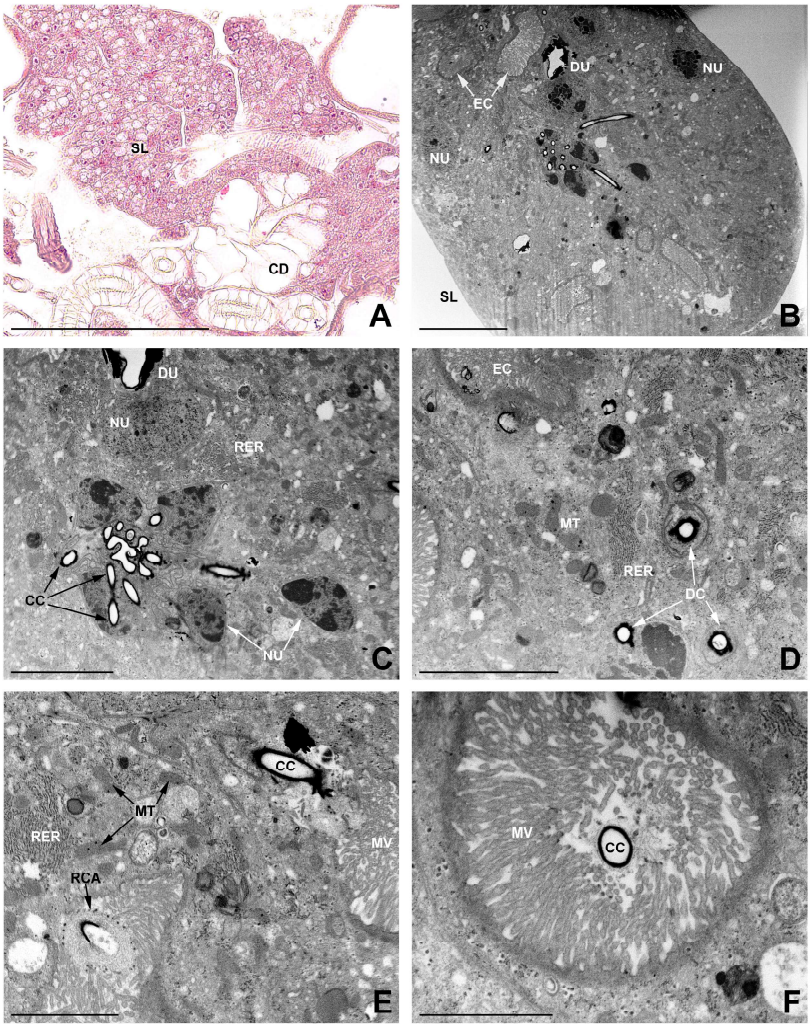
SL
CD
A
DU
NU
EC
NU
SL
B
DU
NU
RER
CC
NU
C
EC
MT
RER
DC
D
CC
MT
RER
MV
RCA
E
MV
CC
F

Figure 2

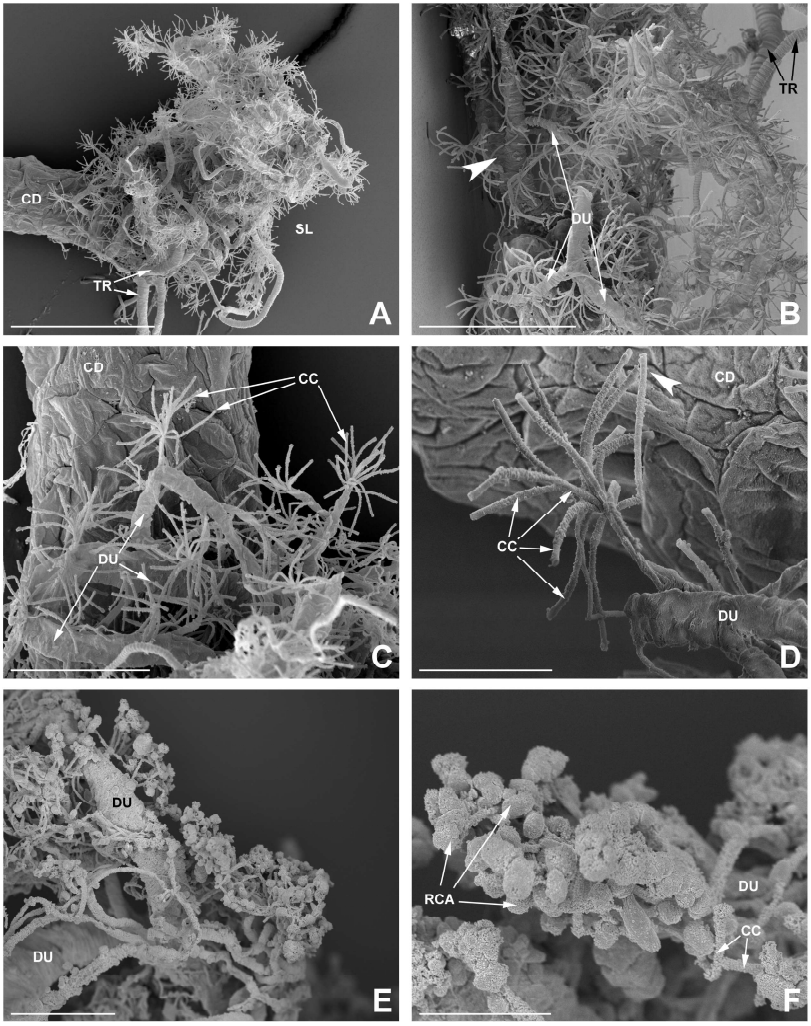

Figure 3

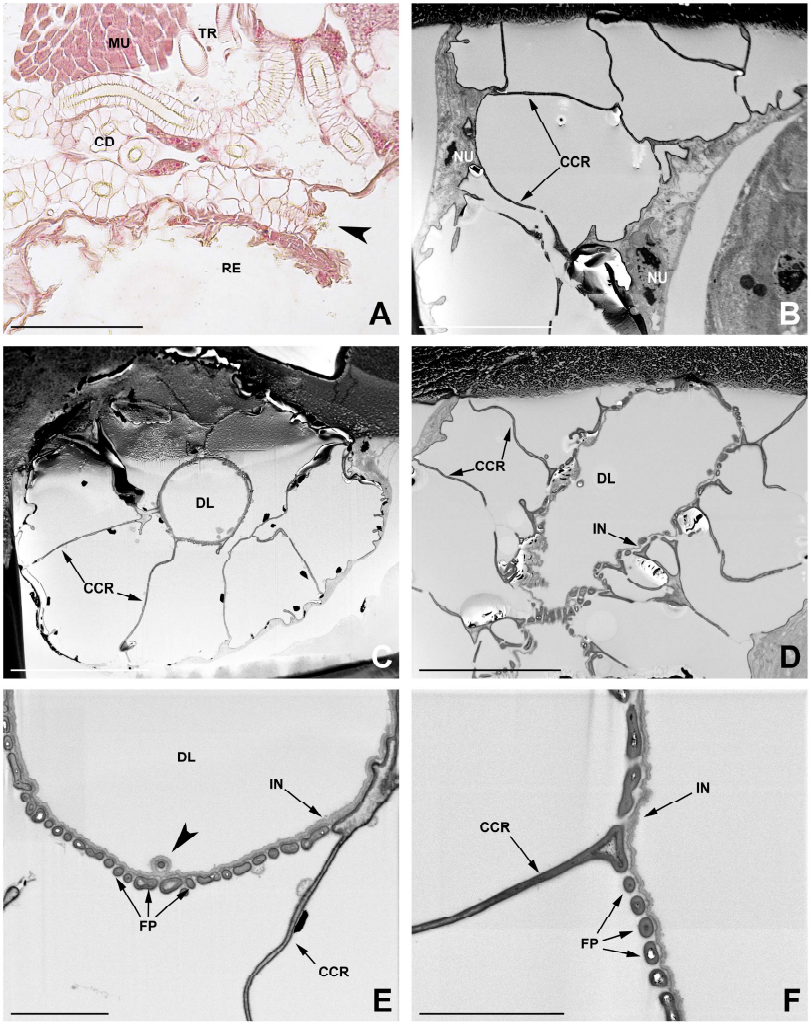

Figure 4

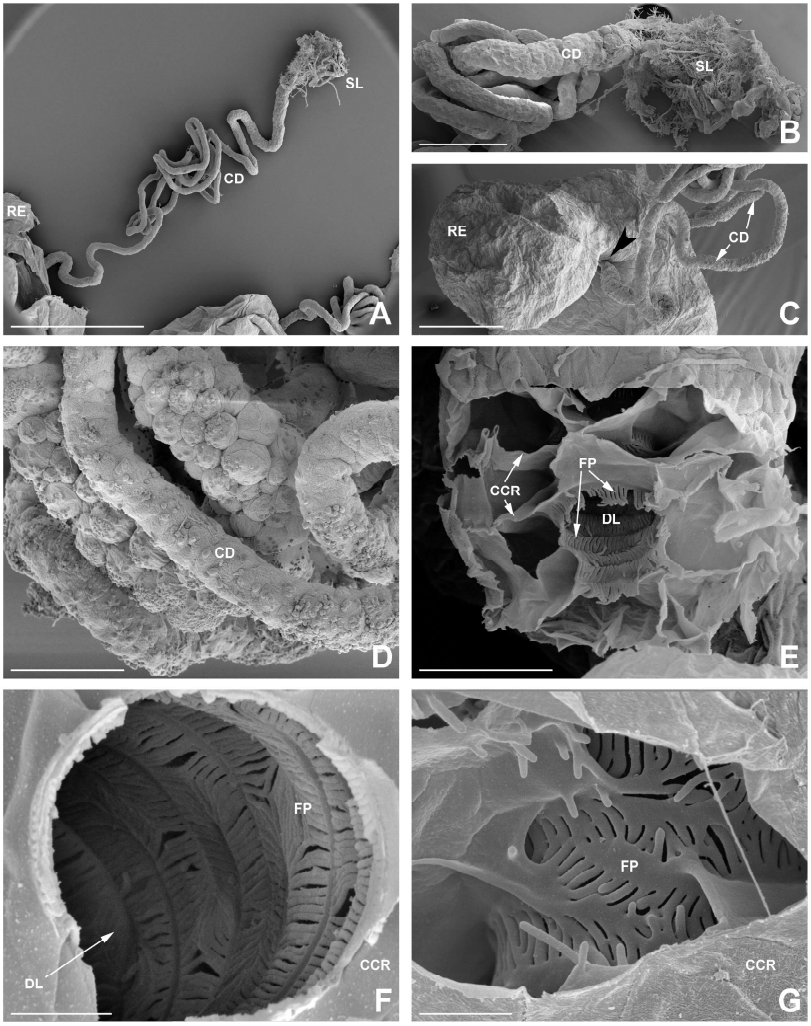

Figure 5

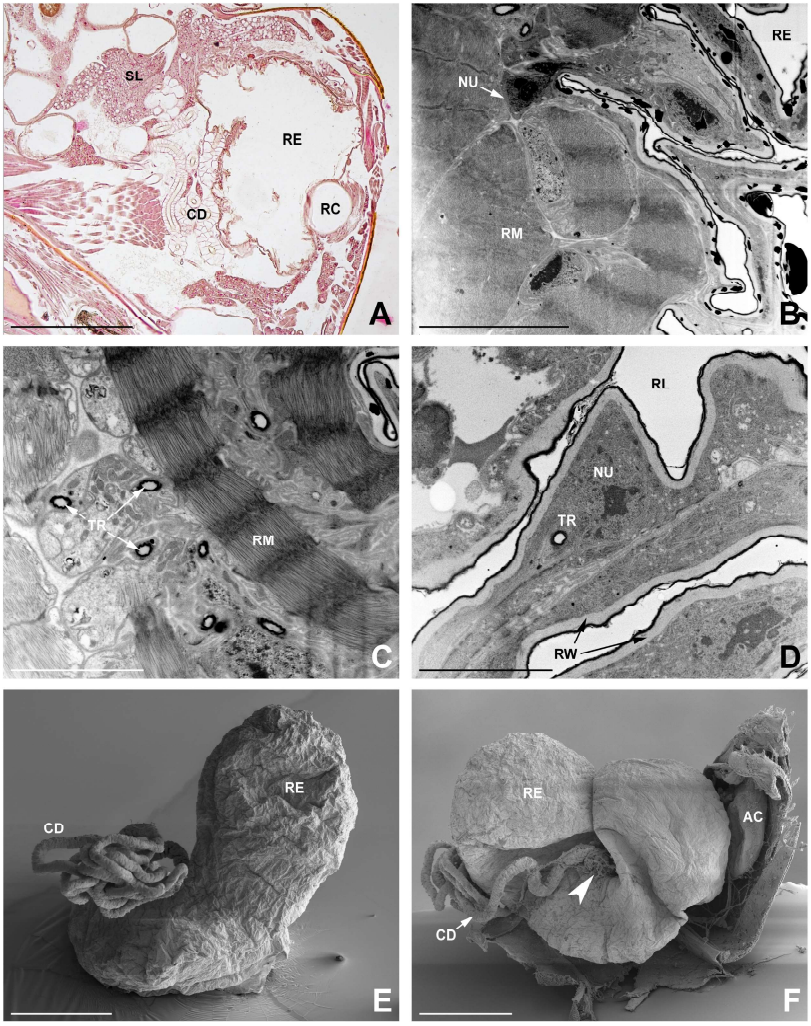

Figure 6

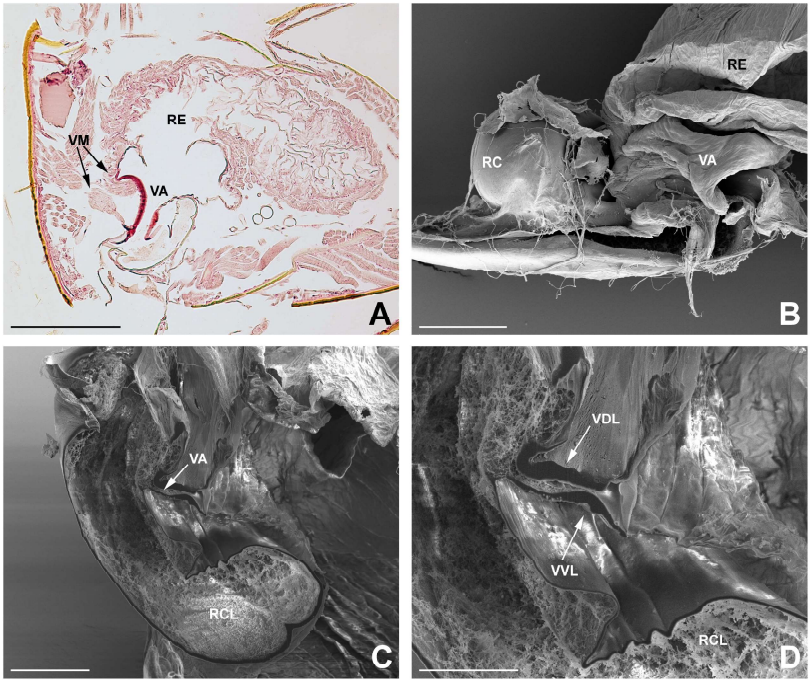

Figure 7

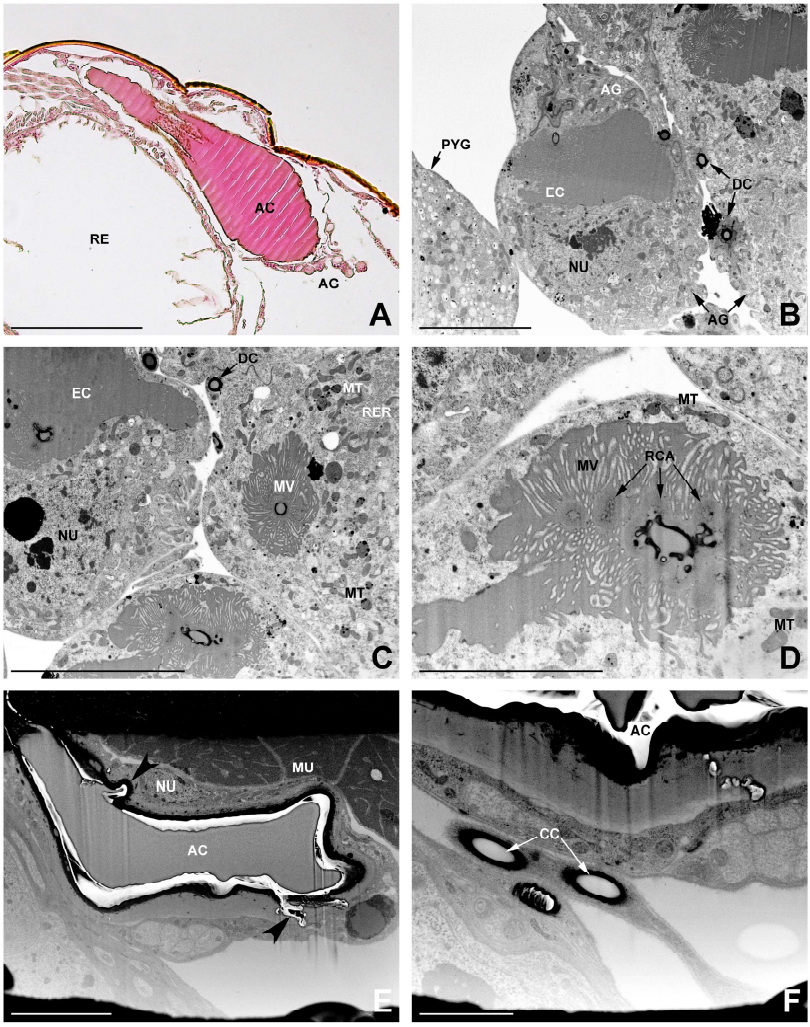
AC
RE
AC
A
AG
PYG
EC
DC
NU
AG
B
DC
EC
MT
RER
MV
NU
MT
C
MT
MV
RCA
MT
D
MU
NU
AC
E
AC
CC
F

Figure 8

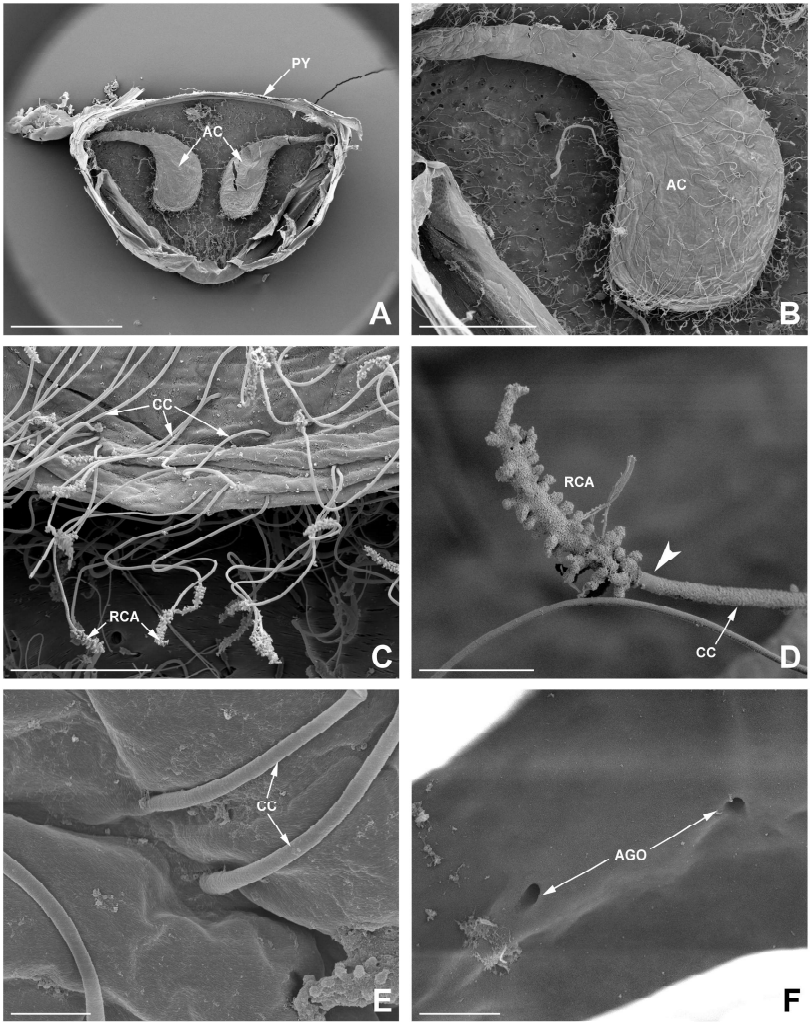

Figure 9

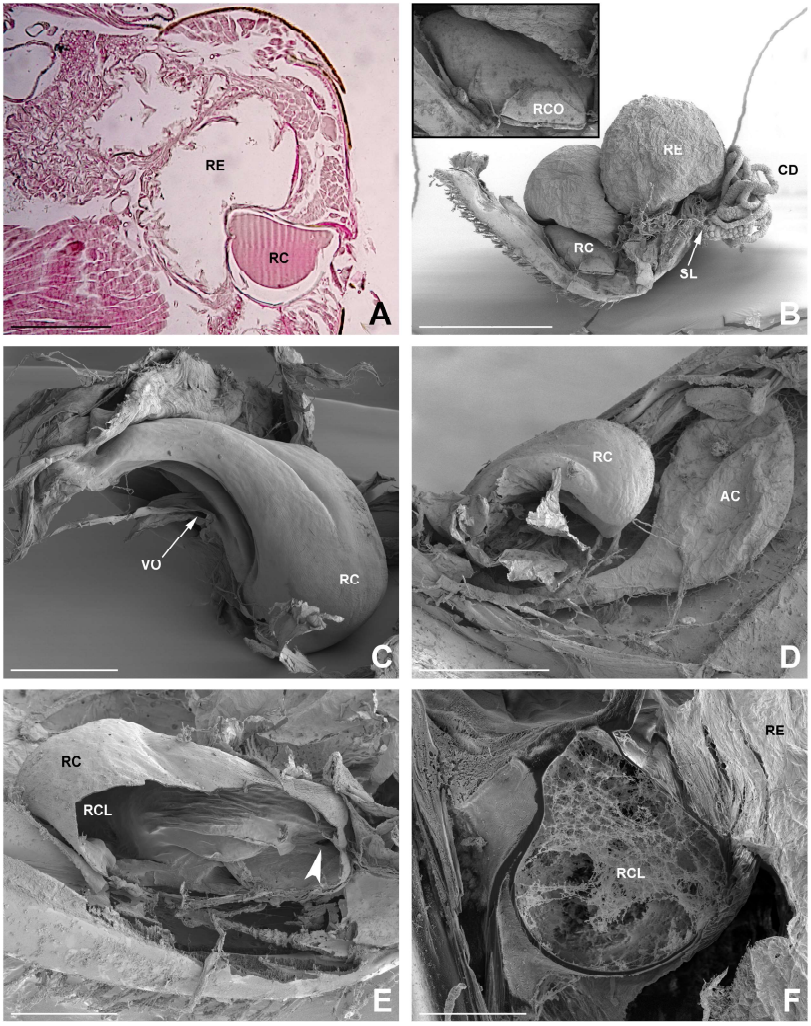

Figure 10

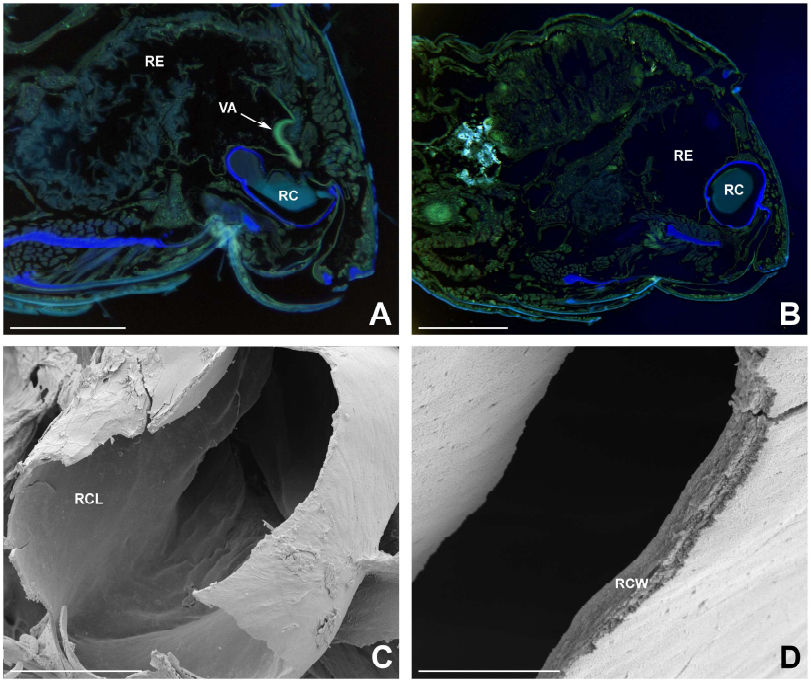

Figure 11

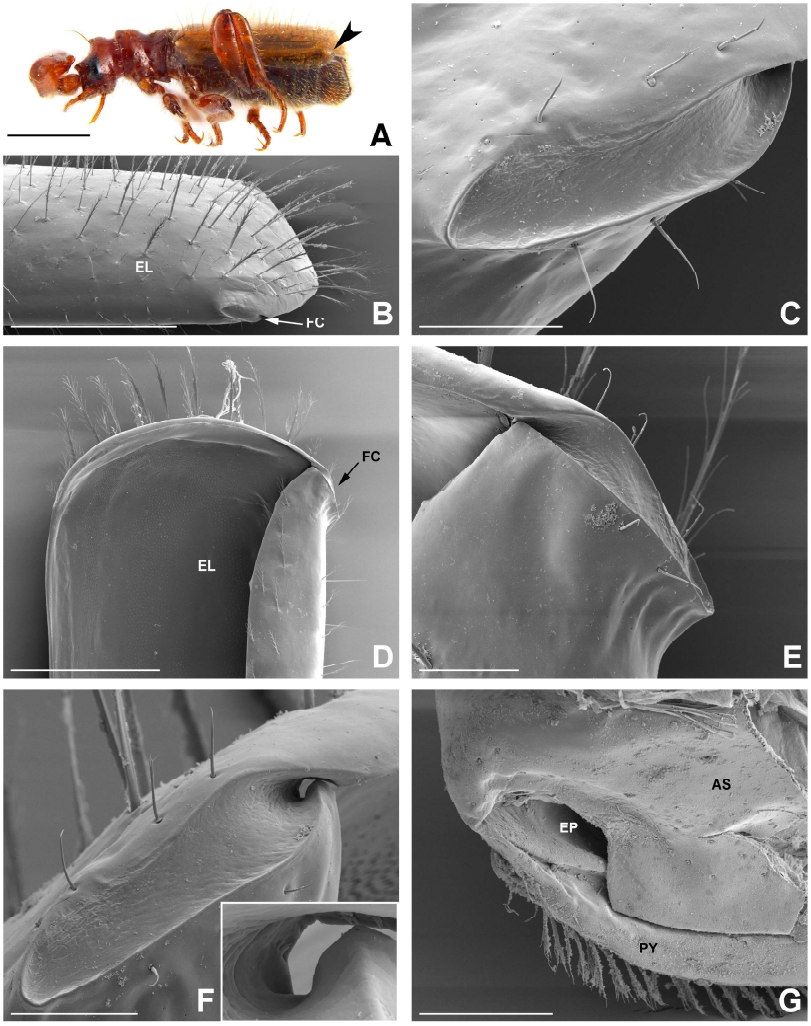

Figure 12

Captions of Figures

Fig.1. A. *Paussus favieri* interacting with *Pheidole pallidula* minors and queen. B. Localization of the pygidial glandular system; drawing modified from Casale et al., 1982. C. Schematic drawing of the explosive defensive system of *Paussus favieri*; the lateral boxes show histological details of the components. *AC* accessory chamber, *CD* collecting duct, *RC* reaction chamber, *RE* reservoir chamber, *SL* secretory lobe.

Fig.2. Secretory lobes of *P. favieri.* A. Histological section showing the secretory lobes and the expanded apical part of the duct. B-F. FIB/SEM analysis of cross sectioned secretory lobe, showing the anatomy of secretory cells, duct cells and ductules at different magnifications.
CC conducting canal, CD collecting duct, DC duct cell, DU ductule, EC extracellular cavity, MT mitochondrion, MV microvilli, NU nucleus, SC secretory cell, SL secretory lobe, RCA receiving canal, RER rough endoplasmic reticulum. Scale bars: A=100 µm; B=10 µm; C=5 µm; D=3 µm; E=3 µm F=2 µm.

Fig. 3. Secretory lobes of *P. favieri* cleared in KOH (A-D) and after a mild maceration in KOH (E-F). A. general structure of the secretory lobes. B. Insertion of the ductules in the collecting duct; arrowhead indicates the basal dichotomous splitting of the ductule. C. Detail of the ductules showing branches of different diameter D. Close up of the converging conducting canals; arrowhead indicate the smooth transition zone. E-F. Samples incompletely digested showing the ovoid receiving canals of the secretory units. CC conducting canals, CD collecting duct, DU ductule, RCA receiving canal, SL secretory lobe, TR tracheae. Scale bars: A=100 µm; B=50 µm; C=30 µm; D=10 µm; E=30 µm F=10 µm.

Fig. 4. Collecting duct of *P. favieri.* A. Histological section showing the tangled collecting duct; the arrowhead indicates the insertion of the duct in the reservoir chamber, note the augmented diameter. B. Peripheral section of the collecting duct showing the collecting duct cells and the cuticular cristae. C. Transverse section of collecting duct showing the duct lumen and the radial cuticular cristae. D. Longitudinal section of collecting duct. E-F. Transverse section showing the cuticular intima lining the fringed cuticular protuberances in cross-section; arrowhead indicates individual cuticular projection completely surrounded by cuticular intima, possibly serving as attachment point. CCR cuticular crista, CD collecting duct, DL duct lumen,

FP fringed projections, IN intima, NU nucleus, RE reservoir chamber. Scale bars: A=100 µm; B=10 µm; C=20 µm; D=10 µm; E=3 µm F=3 µm.

Fig. 5. Fine structure of *P. favieri* collecting duct. A. Entire collecting duct, partially untangled. B. Apical expanded part of the collecting duct bearing the secretory lobes. C. Distal insertion of the collecting duct inside the reservoir chamber, arrowhead indicate the insertion point. D. Bulged and bubble-like appearance of the collecting duct wall at the level of the secretory lobe insertion. E. Cross section of the collecting duct showing cuticular cristae and the internal fringed projections; the thin cuticular intima was digested by KOH treatment. F-G. Close-ups of the fringed projection seen from the duct lumen (F) and from the outside after the removal of the wall (G). CCR cuticular crista, CD collecting duct, DL duct lumen, FP fringed projections, RE reservoir chamber, SL secretory lobe. Scale bars: A=500 µm; B=100 µm; C=200 µm; D=50 µm; E=10 µm F=3 µm; G=2 µm.

Fig. 6. Anatomy and fine structure of *P. favieri* reservoir chamber. A. Histological section showing the wide posterior lobe of the reservoir chamber. B. Multi-folded reservoir wall surrounded by muscles. C. Longitudinal section of the reservoir muscles with the associated tracheae. D. Close up of the reservoir wall showing the different electron density of the two cuticular layers. E-F. Cuticular part of the reservoir chamber after KOH treatment; note the bilobed shape of the reservoir and the ventral attachment of the collecting duct (arrowhead). AC accessory chamber, CD collecting duct, NU nucleus, RC reaction chamber, RE reservoir chamber, RL reservoir lumen, RM reservoir muscles, RW reservoir wall, SL secretory lobe, TR tracheae. Scale bars: A=200 µm; B=10 µm; C=5 µm; D=5 µm; E=250 µm F=250 µm.

Fig. 7. Anatomy and fine structure of *P. favieri* valve. A. Histological section showing the ventral and dorsal layers of the valve and the associated muscles. B. Valve after KOH treatment. C. Valve longitudinally sectioned by FIB. D. Close up of C showing dorsal and ventral layers; note the increased thickness of the dorsal layer. RC reaction chamber, RCL reaction chamber lumen, RE reservoir chamber, RL reservoir lumen, VA valve, VDL valve dorsal layer, VM valve muscles, VVL valve ventral layer. Scale bars: A=200 µm; B=100 µm; C=50 µm; D=30 µm.

Fig. 8. Anatomy of the accessory chamber and related glands in *P. favieri*. A. Histological section showing the accessory chamber and rounded individual

accessory glands. B-F. FIB/SEM analysis of the former showing: general structure of the cells (B), sub-cellular details of both secretory cells (C-D) and duct cells (C, E-F); note the presence of electron-dense substance inside the accessory chamber lumen (A, E), the individual insertion of the conducting canals (E, arrowheads) and the presence of abdominal muscles close to the accessory chamber (E). AC accessory chamber, AG accessory glands, CC conducting canal, DC duct cell, EC extracellular cavity, MT mitochondria, MU muscles, MV microvilli, NU nucleus, PYG pygidial glands, RCA receiving canal, RE reservoir, RER rough endoplasmic reticulum. Scale bars: A=300 μm; B=10 μm; C=10 μm; D=5 μm; E=5 μm F=2 μm.

Fig. 9. Fine structure of *P. favieri* accessory chamber and related glands after KOH treatment. A. Internal view of the pygidium showing the position of the two accessory chambers, other part of the explosive system removed. B. Right accessory chamber showing the peculiar "bota-bag" shape and differential density of the individual accessory glands. C. Close up of B showing the long conducting canals and the relative receiving canals at the bottom of the chamber. Close up of the receiving canal, the arrowhead shows the smooth transition zone. E. Insertion of the conducting canals inside the accessory chambers. F. Internal view of the accessory chamber showing the insertion of the conducting canals, visible as pores. AC accessory chamber, AGO accessory gland opening, CC conducting canal, PY pygidium, RCA receiving canal. Scale bars: A=500 μm; B=150 μm; C=30 μm; D=4 μm; E=3 μm F=3 μm.

Fig. 10. Anatomy and fine structure of *P. favieri* reaction chamber. A. histological section showing the presence of a dense substance in the reaction chamber lumen. B-F. Cuticular part of the reaction chamber after KOH treatment. B. Lateral view of the explosive defensive system showing the relative position of the reaction chamber; the window on the upper left showing a close up of the reaction chamber opening. C. Ventral view of the reaction chamber showing the valve opening and the adjacent cuticular invagination forming the internal longitudinal crista. D. Apical view of the reaction chamber showing the enlarged basal part. E. internal view of the reaction chamber after breaking of the cuticular wall; note the internal cuticular crista and the opening of the accessory chamber (arrowhead). F. Cross section of the reaction chamber at the level of the posterior hemispherical region, note the spongy appearance of the dehydrated catalytic substance. AC accessory chamber, CD collecting duct, RC reaction chamber,

RCL reaction chamber lumen, RCO reaction chamber opening, RE reservoir chamber, SL secretory lobe, VO valve opening. Scale bars: A=100 µm; B=500 µm; C=100 µm; D=50 µm; E=100 µm F=50 µm.

Fig. 11. Anatomy and fine structure of *P. favieri* reaction chamber. A-B. Fluorescence microscopy images of histological sections of the reaction chamber at different levels showing the presence of resilin (in blue) by using DAPI filter; note the absence of resilin at the valve level (A). C-D Cuticular part of a broken reaction chamber, after KOH treatment, showing the irregularly sculptured internal surface (C) and the thickness of the multi-layered wall (D). RC reaction chamber, RCL reaction chamber lumen, RCW reaction chamber wall, RE reservoir, VA valve. Scale bars: A=200 µm; B=200 µm; C=50 µm; D=5 µm.

Fig. 12. Fine structure of the flange of Coanda in *P. favieri*. A. Left ventro-lateral view of the beetle showing the position of the flange (arrowhead) and the thin cuticle of the elytra ventrally adhering to the sterna. B. Left elytron showing the subapical flange of Coanda in latero-dorsal view. C. Flange of Coanda in latero-dorsal view; note the faint grooved microscuplture. D. Ventral view of right elytron showing the flange of Coanda from bottom. E. Close up of the flange presented in D. F. Lateral view of the flange showing the cuticular folding creating the elytral orifice (see a close up of the orifice in the right bottom window showing the fine digitiform microsculpture). G. Ventral view of the abdominal exit pore of the defensive system. AS abdominal sternum, EL Elytron, EP exit pore, FC flange of Coanda, PY pygidium. Scale bars: A=1 mm; B=500 µm; C=50 µm; D=400 µm; E=50 µm F=50 µm; G=100 µm.

Discussion

Pygidial glands are a synapomorphy of Adephaga and represent an important innovation that enables the insect to produce a variety of defensive secretion, stored in a cuticular chamber and promptly released in response to predators and aggressors attacks (Forsyth, 1968, 1970a,b; 1972; Dettner, 1987). Pygidial glands in the adephagan family Carabidae show a broad variability, both in terms of produced chemicals (Moore and Wallbank, 1968; Balestrazzi et al., 1985; Dettner, 1987; Will et al., 2000) and gland morphology (Forsyth, 1970a,b, 1972; Balestrazzi et al., 1985). In spite of sharing a common ground plan, the components of the system (secretory lobes, collecting duct, reservoir and valve) show remarkable morphological differences but it is worth noting that not all of the structural similarities reflect phylogenetic relationships. Similar characters are often found in distant and unrelated groups and the same is true for chemical substances as some of them are quite widespread and shared by phylogenetically distant taxa. Thus, the independent evolution of bio-chemical pathways, underlying the production of a particular defensive secretion, or the presence of a similar structure should not be particularly surprising. Nevertheless, the exceptionality of the two-cambered explosive defensive system led many authors to consider bombardier beetles as a monophyletic lineage, emphasizing the striking chemical similarities and the presence of a second highly sclerotized compartment (reaction chamber) as the main arguments to support the hypothesis of a sister group relationship between Paussinae and Brachininae (Eisner et al., 1977, 2000, 2001; Aneshansley et al., 1983; Erwin and Sims, 1984; Bousquet, 1986). While the explosive system may represent a synapomorphy of the bombardier beetles, many other authors hypothesized that the similarity is likely an example of convergent evolution as the analysis of adult and larval morphological characters suggests that Paussinae and Brachininae are distantly related groups with Paussinae as basal and Brachininae as highly derived carabids (Forsyth, 1972; Ball and McCleve, 1990; Beutel, 1992, 1993, 1996; Deuve, 1993; Arndt, 1998; Liebherr and Will, 1998). Unfortunately, molecular phylogenetic analyses have not yet provided conclusive results concerning the controversial phylogenetic relationship between the two bombardier beetles groups. This is largely because the subfamily Paussinae is subtended by a long branch in trees inferred by molecular sequence data and therefore it is prone to long branch attraction issues and the phylogenetic placement of this subfamily relative to all other carabids is uncertain (Maddison et al., 1999, 2009).

A critical and detailed morpho-anatomical analysis of explosive defensive systems has never been made before and even some of the already known differences between Paussinae and Brachininae have been frequently disregarded. For example, the aiming of the defensive substances is achieved in totally different ways as highlighted by the remarkable contributions of Eisner and Aneshansley (1982, 1999). In brachinines the glands open medially on the abdominal apex and the secretions are aimed in virtually every direction by revolving the hypermobile abdominal tip, which is left free to move thanks to truncated shape of elytra. In paussines, instead, the glands open laterally and the secretions are forwardly aimed using the elytra as launching guide. One of the reasons of this different pointing strategy is probably related to the almost fixed abdomen of paussines, unable to bend to such an extent to forwardly direct the defensive secretions. These two aiming strategies are extraordinarily different but equally functional as they both allow a precise addressing of the spray against the source of disturbance, therefore the hypothesis that one of the two evolved from the other appears extremely unlikely.

One of the main results of the present work is the characterization of the fine morphology of the reaction chambers in Brachininae and Paussinae that allowed a deeper knowledge of the different level of complexity found in these two subfamilies. Often reaction chambers have been considered as slight variations of the same structure, emphasizing their high level of sclerotization and the fact that they represent the exclusive component that distinguishes the explosive defensive system from other pygidial glands. There is no doubt that reaction chambers of Paussinae and Brachininae share a specific functional role, being the compartments where the explosive reaction between precursors (hydroquinones and hydrogen peroxide) and enzymes (catalases and peroxidases) takes place. Therefore, it is possible that some similarities, like the high level of sclerotization and the thickening of the cuticular wall, represent essential modifications needed to face the increase of pressure and temperature caused by the explosive production of quinones. It is still interesting to note that despite the functional analogies, paussines and brachinines reaction chambers are quite different in position and shape. While brachinines exhibit symmetrical funnel shaped compartments, medially positioned near the abdominal tip, paussines have asymmetrical kidney-shaped reaction chambers, laterally located on the side of the ninth abdominal tergum. The funnel shaped reaction chambers of brachinines are distally produced in a turret, a cylindrical apical region that is used to enhance the efficiency and range of the spray. On the contrary, the reniform reaction chambers of paussines lack turrets or similar regions as they

open directly to the outside (where the addressing of the spray is assigned to the elytral margin). Even the level and degree of sclerotization of the chambers show remarkable differences between the two bombardier beetles groups. In brachinines the chambers have a differential degree of sclerotization both at the level of the turret and at the level of the basal part; the first one is mainly membranous while the second one is mainly hard and thickened, showing only a thin unsclerotized belt that provides elasticity and reduces the recoil caused by the internal explosions. In paussines, instead, chamber is uniformly sclerotized and does not show any membranous areas; however, the reduction of mechanical stress is likely provided by the presence of resilin throughout the entire reaction chamber wall. The presence of resilin in reaction chamber is not exclusive of Paussinae but in Brachininae is limited to a specific unsclerotized region of the turret suggesting a different function (limiting the recoil during discharges). The use of electron microscopy highlighted additional differences concerning the complexity of the internal surface of the reaction chamber. While Paussinae chambers are internally smooth or show only slightly corrugated surfaces, Brachininae reaction chambers bear different types of complex sculpticels (spiniform, hair-like, alveolate, etc.) used to keep the catalytic secretion attached to the reaction chamber wall. The different microsculpture mirrors a completely different way of conveying and storing the catalytic enzymes produced by the accessory glands. In brachinines, accessory glands enter directly inside reaction chambers, where they pour their dense secretions; in paussines, instead, accessory glands do not release their catalytic secretions directly inside the reaction chamber but they discharge them in a specific accessory chamber, which enters laterally in the reaction chamber.

The valve usually shows a low degree of variability in carabid beetles (Forsyth, 1970b, 1972) so, a certain similarity was expected even between Paussinae and Brachininae. Nevertheless, while the shape of the valve is quite similar (U shaped in paussines and V shaped in brachinines) a major difference has been highlighted by fluorescence microscopy. In brachinines the ventral layer of the valve exhibits the presence of resilin while both ventral and dorsal layer of paussines lack this elastomeric protein. This difference is likely related to a distinct way of discharging the spray, in fact, most of the brachinines shows a pulsed discharge of the quinones while paussines appear unable to pulse their secretory emissions (Dean et al., 1990; Eisner et al., 2001; Arndt et al. 2015). The exclusive presence of resilin in Brachininae probably enables their valve to better withstand the repeated mechanical stress involved in pulsed discharges as these are achieved by fast

passive oscillations of the valve (Dean et al., 1990; Eisner et al. 2001; Arndt et al., 2015).
Reservoirs in carabids show great variability in shape and volume, nevertheless some correlations have been made between the different reservoir shapes and the different types of stored chemicals (Moore and Wallbank, 1968). Paussinae and Brachininae, however, have completely different reservoirs even if they store similar substances. The reservoir chamber in paussines is distinctly bilobous while brachinines display a curved and tubular multi-folded chamber with pronounced folds and internal incomplete septa that cannot be found in paussines. In both bombardier beetles groups the muscles encasing the reservoir create 2-3 continuous layers; nevertheless Brachininae display an increased level of complexity exhibiting additional longitudinal strands of muscles that connect adjacent folds of the bellows-like reservoir.
Collecting ducts of both bombardiers share a distinctive character, they are extremely long (up to 10 times the beetle length) and tangled on themselves. Among the possible explanations of this exaggerated length have been proposed the maturation of the secretions or a role in preventing the backflow of the secretions towards the secretory lobes (Forsyth, 1970b, 1972). In addition, it is also possible that the extended length could enable the duct to act as a reserve for secretions, allowing a prompt refilling of the reservoir after relaxation of muscles. Another similarity concerns the reduced metabolic activity of the cells responsible for the creation of the duct. These cells, after the completion of the duct, appear depleted of cytoplasm and organelles in both paussines and brachinines. However the strong reduction of metabolic activity in this kind of cells seems to be widespread in all carabid and adephagan beetles (Forsyth, 1970b, 1972; Balestrazzi et al., 1985). Excluding the exaggerated length and their specialized epidermal cells, the collecting ducts of paussines and brachinines show many differences starting from their cuticular wall. The bulged and swollen surface characterizing the outer wall of paussines is completely different from the corrugated one exhibited by brachinines. Moreover, even if both ducts have an internal lumen lined by a thin epicuticular intima, this latter is secured to the duct by totally diverse structures, namely match-like projections in Brachininae and fringed projections in Paussinae. In addition Paussinae collecting duct is always single while Brachininae can present either one, two or multiple ducts. Another remarkable difference concerns the diameter of the duct; in Brachininae it is constant while in Paussinae is variable as the duct shows augmented basal and apical regions.

Secretory lobes are responsible for the production of hydroquinones and hydrogen peroxide in both brachinines and paussines, however, histological analysis showed marked differences. The glandular tissue of paussines is made of rounded irregular elements, consisting of compacted cells irregularly disposed around a cuticular ductule. On the contrary the analogous tissue in brachinines consists of digitiform elements, made up of orderly arranged conical cells that encircle the cuticular ductule. In both cases the glandular tissue is made of bi-cellular units assignable to class III cells according to Noirot and Quennedey (1974, 1991) but it is interesting to note that in paussines, nuclei and extracellular cavities of the secretory cells exhibit a variable and irregular distribution within the cytoplasm, while they appear constantly and regularly located near the basal periphery of the cell in brachinines. The conducting canals of Paussinae are arranged in converging clusters (called "florets" by Eisner et al., 2001) while the ones of Brachininae insert in the ductule lumen individually and without clustering. A notable exception among Brachininae is represented by Crepidogastrini (Eisner et al., 2001) where the glandular tissue appears digitiform but the collecting canals converge in clusters similar to those of paussines. Even the cuticular ductules, which convey the secretions towards the collecting duct, are structurally very different as paussines possess only a pair of finely branched and ramified ductules while brachinines exhibit a higher number (usually 10-15) of unbranched blind-ended cuticular ductules.

The results of this work represent a contribution to the debate concerning the evolution of the explosive defensive system in carabid beetles, supplying additional fine morphological and ultrastructural data on the pygidial glands of Paussinae and Brachininae. Moreover, the present analysis confirms that within Paussinae, Metriini represents the basal group according to their simplified glandular and addressing system, which lacks a proper flange of Coanda; within Brachininae the Crepidogastrini appears basal showing a plesiomorphic organization of the collecting duct in "florets".

Comparative analysis of the two subfamilies systems revealed many remarkable morpho-anatomical and ultrastructural differences that add up to the acknowledged ones concerning the addressing systems and the position of the reaction chamber. Despite the remarkable chemical analogies of their defensive chemicals, the lack of morphological similarity between the two explosive defensive systems suggests that Paussinae and Brachininae may very well have evolved independently a bombarding mechanism. Undoubtedly, explosive defensive systems represent a big step forward in efficiency compared to the non-explosive glands of all other adephagan beetles; a distinct advantage that comes at a cost that is linked to a higher

structural complexity and to the production of an increased number of toxic chemicals (including the cytotoxic hydrogen peroxide). It is possible to hypothesize the evolution of a bombarding strategy as a response to an increased predatory/disturbance pressure. In fact, Brachininae are opportunistic predators or scavengers on organic matter that inhabit riparian zones, areas where they are particularly subject to a vast array of predators like birds, amphibians, reptiles and small mammals (Eisner, 1958; Dean, 1980a,b; Eisner et al., 2005, 2006). On the contrary, members of the subfamily Paussinae have always some kind of interaction and/or associations with ants (Moore, 2008; Moore and Di Giulio, 2008; Moore et al. 2011). In fact, the evolution of an effective explosive defensive strategy in Paussinae could have been very advantageous for both myrmecohagous species and myrmecophilous species. It is worth noting that, despite its full integration and acceptance inside the ant nest, which is one of the most protected environment, the myrmecophilous species *Paussus favieri* not only retains the explosive glands but shows one the most refined explosive defensive system in Paussinae. In the past Crowson (1981) considered the presence of efficient pygidial glands as an essential preadaptation for the evolution of myrmecophily in Paussini. Similarly, the presence of tergal glands has been considered one of the primary preadaptation promoting colony exploitation in aleocharines (Staphylinoidea), one of the most successful group of myrmecophilous beetles (Parker, 2016). The retention of defensive glands even in highly integrated taxa has been interpreted as a "backup" mechanism in rare cases of detection by hosts, or for defence during host colony switches and nest migration (Hölldolber et al., 1981). In view of the above, the presence of explosive defensive glands in Paussinae could represent an essential preadaptation for the multiple evolution of myrmecophily in this subfamily, since this strategy evolved at least four times in Ozaenini (Moore, 2008; Moore et al., 2011) and one in Protopaussini + Paussini (Di Giulio et al., 2003).

References

Aneshansley, D.J., Jones, T.H., Alsop, D., Meinwald, J. and Eisner, T., 1983. Thermal concomitants and biochemistry of the explosive discharge mechanism of some little known bombardier beetles. Experientia 39, 366-368.

Arndt, E., 1998. Phylogenetic investigation of Carabidae (Coleoptera) using larval characters. Phylogeny and classification of Caraboidea (Coleoptera: Adephaga). In: Ball, G.E., Casale, A., Taglianti, A.V. (Eds.), International Congress of Entomology, Phylogeny and Classification of Caraboidea (Coleoptera:Adephaga): Proceedings of a Symposium, 28 August 1996, Florence, Italy: XX International Congress of Entomology. Museo regionale di scienze naturali, Torino, pp. 171-190.

Arndt, E.M., Moore, W., Lee, W.K. and Ortiz, C., 2015. Mechanistic origins of bombardier beetle (Brachinini) explosion-induced defensive spray pulsation. Science 348, 563-567.

Balestrazzi, E., Valcurone Dazzini, M.L., Bernardi, M.D., Vidari, G., Vita-Finzi, P., Mellerio, G., 1985. Morphological and chemical studies on the pygidial defence glands of some Carabidae (Coleoptera). Naturwissenschaften 72, 482-484.

Ball, G.E. and McCleve, S., 1990. The middle American genera of the tribe Ozaenini, with notes about the species in southwestern United States and selected species from Mexico. Quest. Ent. 26, 30-116.

Beutel, R.G., 1992. Study on the systematic position of Metriini based on characters of the larval head (Coleoptera: Carabidae). Syst. Entomol. 17, 207-218.

Beutel, R.G., 1993. Phylogenetic analysis of Adephaga (Coleoptera) based on characters of the larval head. Syst. Entomol. 18, 127-147.

Beutel, R.G. and Haas A., 1996. Phylogenetic analysis of larval and adult characters of Adephaga (Coleoptera) using cladistic computer programs. Insect Syst. Evol. 27, 197-205.

Bousquet, Y., 1986. Description of first-instar larva of *Metrius contractus* Eschscholtz (Coleoptera: Carabidae) with remarks about phylogenetic relationships and ranking of the genus Metrius Eschscholtz. Can. Entomol. 118, 373-388.

Crowson, R.A., 1981. The Biology of the Coleoptera. Academic Press, London

Dean, J., 1980a. Effect of thermal and chemical components of bombardier beetle chemical defense: glossopharyngeal response in two species of toads (*Bufo americanus*, *B. marinus*). J. Comp. Physiol. 135, 51-59.

Dean, J., 1980b. Encounters between bombardier beetles and two species of toads (*Bufo americanus*, *B. marinus*): speed of prey-capture does not determine success. J. Comp. Physiol. 135, 41-50.

Dean, J., Aneshansley, D. J., Edgerton, H. E. and Eisner, T., 1990. Defensive spray of the bombardier beetle: a biological pulse jet. Science, 248 1219-1221.

Deuve, T., 1993. L'abdomen et les genitalia des femelles de Coléoptères Adephaga. Mémoires du Muséum national d'histoire naturelle. Editions du Muséum, Paris.

Dettner, K, 1987. Chemosystematics and evolution of beetle chemical defenses. Annu. Rev. Entomol. 32, 17-48.

Di Giulio, A., Fattorini, S., Kaupp, A., Taglianti, A.V. and Nagel, P., 2003. Review of competing hypotheses of phylogenetic relationships of Paussinae (Coleoptera: Carabidae) based on larval characters. Syst. Entomol. 28, 509-537.

Eisner, T., 1958. The protective role of the spray mechanism of the bombardier beetle, *Brachynus ballistarius* Lec. J. Insect Physiol. 2, 215-220.

Eisner, T., Jones, T.H., Aneshansley, D.J., Tschinkel, W.R., Silberglied, R.E. and Meinwald, J., 1977. Chemistry of defensive secretions of bombardier beetles (Brachinini, Metriini, Ozaenini, Paussini). J. Insect Physiol. 23, 1383-1386.

Eisner, T. and Aneshansley, D.J., 1982. Spray aiming in bombardier beetles: jet deflection by Coanda effect. Science 215, 83-85.

Eisner T. and Aneshansley, D.J., 1999. Spray aiming in the bombardier beetle: photographic evidence. P. Natl. Acad. Sci. U.S.A. 96, 9705-9709.

Eisner, T., Aneshansley, D.J., Eisner, M., Attygalle, A.B., Alsop, D.W. and Meinwald, J., 2000. Spray mechanism of the most primitive bombardier beetle (*Metrius contractus*). J. Exp. Biol. 203, 1265-1275.

Eisner, T., Aneshansley, D.J., Yack, J., Attygalle, A.B. and Eisner, M., 2001. Spray mechanism of crepidogastrine bombardier beetles (Carabidae: Crepidogastrini). Chemoecology 11, 209-219.

Eisner, T., Eisner, M. and Aneshansley, D., 2005. Pre-ingestive treatment of bombardier beetles by jays: food preparation by "anting" and "sand-wiping". Chemoecology 15, 227-233.

Eisner, T., Aneshansley, D.J., del Campo, M.L., Eisner, M., Frank, J.H. and Deyrup, M., 2006. Effect of bombardier beetle spray on a wolf spider: repellency and leg autotomy. Chemoecology 16, 185-189.

Erwin, T.L. and Sims, L.L., 1984. Carabid beetles of the West Indies (Insects: Coleoptera): a synopsis of the genera and checklists of tribes of Caraboidea, and of the West Indian species. Quaest. ent. 20, 351-466.

Forsyth, D.J., 1968. The structure of the defence glands in the Dytiscidae, Noteridae, Haliplidae and Gyrinidae (Coleoptera). Trans. R. ent. Soc. Lond. 120, 159-181.

Forsyth, D.J., 1970a. The structure of the defence glands of the Cicindelidae, Amphizoidae, and Hygrobiidae (Insecta: Coleoptera). J. Zool. 160, 51-69.

Forsyth, D.J., 1970b. The ultrastructure of the pygidial defence glands of the carabid *Pterostichus madidus* F. J. Morphol. 131, 397-415.

Forsyth, D.J., 1972. The structure of the pygidial defence glands of Carabidae (Coleoptera). Trans. Zool. Soc. Lond. 32, 249-309.

Hölldolber, B., Möglich, M. and Maschwitz, U., 1981. Myrmecophilic relationship of *Pella* (Coleoptera: Staphylinidae) to *Lasius fuliginosus* (Hymenoptera: Formicidae). Psyche 88, 347-374.

Liebherr, J.K. and Will, K.W., 1998. Inferring phylogenetic relationships within Carabidae (Insecta, Coleoptera) from characters of the female reproductive tract. Phylogeny and classification of Caraboidea (Coleoptera: Adephaga). In: Ball, G.E., Casale, A., Taglianti, A.V. (Eds.), International Congress of Entomology, Phylogeny and Classification of Caraboidea (Coleoptera:Adephaga): Proceedings of a Symposium, 28 August 1996, Florence, Italy : XX International Congress of Entomology. Museo regionale di scienze naturali, Torino, pp. 107-170.

Moore, B.P. and Wallbank, B.E., 1968. Chemical composition of the defensive secretion in carabid beetles and its importance as a taxonomic character. Proc. R. Entomol. Soc. Lond. Ser. B 37, 62-72.

Moore, W., 2008. Phylogeny of the western Hemisphere Ozaenini (Coleoptera: Carabidae: Paussinae) based on DNA sequence data. Ann. Carnegie Mus. 77, 79-92.

Moore, W. and Di Giulio, A., 2008. *Metrius* Eschscholtz (Carabidae: Paussinae) is not a millipede specialist. Pan-Pac. Entomol. 84, 33-34.

Moore, W., Song, X. B. and Di Giulio, A., 2011. The larva of *Eustra* (Coleoptera, Paussinae, Ozaenini): a facultative associate of ants. ZooKeys 90, 63-82.

Noirot, C. and Quennedey, A., 1974. Fine structure of insect epidermal glands. Annu. Rev. Entomol. 19, 61-80.

Noirot, C. and Quennedey, A., 1991. Glands, gland cells, glandular units: some comment on terminology and classification. Ann. Soc. Entomol. Fr. 27, 123-128.

Parker, J., 2016. Myrmecophily in beetles (Coleoptera): evolutionary patterns and biological mechanisms. Myrmecol. News 22, 65-108.

Will, K.W., Attygalle, A.B. and Herath, K., 2000. New defensive chemical data for ground beetles (Coleoptera: Carabidae): interpretations in a phylogenetic framework. Biol. J. Linn. Soc. Lond. 71, 459-481.